ECONOMICALLY VIABLE SOLAR STILLS

by

Ian Goldie

Dissertation presented for the Degree of
Doctor of Philosophy in Chemistry (Physical)
at the
University of Stellenbosch

Promoter: Prof RD Sanderson
The late Prof WJ Engelbrecht
(original promoter)

STELLENBOSCH
December 2003

DECLARATION

I, the undersigned, hereby declare that the work contained in this dissertation is my own original work and has not previously in its entirety or in part been submitted at any university for a degree.

Ian Goldie

SUMMARY

The use of solar distillation as a means of desalination to provide potable water to communities in remote and arid regions has often been discarded on economic grounds mainly because of the inherent low efficiency of relatively expensive solar distillation units (solar stills). Closer analysis of this constraint showed that by following a mainly Physical Chemistry approach (rather than the traditional engineering one), the technology could be made more economically attractive through (1) lowering the construction cost of the solar still and / or (2) increasing its operational life and / or (3) increasing its efficiency.

The study into different solar still designs showed that, despite its limitations, the basin solar still is preferred due to its simplicity, ease of operation and low maintenance. Given the solar distillation process as formulated in this study, substitute durable components could be identified and optimised for this design. A basin solar still that costs about 80% less than a reference unit without an apparent drop in performance was consequently developed and successfully tested up to full plant scale.

An in-house experimental facility that simulates solar still behaviour under controlled environmental conditions was developed to simulate conditions of lower radiation intensity and productivity, which enabled research into performance enhancement and microbiological water quality. It was found that (a) absorption of the radiation by the water plays an important part in productivity and that a productivity decrease of up to 33% can be expected as the black interior lining becomes contaminated, (b) the simulated winter productivity of the basin still was about 25% of the summer value due to the lesser amount of solar radiation hours, the lower angles of radiation incidence onto the cover and the decrease in water area receiving direct radiation, (c) an annual productivity increase of about 10% can be obtained when a particular reflector configuration is fixed behind the basin, and (d) the microbiological pasteurisation temperature is less than the distillation onset temperature .

This study played an important role in making solar still technology affordable for use by poor, rural communities, as was demonstrated by the successful use of the research product (basin solar still) in a pilot drinking water plant at a typical target community. This was made possible through the use of evaluation models developed as part of this research, which addressed relevant construction and performance factors influencing the economic viability of the specific solar still.

The following outcomes of this study can be regarded as new contributions to the field of solar distillation technology, namely (a) a test matrix that can be used to screen solar still construction materials at component level, (b) an evaluation model that can be used to determine the economic viability of solar stills at a given location, (c) a laboratory testing facility to study solar still behaviour under controlled conditions and (d) a solar still design that has been optimised and tested for local field application.

OPSOMMING

Die gebruik van son-energie om brakwater deur middel van distillasie te ontsout en sodoende drinkwater aan afgeleë gemeenskappe te verskaf, is herhaaldelik in die verlede as ekonomies nie-lewensvatbaar aangetoon. Dit is hoofsaaklik toeskryfbaar aan die inherente lae effektiwiteit van sodanige stelsels, asook die hoë kapitaalkoste daaraan verbonde. Die hoofsaaklike faktore wat die tegnologie bekostigbaar kan maak, is egter hieruit afgelei en volgens 'n Fisiese Chemie benadering geoptimeer, naamlik (1) vermindering van die konstruksiekoste van die sondistilleerder-eenhede, en / of (2) verlenging van die operasionele leeftyd daarvan, en / of (3) verhoging van effektiwiteit van die stelsel.

Die literatuurstudie het aangetoon dat die pan-tipe sondistilleerder-eenheid verkieslik as navorsingsbasis is omdat dit eenvoudig en maklik bedryf- en onderhoudbaar is. Vanuit die geformuleerde beskrywing van die sondistillasie-proses kon plaasvervangende komponente vir die sondistilleerder-eenheid geïdentifiseer en getoets word, wat daartoe gelei het dat 'n eenheid met dieselfde funksioneringseienskappe vir sowat 80% goedkoper ontwikkel kon word.

'n Laboratoriumopstelling waarmee lae bestralingskondisies gesimuleer kan word, is ontwikkel om navorsing op produktiwiteitsverbetering en mikrobiologiese produkwaterkwaliteit te doen. Dit is aangetoon dat (a) absorpsie van die inkomende bestraling deur die water belangrik is en dat 'n sondistilleerder-eenheid tot 33% minder produktief kan wees indien die swart voering binne die eenheid besoedel sou word, (b) winterproduktiwiteit daal tot 25% van somerproduktiwiteit as gevolg van die verminderde sonlig-ure, die laer invalshoek van die bestraling op die glasdeksel, en die gepaardgaande verkleining van die blootgestelde water-oppervlakte, (c) 'n gemiddelde produktiwiteitsverhoging van 10% deur weerkaatsers agter die sondistilleerder-eenheid teweeggebring kan word, en (d) die distillasie-temperatuur die water-ontsmettingstemperatuur oorskry.

Hierdie navorsing het 'n belangrike rol gespeel om sondistilleerder-tegnologie bekostigbaar vir behoeftge gemeenskappe in landelike gebiede te maak. Dit is

gedemonstreer deur die suksesvolle toepassing van die navorsingsproduk (sondistilleerder-eenheid) in 'n drinkwatervoorsieningsprojek by 'n tipiese teiken-gemeenskap. Dit is vermag deur die gebruikmaking van evaluasie-modelle wat gedurende hierdie studie ontwikkel is, en wat die toepaslike konstruksie- en funksioneringsfaktore wat die ekonomiese lewensvatbaarheid van die eenheid beïnvloed, aanspreek.

Die volgende navorsingsprodukte kan beskou word as nuut in die veld van sondistillasie-tegnologie, naamlik (a) 'n toetsmatriks wat gebruik kan word om komponente vir sondistilleeerders te evalueer, (b) 'n ekonomiese evalueringsmodel wat gebruik kan word om die bekostigbaarheid van sondistilleerders in 'n bepaalde gebied te bepaal, (c) 'n laboratorium-toetsfasiliteit om die werking van sondistilleerders onder beheerde kondisies te ondersoek en (d) 'n sondistilleerder-eenheid wat doelgeskik vir plaaslike omstandighede ontwikkel en getoets is.

ACKNOWLEDGEMENTS

The author wishes to express his sincere thanks to the following people and institutions:

First and foremost:

The late **Prof Willem Engelbrecht** (original study leader, deceased 5 September 2003). Prof – thank you for your support and guidance throughout my postgraduate study years. I consider it a privilege to have known you, been in a position to learn from you, and had you as my supervisor and promoter. This dissertation is dedicated to you – with sincere thanks and appreciation.

Also:

Prof Ron Sanderson (who assumed study leadership) for initialising this research and for his expert advice and guidance throughout the study.

Dr Gerhard Offringa (Water Research Commission of South Africa) for his discerning advice and scientific guidance especially during our field trials.

Johan Bonthuys, Andrew Theunissen, Reynold Heneke, Valeska Cloete and **Calvin Maart,** for their dedication and unselfish contributions especially after-hours.

Dr Margie Hurndall and the personnel of **Polymer Science, Department of Chemistry,** for their kind assistance and encouragement.

The **Water Research Commission** of South Africa for financial assistance.

The **University of Stellenbosch** for financial assistance through Harry Crossley Trust and THRIP.

My dear family (**Isolde, Niel** , **Carl** and **Pona**) for their love and support.

TABLE OF CONTENTS

LIST OF FIGURES

LIST OF TABLES

CHAPTER 1

INTRODUCTION

1.1 Background

Latitude, and its influence on the amount of solar radiation received, is one of the main factors influencing the climate of a particular geographical area. Since the input of energy into the earth's system is greatest in the equatorial regions, more water is evaporated and more energy is stored (as latent energy in water vapour and sensible heat in ocean water) in this region than in any other. Water vapour and its stored energy can then be re-distributed around the globe via the global circulation system (http://www.math.montana.edu/~nmp/materials/ess/hydrosphere/expert/runningwater/runningback.html). The balance between regional or local gain and loss of water will determine climate, insofar as moisture is concerned. The major ocean currents play an important role in the moisture distribution system. These currents are initiated by winds and earth rotation, and the global current patterns resemble the global air circulation patterns. Precipitation maps (Figure 1.1) show rainfall patterns that originate from these moisture-distribution cycles.

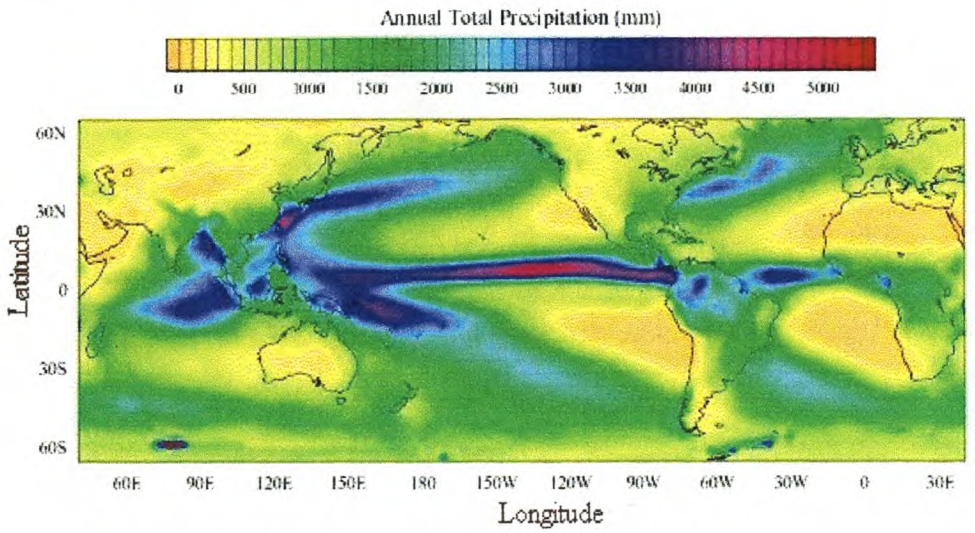

Figure 1.1: Annual global precipitation.
(*http://www.jisao.washington.edu/legates_msu/*).

Southern Africa, under the influence of the Benguela current along its West Coast, has areas of particularly low mean rainfall, as shown in Figure 1.2 (Lynch 1998).

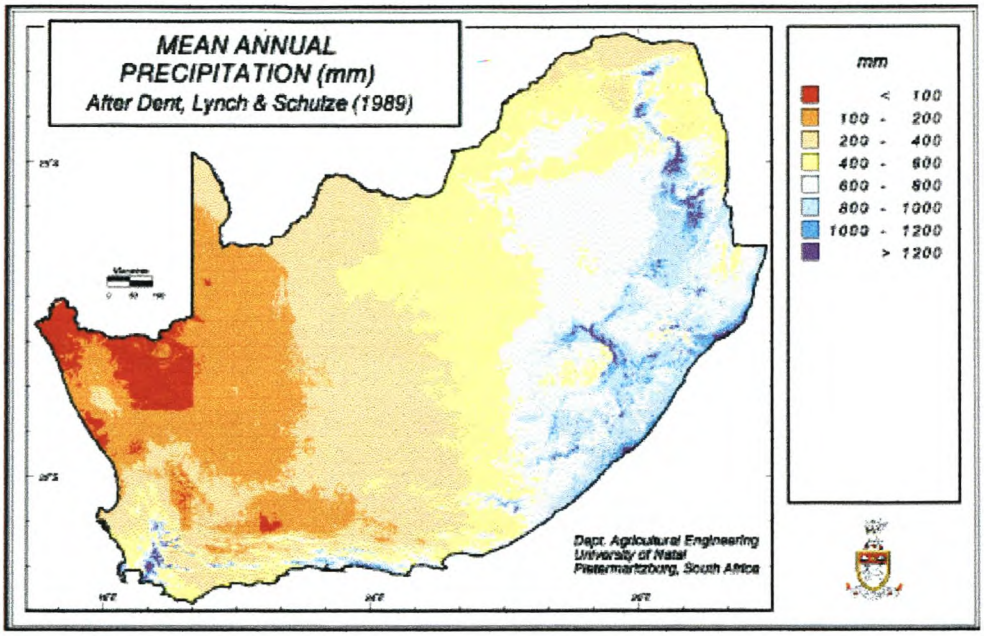

Figure 1.2: Mean annual precipitation of South Africa.

The areas of low rainfall for South Africa correspond to a large degree with areas of high annual solar radiation (Figure 1.3).

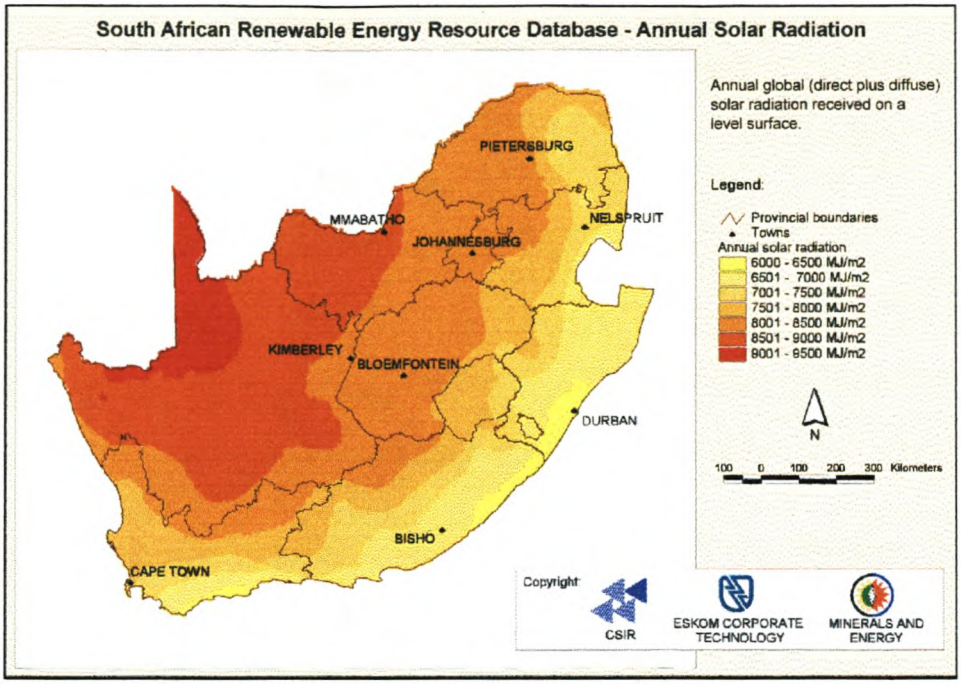

Figure 1.3: Mean annual global radiation map of South Africa (http://www.csir.co.za/websource/ptl0002/images/environmentek/sarerd/maps/solar.jpg).

When South Africa's groundwater quality is viewed in terms of total dissolved solids (TDS), it is seen that the geographical areas with high TDS values (Figure 1.4) overlap to a large extend with the arid areas presented in Figures 1.2 and 1.3.

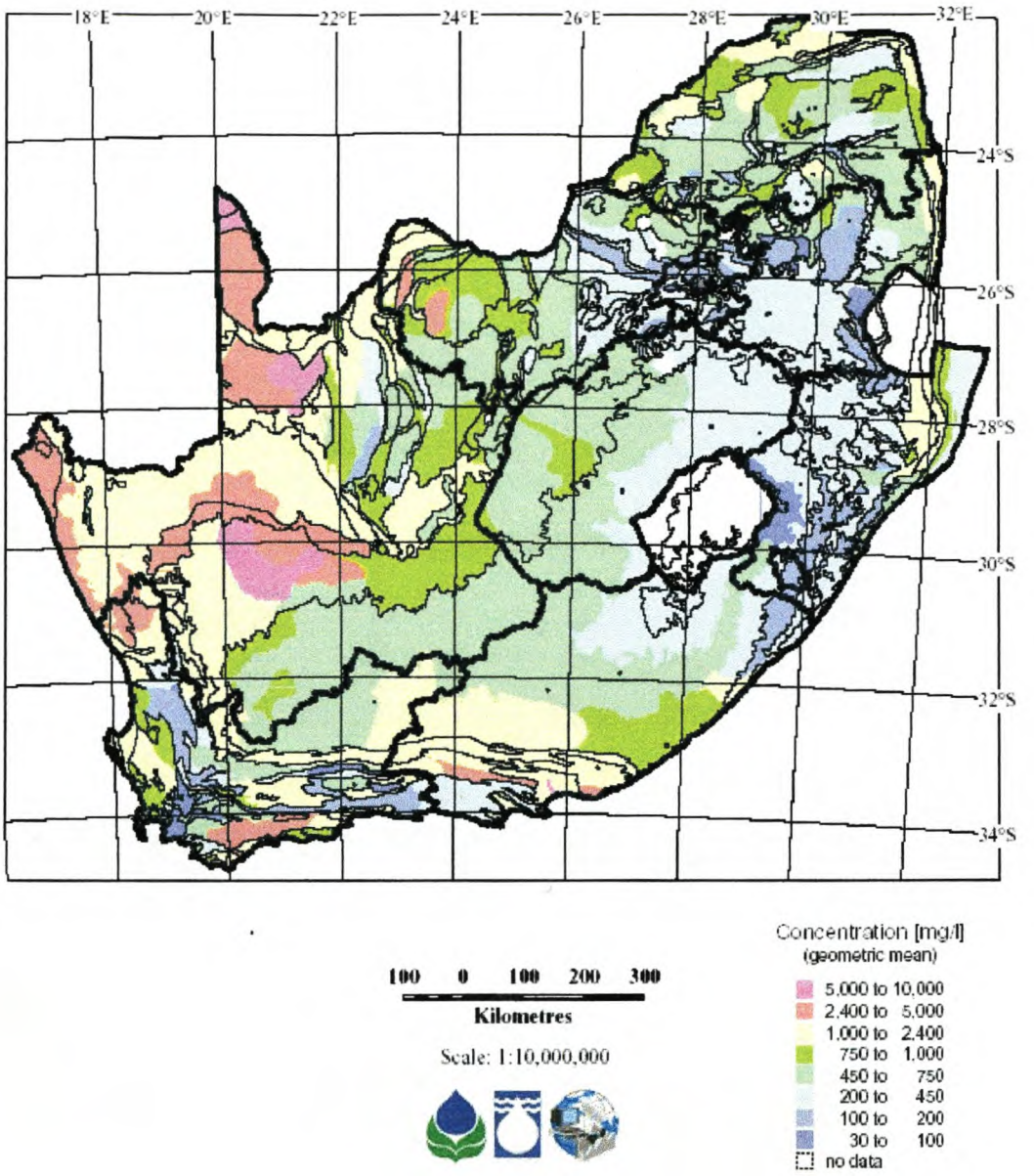

Figure 1.4: Groundwater quality map of South Africa (Simonec 1999).

Figure 1.5 shows the 1998 population density distribution for South Africa. It is clear that, throughout the country, the arid regions have the lowest population density.

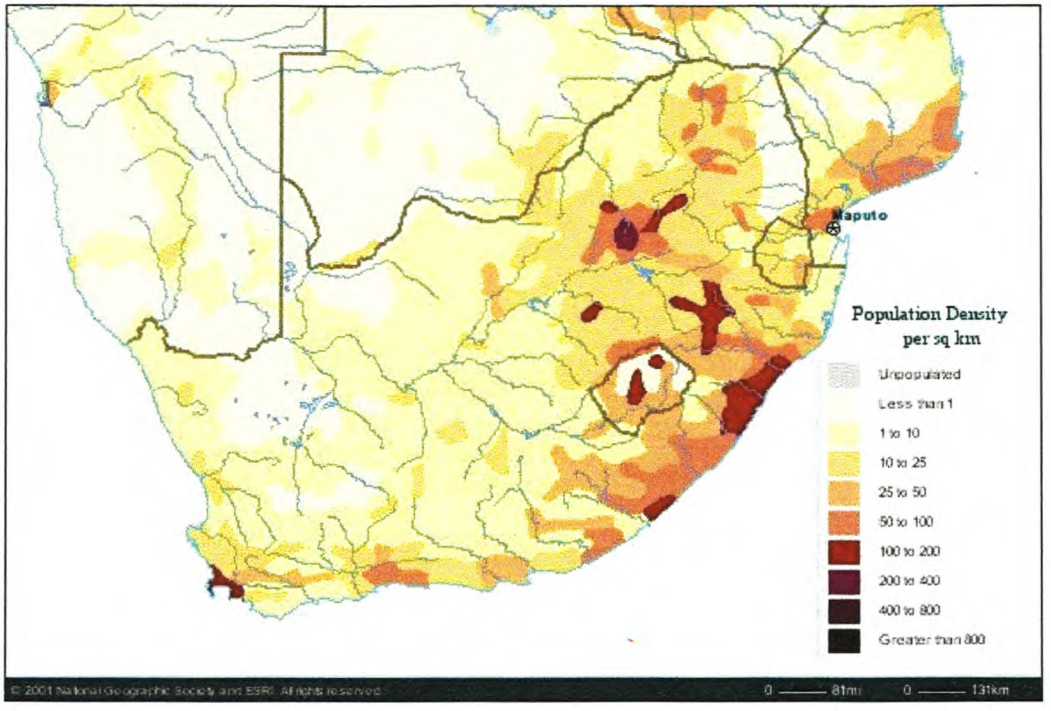

Figure 1.5: 1998 population density distributions of South Africa.
(from National Geographic MapMachine, http://plasma.nationalgeographic.com/)

The maps in Figures 1.2 to 1.5 show that the arid areas of Western and central South Africa have the following features:

- the population density is low,
- the annual rainfall is low and inconsistent,
- groundwater quality is unacceptable for potable purposes; and
- the annual solar radiation is high.

1.2 Rural water supply options

Provision of potable water conforming to required national standards to households of the smaller-sized communities in sparsely populated areas is problematic. To supply such small remote communities with fresh water, at least three alternatives exist, namely (1) to construct a modern, sophisticated and costly desalination plant to treat saline groundwater or seawater, (2) to transport

potable water over long distances by pipes or other transportation means, or (3) to utilise solar energy to desalinate brackish groundwater or seawater.

A variety of desalination technologies can be used to separate fresh water from saline water, including multi-effect distillation (ME), multi-stage flash distillation (MSF), mechanical vapour compression (MVC), reverse osmosis (RO) and electrodialysis (ED) (KS Spiegler 1994). These technologies are however often too expensive for the production of relatively small amounts of fresh water. The use of long-distance piping or mechanical transport in harsh conditions is usually costly (Abdul-Fattah 1986). Solar distillation plants may be suitable to provide desalinated water especially where solar radiation is abundant and large land areas are available at low or no cost (EE Delyannis 1995). In such areas, the water demand is often directly proportionate to the solar radiation intensity, creating the potential benefit of applying solar energy to provide for the increased water demand. When it rains, the distilled water production stops but another source of fresh water is available to utilise. This technology is further made attractive by not requiring any moving parts, membranes or electricity (Agua del Sol Newsletter 1997). Small-scale solar powered distillation thus becomes an attractive, and sometimes the only, method by which to provide potable water, provided that it can be implemented economically.

1.3 Historical and current application of solar stills

The oldest large-scale application of solar energy appears to be the burning of the Roman Fleet in the bay of Syracuse by Archimedes, who concentrated solar radiation by mirrors using the ships as focus (AA Delyannis 1981). Principles of solar distillation have also been around for centuries. Greek navigators used to boil seawater and condense the vapours on sponges to produce fresh water. In 4 BC, Aristotle suggested a method for evaporating seawater to produce potable water. In 1551 Arab alchemists practiced solar distillation using glass vessels. Ghezzi, an Italian philosopher, also made specific reference to the possibilities of solar distillation in 1742. The solar still can therefore rightfully be regarded as the oldest device that can be used to provide drinking water (Gomkale 1988).

In 1874 J Harding and C Wilson built the first solar still plant near Las Salinas in Chile (M Telkes 1956). This plant had a glass covered area of 4 757 m^2 and produced about 27 000 liters of water per day from brackish wells. It was used to supply fresh water to workers and animals working for a nearby nitrate mining company. This plant ran for 40 years until the mine was closed, and yielded more than 4.9 kg distilled water per m^2 during the summer.

Between 1920 and 1938 research effort went into increasing the distilled water yield of solar distillation devices, which included the use of metal-coated reflectors and lenses. During World War II considerable work went into making air-inflated small plastic solar stills for use on life rafts (Tiwari 1997). Seawater was evaporated inside the still on a porous felt pad and collected in bottles at the bottom.

Intensive research into solar stills and solar distillation was undertaken from 1958 at the Solar Distillation Research Station at Daytona Beach, Florida (Lof 1961). Much of the current understanding of solar distillation stems from this research, and other researchers often reference this research by Lof.

Many solar distillation plants were built in the 1960's (AA Delyannis 1983). Then, as other desalination technologies became available, application thereof began to decrease. Recently however, as research lead to design and operational improvements, interest in its potential began to increase again.

There is agreement that the suitability of solar still plants is determined by the availability of a saline water source, specific hot weather conditions and a relatively small daily demand (Ashboren 1979). Typically, this demand can be described as modest, typically less than 5 000 liters per day. The overall simplicity of solar stills makes them attractive for use with all types of feed water, an advantage over the more complicated technologies. This means that water from the sea, streams, rivers, wells and rain catchment tanks can be purified.

The future application potential of solar stills must also be viewed in terms of the global energy scene. Exploring renewable energy sources, especially solar energy, will become increasingly important in the next decade or so (Belessiotis 1996). Energy efficient and, more importantly, renewable energy technologies offer the means to avoid a trade-off between energy use, environmental pollution and economic growth. Add to this the ever-increasing rate of fossil energy depletion; the need for refocusing on renewable energy sources becomes obvious. Of all the available natural energy resources, solar energy has the second greatest capacity of energy delivery (0.4×10^{14} kW), second only to geothermal energy (capacity 4×10^{17} kW).

Research into the utilisation of solar energy for distillation, demands increased yields of the stills, and / or cheaper construction methods, both of which are aimed at making solar distilled water available at acceptable cost. Consideration must also be given to developing units which are simple, robust, easy to maintain and easy to repair (Ouahes 1987). Mention is made of attempts to combine solar still technology and other solar collectors, thus increasing the yield substantially, but also its complexity (Kumar 1998). The long-term storage of distilled or blended water is also being addressed, as these factors influence the taste and the quality thereof (AA Delyannis 1983).

1.4 Objectives of this study

It is against the above background of the need to provide rural communities in arid regions of South Africa with adequate potable water, the abundance of sunlight in these areas and the potential of solar distillation, that the aims for this study are formulated as follows, namely:

(A) to understand the factors influencing solar still operation and performance;
(B) to identify the factors contributing to the cost of distilled water produced by solar distillation;
(C) to research and economically optimise the above factors in terms of solar still design and performance to reach a distilled water cost of less than R50/m^3, and

(D) to develop a low cost, low maintenance solar still suitable for use by rural communities and households in arid regions of Southern Africa.

1.5 Layout of study tasks

This study was undertaken by carrying out the following tasks:

- A comprehensive literature study on different solar still designs (Chapter 2), the quality of solar distilled water (Chapter 4), and economic factors determining the viability of solar stills (Chapter 12);
- selection, from the literature study, of a solar still design that theoretically suits the research goals of this study best (Chapter 2),
- the theoretical and experimental evaluation of the selected solar still design to quantify performance properties that can be improved (Chapter 3),
- the theoretical and experimental evaluation of the quality of water produced by solar distillation (Chapter 4),
- an experimental investigation into the functional properties of the different construction materials of the selected solar still design, and the identification and evaluation of cheaper replacement materials in order to reduce the manufacturing cost of the solar still (Chapter 5),
- a further theoretical and experimental study into the role of the most important performance factors (solar radiation, solar transmission and radiation absorbance inside the still) (Chapter 6),
- the design and testing of laboratory solar still equipment to study performance improvement factors under controlled conditions (Chapter 7),

- a study into the performance improvement of solar stills using the above-mentioned laboratory equipment combined with the results of Chapter 3 (Chapters 8, 9, 10 and 11),
- determine the economic viability of the selected solar still design by combining the results of the performance improvement study (Chapters 8 to 11) and improved construction costs (Chapter 5), and
- compare the results obtained with the objectives of this study (Section 1.4) (Chapter 13).

An example to illustrate the application of the results of this study are given in an addendum.

CHAPTER 2

LITERATURE OVERVIEW OF DIFFERENT TYPES OF SOLAR STILLS AND THEIR APPLICATION POTENTIAL

2.1 Solar still designs

A literature study of recent publications and patents was undertaken to determine the status of solar distillation technology. Several designs were identified, most being either of the basin or inclined type (Figure 2.1).

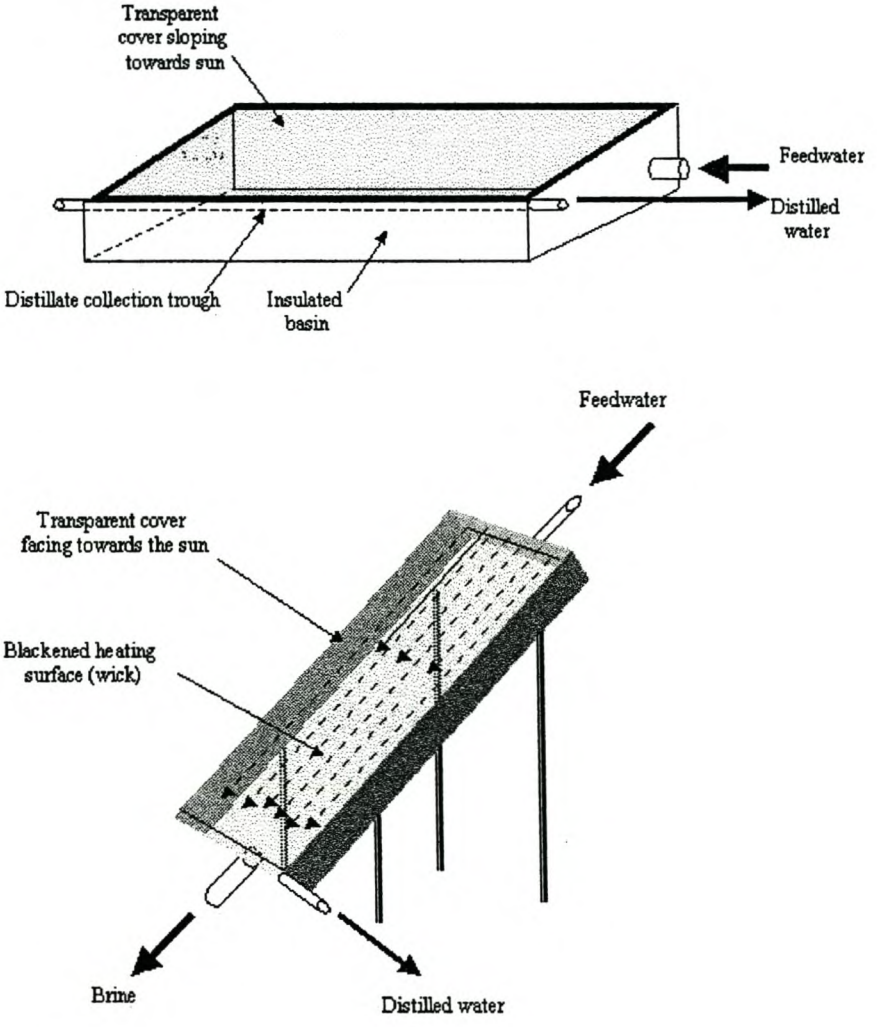

Figure 2.1: Typical basin still (above) and inclined still (below).

Secondary design differences can be related to productivity enhancements, the use of lower cost construction materials and improved ease of operation and maintenance.

2.1.1 Basin solar stills

This is the only solar still design that has been commercialised successfully due to its long operational life and low operating and maintenance costs (Delyannis 1985). All basin-type stills operate on the same principle. Sunlight passes through a transparent cover and through a layer of saline water and is absorbed by the basin. The heat is transmitted to the water and the heated water evaporates and then condenses against the relatively cooler inner surface of the cover. The distilled water flows down the sloped cover and is collected at the base of the slope. This distillate is drained out and collected in a receiving container. Normally these stills have blackened interiors and insulated basin floors to increase heat transfer to the saline water.

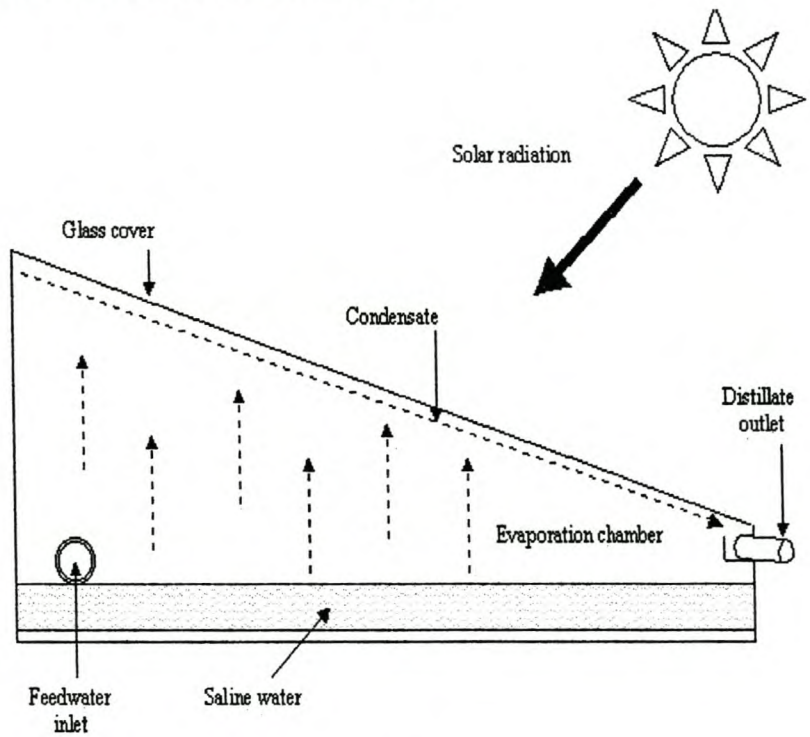

Figure 2.2: Single-slope basin solar still operation.

Another type of basin still commonly used in countries near the equator is the

double-slope basin still, also called the 'greenhouse still' (Figure 2.3). Comparison of the above two configurations of basin stills shows that, given the motion of the sun, in different seasons and locations, maximum radiation may be higher for double-slope stills and their performance may be better (Fath 1998). Single-slope stills have less convection and radiation losses, while the shaded region may be utilised for additional condensation.

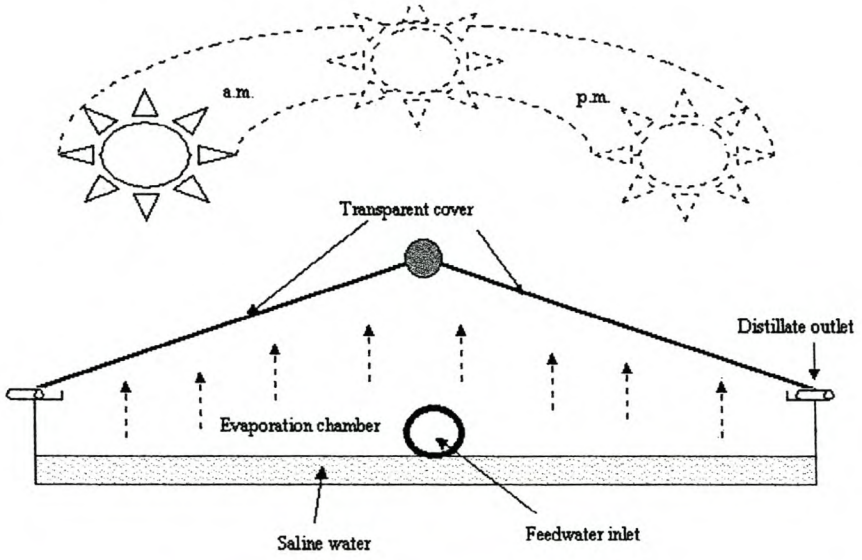

Figure 2.3: Double-sloped basin solar still.

Solar stills suffer inherently from low efficiency, and many aspects of still design are being studied to optimise productivity. Recently, the double effect basin solar still was developed; it re-utilises the latent heat in two or three stages (Figure 2.4, Fath 1998).

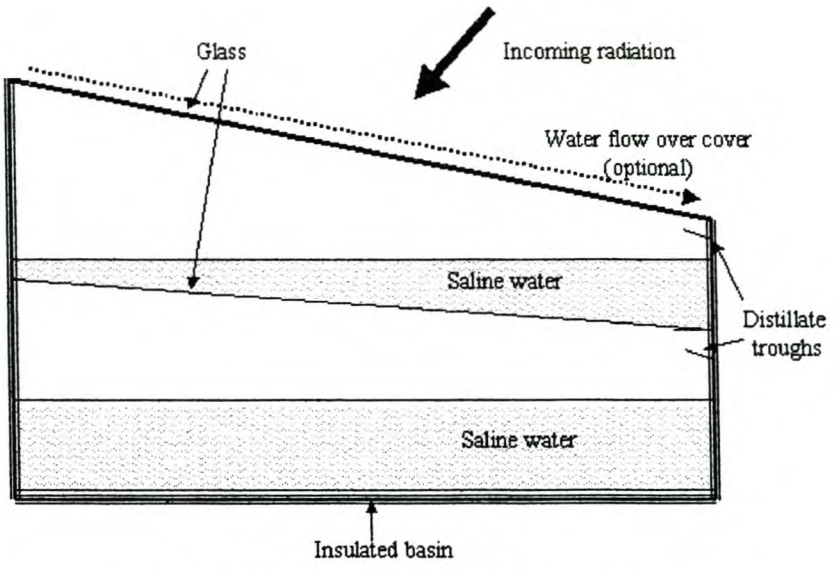

Figure 2.4: Double-effect basin solar still (Fath 1998).

In the double-condensing chamber solar still water vapour is formed in the first chamber when the saline water is heated by solar radiation. Due to pressure differences, the vapour passes to a second chamber through a vent connecting the two chambers. The vapour is then condensed against a metallic surface behind a partition wall as well as on the inner surface of the double glass cover of the solar still (see Figure 2.5).

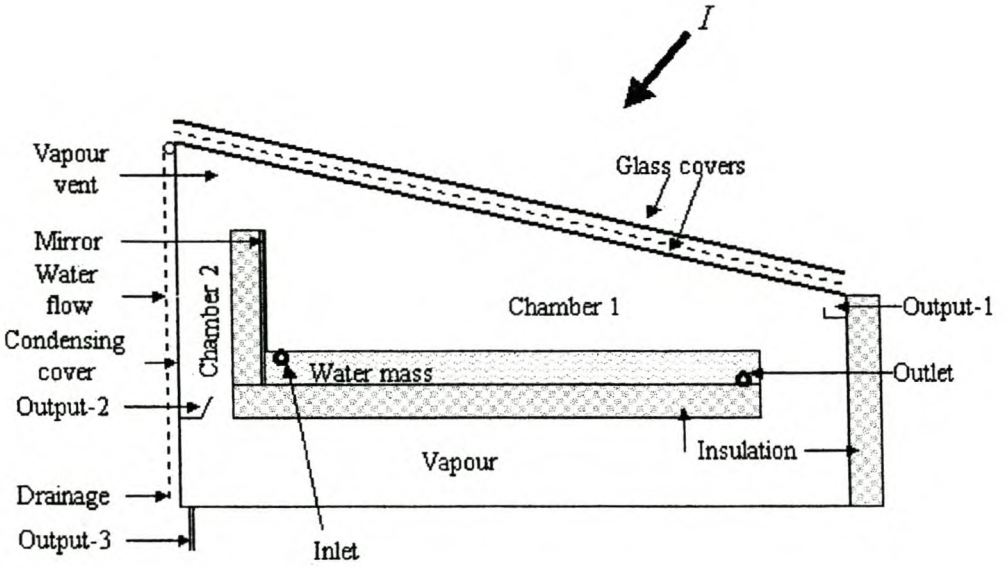

Figure 2.5: Double-condensing solar still (Tiwari 1997).

The use of a passive condenser in the shaded region of a single-sloped basin still to increase efficiency has also been reported (Figure 2.6, Fath 1998).

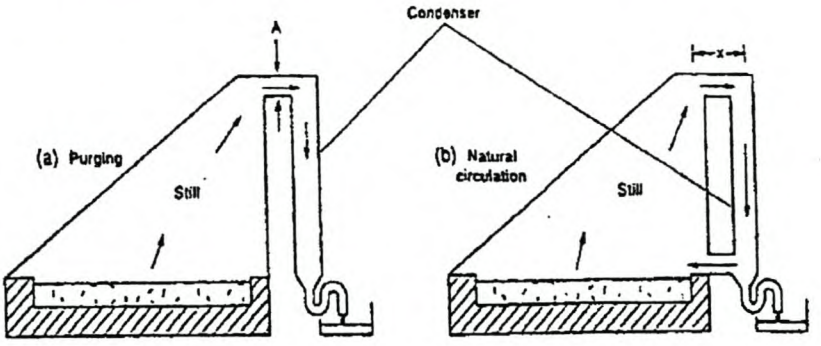

Figure 2.6: Solar still with passive condenser (Fath 1998).

2.1.2 Inclined stills

Inclined stills overcome the drawback of basin stills, namely that the water receives less solar radiation during the winter months (than with tilted stills). The productivity of inclined stills is therefore higher than conventional basin stills because of the smaller thermal capacity of the water moving across the inclination. It was found that an inclined still yielded up to 50% more distilled water when exposed to solar radiation for the same period (Rahim 1995). It was also found that the brine flow rate, the inlet temperature and the insulation are the main factors influencing the efficiency of these types of stills (Gandhidasan 1984).

Non-wick inclined stills were investigated (Rahim 1995). Here water is allowed to be preheated by passing through the gap of the double-glazing cover before entering the main basin of the still. A productivity increase of 1.5 times above the reference single-slope inclined-stepped still was reported after factors such as the distance between evaporation and condensation surfaces, and the number of steps were optimised (see Figure 2.7).

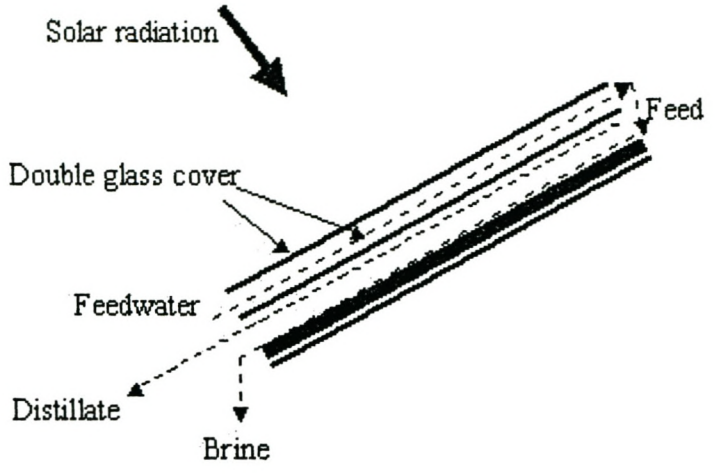

Fig 2.7: Inclined non-wick solar still (Rahim 1995).

Normally, however, inclined stills have wicks through which the saline water passes while being heated. There are single- and double-sloped wick stills, and the application of each is normally influenced by geographical position (distance from the equator). Fig 2.8 illustrates these two still types.

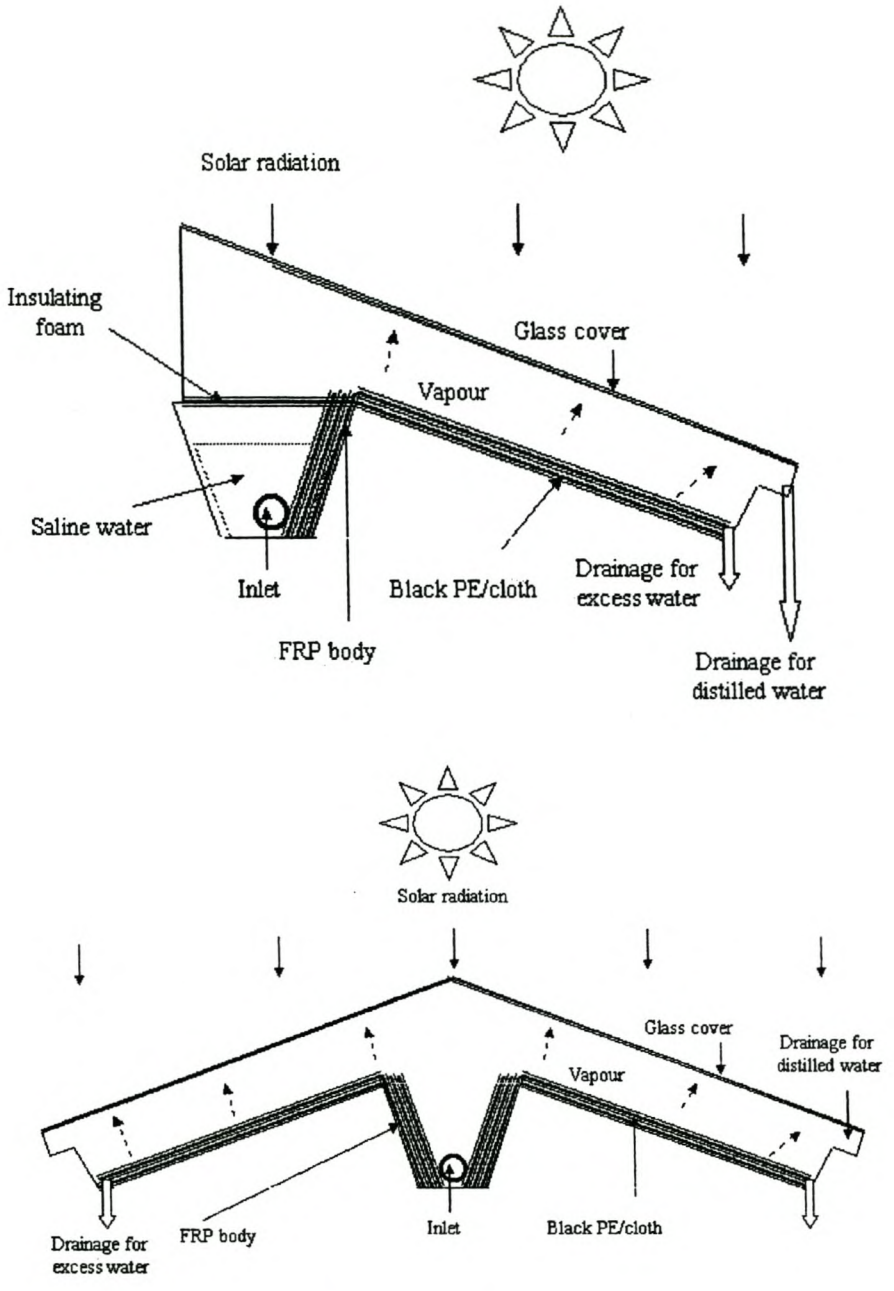

Fig 2.8: Single-sloped inclined wick still (top, Fath 1998) and double-sloped wick still (bottom, Tiwari 1991) (FRP: Fibre-reinforced plastic).

The availability of latent heat of evaporation is maximally exploited through the use of multi-effect inclined wick stills. Productivity increases of up to 10 times compared to a normal basin still are reported (Figure 2.9, Bouchekima 1998).

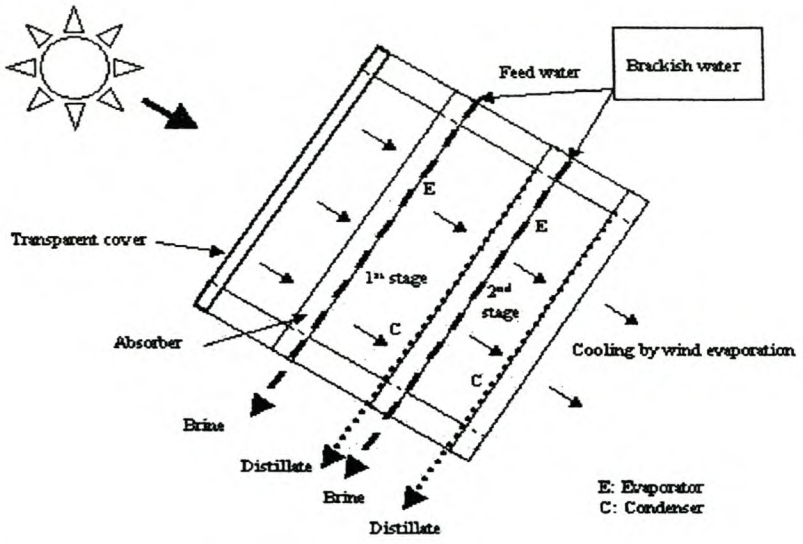

Figure 2.9: Multi-effect, multi-wick inclined solar still (Bouchekima 1998).

2.1.3 Other designs

Other solar still designs include: spherical stills (Dhiman 1988), active stills connected to solar collectors (Yadav 1989) and stills that utilise waste heat channelled through heat exchangers heating feed-water during nocturnal and sunless periods (Yadav 1993).

2.2 Design choice

In order to identify the solar still design(s) most suited for further research into the production of low cost distilled water, certain design comparison criteria were identified through literature and patent studies. These criteria were: (A) the availability and properties of the construction materials, (B) the degree of sophistication of the operational system and (C) still performance.

There is agreement that, generally speaking, solar stills are ineffective and thus their water production is expensive and normally uneconomical. Most research is therefore focussed on ways and means of improving efficiency to produce more water per solar still unit area (C), while less attention is given to capital cost (A) and operational maintenance (B).

The following Table compares the different solar still designs discussed in Section 2.1 on the basis of these three criteria:

Table 2.1: General comparison of different solar still designs
(**A**: *are proper construction materials freely available*, **B**: *is the solar still unsophisticated and easy to operate*, **C**: *has the still design a proven performance track record*)

Solar still type	A	B	C	Limitations
Single-slope, single-effect basin	Yes	Yes	Yes	Low winter productivity
Double-slope, single-effect basin	Yes	Yes	No	For use in equatorial countries
Single-slope, double-effect basin	Yes	No	No	Expensive construction
Single-slope inclined wick	No	No	No	Wick maintenance
Double-sloped wick	No	No	No	Wick maintenance
Inclined multi-effect, multi-wick	No	No	No	Wick maintenance
Active solar stills	Yes	Yes	No	Expensive infrastructure

Table 2.1 provides the motivation for the single-slope basin solar still being chosen for this study:

- It is the only design with reference to commercial use.
- The design is relatively simple and the construction materials freely available.
- The absence of moving and / or replaceable and / or control components in the still favours limited operational and maintenance supervision.
- The design is modular, i.e. it is relatively easy to increase the plant capacity by increasing the number of solar stills.

2.3 Cost of distilled water from a basin solar still

The cost of distilled water has been calculated for various efficiencies and assumed construction and maintenance costs (Figure 2.10).

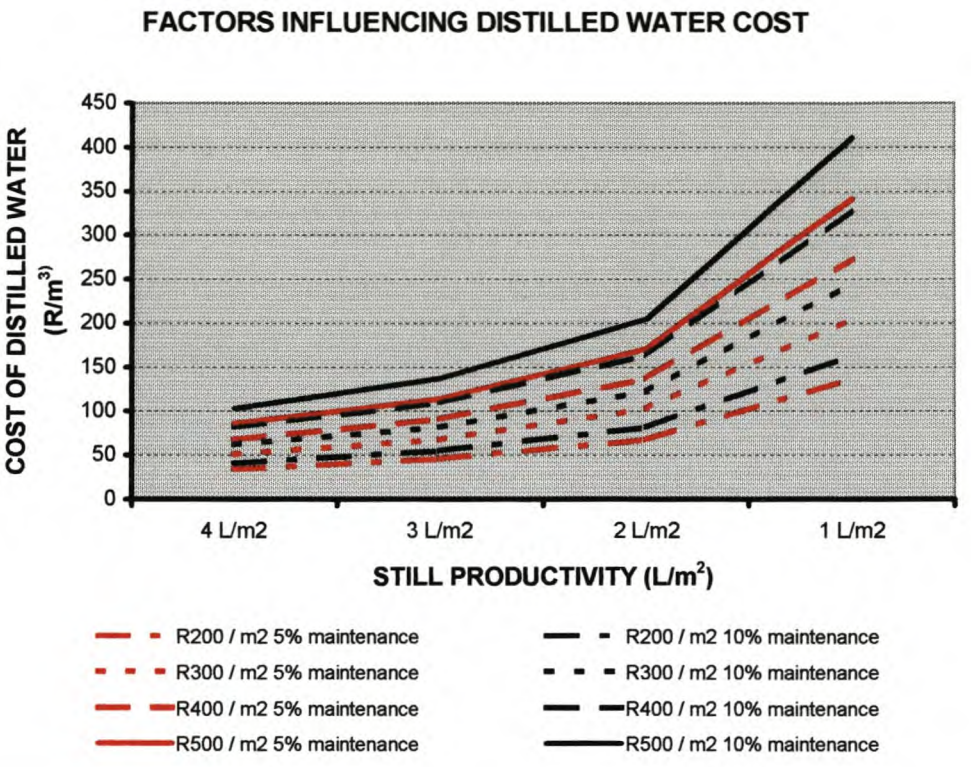

Figure 2.10: Calculated distilled water cost as a function of still construction cost (amortized over five years without interest), maintenance cost (assumed as a percentage of still cost) and productivity (reported on an average daily basis over one year).

From the above Figure it can be seen that reducing the construction cost can be just as cost effective as increasing the productivity. As an example: the cost of producing 1,5 liters per m^2 distillate per day from a still constructed at R200 per m^2 will be the same as that of a still producing about 2,3 the volume but costing 2,5 times as much. As another example: if both the productivity and the capital cost are doubled, the distilled water cost will increase. Increased maintenance will lead to increased running cost, thus increasing the distilled water cost.

2.4 Conclusions drawn from literature study

The following conclusions were reached:

- The conventional basin-type solar stills suffer from some serious drawbacks, one of the important ones being the horizontal surface which intercepts less solar radiation than an inclined solar still does.
- The large volume of water in the basin and the shadows of the walls further limit productivity.
- Further negative characteristics include: the low temperature gradient over the 'condenser' (cover), a decrease in glass transparency due to water droplets forming on the condensing surface, poor wettability of the cover and re-evaporation of the distillate in the collecting troughs.
- Basin stills are generally characterised by low efficiency and low winter production rate, producing little distillate while occupying a wide area.
- Stills coupled to solar collectors show improved efficiency, but have the disadvantage of a further increase in capital costs and often requiring electricity to operate efficiently.
- The productivity of wick stills is always higher than conventional basin stills due to the negligible heat capacity of the water mass in the multi-wick still.
- Main problems associated with wick stills include the maintenance of the wick, the limiting capillary action of the wick around noon on sunny days and wastage of hot water during early and late work hours, damage to the wick due to drying and high investment costs (Ouahes 1987, Dhiman 1988, Toyama 1987, Tiwari 1991). Deposition of salts is problematic where saline water flow through the wick is necessary (Murase 1989).
- In theory, a wick solar still plant can be more economical but, in practice, it was found that a basin still is cheaper to operate because of its simplicity and low maintenance cost (Fath 1998).
- Despite attempts to develop improved stills, the basin still remains the only design that has been commercialised successfully due to its long operational life and low operating and maintenance cost compared to other alternatives.

It was therefore decided to use the normal basin still design as departing point for this study. At the time (1999), the local construction cost of a benchmark low-maintenance overseas design was equivalent to R500/m ^{2}. It was then necessary to determine its distilled water cost in order to determine its position on Figure 2.10.

CHAPTER 3

THEORETICAL AND EXPERIMENTAL PROPERTIES OF THE BASIN SOLAR STILL

3.1 General description

The term 'basin solar still' refers to the definition and description given in Section 2.1.1 and Figure 2.1, i.e. a single-sloped basin solar still, hereafter referred to as the still. The main components of such a still are normally the transparent cover, frame (including distillate trough), insulation, waterproofing (or lining) and piping (for feed water and distillate collection). Figure 3.1 shows these different components of a typical basin still.

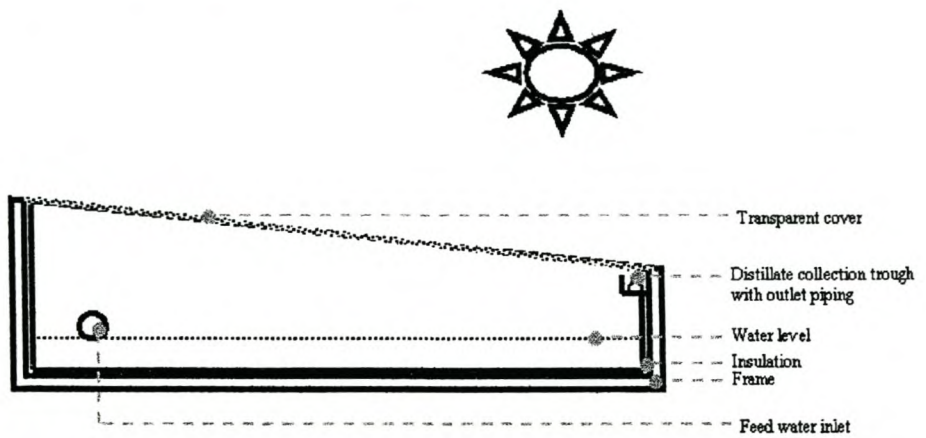

Figure 3.1: Single slope basin solar still.

3.2 Theoretical properties

A literature study was carried out in order to determine the operational mechanisms of the still. Most researchers have approached this subject from a heat flow point of view. The following summary is presented as a basis for further reference.

3.2.1 Basic heat flow

Saline water is supplied to the basin, usually intermittently. Solar radiation is transmitted through the cover and absorbed by the saline water and the solar still basin. The water is heated; thereby increasing its water pressure, and so partial vaporisation into the air begins. The moist air rises to the cover by convection, where it condenses on the cooler underside of the cover. The heat of condensation is conducted through the cover to the surrounding atmosphere, while the partially dehumidified air is convected back to the water surface for further moisture addition. A thin film of condensate flows down the transparent cover into a collection trough situated at the lower edges of the cover.

The incoming solar energy is composed of both direct and diffuse radiation. This radiation is partially reflected by the outer and inner cover surfaces, slightly absorbed in the cover, slightly reflected by the saline water and by the bottom of the basin; the water and the basin bottom absorb the balance. Minor additional reflections can also occur, but are practically ignored. Of the energy absorbed by the basin bottom, a small portion is lost by conduction into the ground or through insulation under the bottom of the still. The balance of the absorbed energy is transferred to the water. The heat loss by the cover to the outside air is necessary to keep the cover cool and so to maintain operation. Radiation from the water surface is either absorbed or transmitted by the cover (depending on its properties). Glass is opaque to long wave (infrared) radiation and completely absorbs that emitted from the water surface (Lof 1961).

The processes of evaporation and condensation take place in narrow layers on top of the water surface and beneath the cover surface respectively. The bulk of the air mass does therefore not participate in these processes, and thus it is advantageous to keep the distance between the cover and the horizontal water plane as small as possible. The larger the temperature difference between the water surface and the cover, the more intense the circulation becomes (AA Delyannis 1981).

Energy transferred to the cover is conducted through it and is dissipated to the

atmosphere by radiation and convection. Some sensible heat may be supplied to the system through the feed water; also, there may be sensible heat loss through the condensate. Mass flow for solar stills involves the quantity of feed water introduced into the still and water leaving the still in the form of distillate, leakages and vapour losses.

Figure 3.2 illustrates the different heat flows in and around the still.

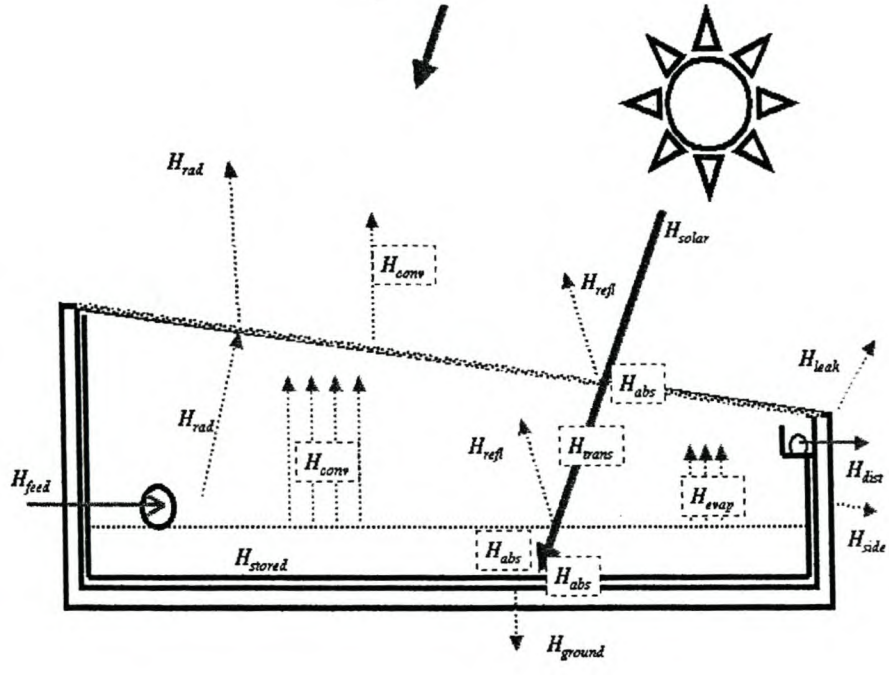

Figure 3.2: Proposed heat flows for basin solar still (Al Kasabi 1981).

According to the above presentation, direct and diffuse solar radiation (H_{solar}) arrive at the still cover. Depending on the characteristics of the cover, the radiation wavelength and the angle of incidence, this energy is transmitted (H_{trans}), reflected (H_{refl}) and absorbed (H_{abs}) by the cover in different ratios. The fraction of transmitted radiation energy H_{trans} passes through the air inside the basin and is again partially reflected off the surface of the saline water. The remainder passes through the water and is absorbed by the water and the lining. Reflection from the lining is also possible. The saline water heats due to the absorbance of the incoming radiation and the heat convected from the basin lining. The water mass loses heat to the air inside

the still through radiation, convection (H_{conv}) and evaporation, as well as through heat loss to the environment through leaks (H_{leak}), the still base (H_{ground}), sidewalls (H_{side}) and the distillate (H_{dist}). Heat loss into and through the cover occur through absorption, convection and radiation.

Figure 3.2 can be represented as follows:

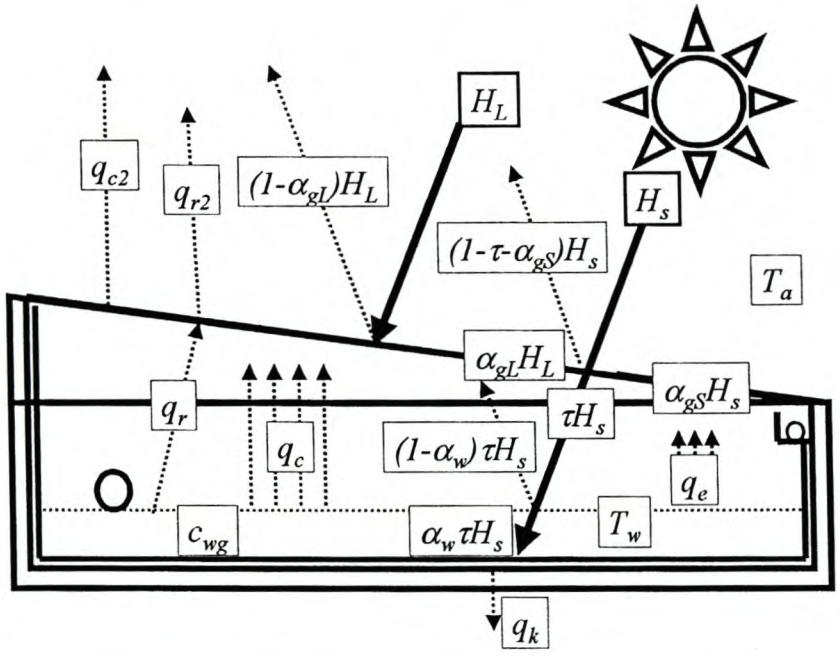

Figure 3.3: Heat flows for basin still according to Dunkle's equations. [H_L , H_S: long / short wavelength solar radiation

$\sigma_{gL}H_L$, $\sigma_{gS}H_s$: fraction of long / short wavelength solar radiation absorbed by glass cover

τH_S: fraction of short wavelength radiation transmitted through glass cover

$\tau\sigma_w H_s$: fraction of short wavelength solar radiation absorbed by the water

$(1 - \sigma_w)\tau H_S$: fraction of solar radiation reflected from water surface

q_e , q_c , q_r , q_k : water heat loss through evaporation / convection / radiation / conduction

q_{c2} , q_{r2} : heat loss through the solar still cover through convection / radiation]

Dunkle's mathematical model for a flat solar still states two important heat balances, namely, over the saline water surface (Still 1991):

$$\tau\sigma_w H_s = q_e + q_c + q_r + q_k$$

and over the cover:

$$q_e + q_c + q_r + \sigma_{gL}H_L + \sigma_{gS}H_s + (1 - \sigma_w)\tau H_S = q_{c2} + q_{r2}$$

The productivity of a still is greatly influenced by the degree of efficiency to which it converts incoming radiation (H_L and H_S) into heat of evaporation inside the still, i.e. q_e, hence T_W, needs to be maximised for increased productivity. These productivity factors are discussed in the following Sections.

3.2.1.1 *Maximising* τH_s

Orientating the still in such a way that cover absorbance and reflectance is at a minimum will increase the radiation intensity inside the still. Arif Ileri (1997) showed that the variation in total transmittance of the cover and the condensate film was negligible for an angle of incidence up to 60 ^{0} for places confined within latitudes 0 ^{0} and 45 ^{0} (glass of varying thicknesses and plastic covers were investigated).

Note: The change in the transmittance of the cover with the incidence angle can be estimated by the following equation by Ileri:

$I = I_o e^{(-kx)}$, where $x = x_o / cos\ I$,

where x = the effective thickness of the cover, x_o = the normal thickness, i = angle of incidence, I and I_o are the transmitted (or τH_S) and the incident (or H_S) radiation (W/m^2) and k = extinction coefficient of the cover (m^{-1}).

Maalej (1991) calculated that the solar energy fraction absorbed by a glass cover amounted to about 15% (versus about 10% by the insulation and 75% by the brackish water and black basin).

H_L will not pass through common types of cover materials.

3.2.1.2 *Cover properties*

The cover should have a low absorbance (high transmittance) over the widest solar radiation spectrum. It was however shown by Maalej (1991) that solar basins with untreated plastic covers often gave markedly reduced output versus

those with glass covers despite plastic cover transmissivity being better - this was due to poorer wettability.

3.2.1.3 *Absorbance in the water / still basin (σ_w)*

Increased energy absorbance of the basin water results in faster heating thereof. Al Kasabi (1981) found that absorbance by the still basin increased from 40% to 57% when the still basin liner is blackened from 0% to 30%. Productivity increases of 70% through the injection of a black dye to the water in basin are reported (El-Hagger 1993). The same research team studied the effect of the addition of charcoal pieces to the still basin. It was observed that a charcoal-lined still is relatively insensitive to basin water depth as long as the charcoal pieces remained uncovered. Productivity increases of up to 68% through the use of such charcoal pieces are reported. Dobrevsky (1983) studied the productivity effect of floating porous black platelets in basin solar stills and found that such particles can enhance the solar distillation process by up to 20%. Bromine and iodine installed in glass containers submerged in the saline water have also been utilized as heat-generating media (Al-Abbasi 1992). With bromine the productivity increase was 65%, while with iodine the increase was 42%.

3.2.1.4 *Insulation*

q_k must be low i.e. the still must be well insulated to minimise conduction losses to the environment. Basin insulation (e.g. through the use of foams) can improve productivity by up to 15% (Maalej 1991). Generally, metallic materials are not suitable for use as insulating materials (Murase 1989).

3.2.1.5 *Heat loss through the cover*

Heat loss through the cover should be maximised. This can be achieved by lowering the cover temperature (multi-effect designs being disregarded). A substantial increase in daily production volume is claimed by US patents 4235679 (Maier) and 4270981 (Stark), where the feed water is circulated through

the cover thus cooling down the cover while simultaneously preheating the feed water. In such a system the cover transmits H_S while (q_{c2} + q_{r2}) is utilised to preheat the feed water.

3.2.1.6 *Convection and radiation losses inside the still*

(q_c + q_r) should be small – this is however difficult to control as it is a function of temperature gradients between the cover and the water. Lof *et al* (1961) showed that the largest single loss was radiation from the basin water to the still cover, varying between 38% (low solar intensity) and 17% (high intensity) and being accompanied by an increase in efficiency from 25% to 41%.

3.2.1.7 *Basin water depth*

Lowering of the water depth in a solar still will improve its performance (Arif Ileri 1997, Fath 1998), as the less water there is to be heated the more heat energy there will be available to apply to evaporation. El-Haggar *et al* (1993) studied the effect of water depth against a reference still and found that a specific still water depth (3 cm) corresponded with the optimum performance. They explained their findings through reference to heat loss from the system, either through the cover (greater water depths) or through the sidewalls (lesser water depths). Tiwari *et al* (1987) found that there was a variation of 30% in daily yield for variation in water depth inside the basin from 1.27 to 30.5 cm, and that this variation was dependant on the initial water temperature and heat transfer coefficient.

3.2.2 Solar radiation and productivity

It is important to know the value of solar radiation during the operation of a solar still as it provides a tool for detecting malfunction. Unlike most other desalination plants, malfunction does not necessarily lead to plant shutdown but rather in reduction of output below its optimum value. Diurnal solar radiation (R) used in efficiency calculations is most accurately measured by means of a calibrated pyranometer. A pyranometer measures radiation from the sun as well

as from the hemispherical space above the instrument. A pyrheliometer measures radiation from the sun alone, and is therefore not used in the calculation of solar still efficiency, as diffuse radiation is (theoretically) not measured. The productivity of a solar still expresses the amount of distillate produced per unit area of water surface.

Lof (1961) reported a near linear relationship between radiation intensity and distillate production (see Figure 3.4). Major short-term influences due to ambient air temperature and wind velocity disappear when long-term averages are used in productivity calculations.

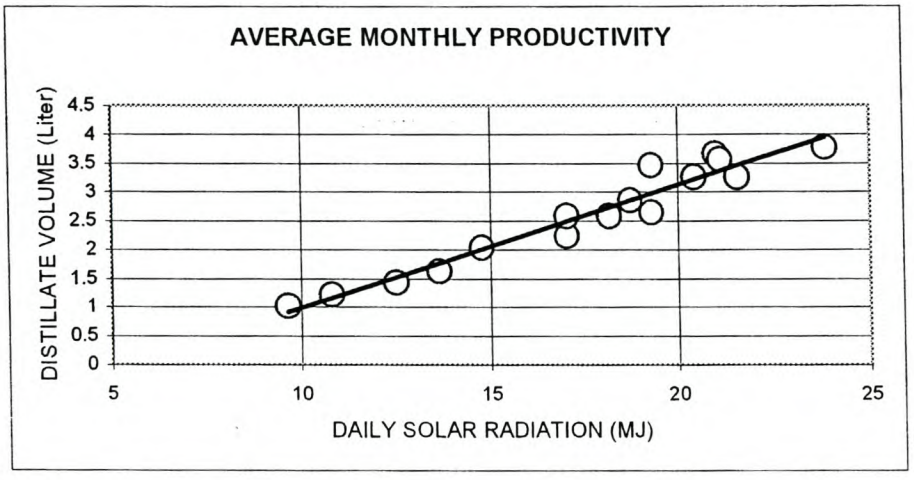

Figure 3.4: Radiation intensity versus distillate production (Lof 1961).

Howe (1986) plotted actual performance data for a basin solar still (see Figure 3.5). As can be expected, data points on cloudy days were scattered, but those for clear days defined a single line:

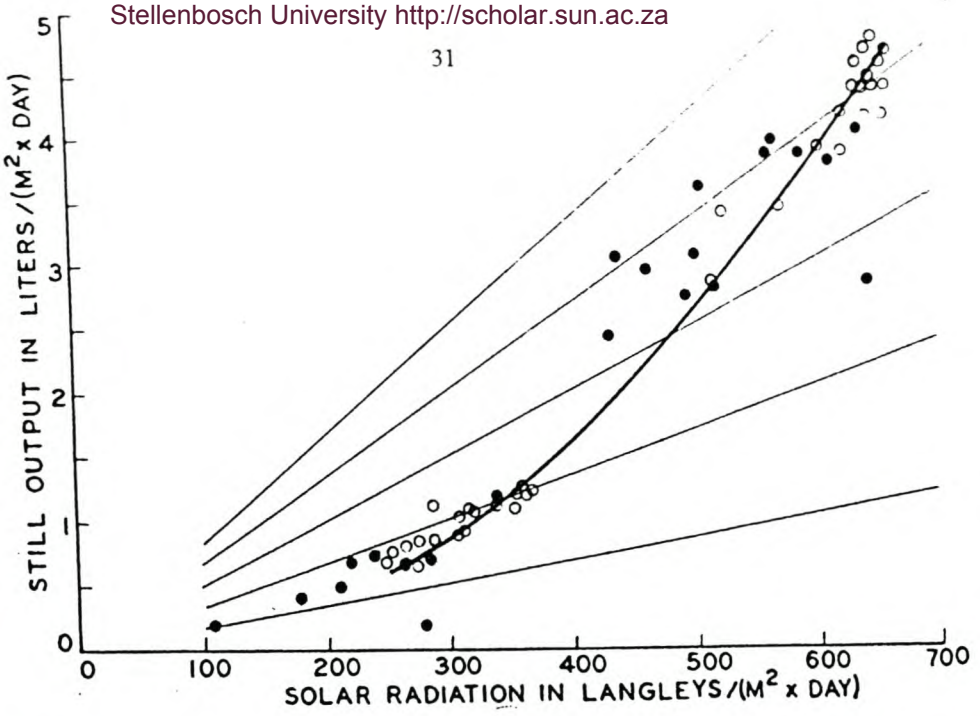

Figure 3.5: Production rate of a basin solar still, latitude 37.6 ° N (circles: clear weather, dots: cloudy skies) (Howe 1986).

The algebraic equation which best fitted the line on the above graph can be represented by the exponential equation: $P = 0.4137\ (R/100)^{2.04}$, where P is the production rate (L/m^2d) and R is the diurnal radiation on a horizontal surface (kJ/m^2d). Madani *et al* (1989) developed the following equation: $D = 1.18\ X\ 10^{-4}.\ I^{1.64}$, where D is the yield (L/m^2) and I is the daily average solar intensity (W/m^2). This relation presented the data within 17%.

Arif Ileri (1997) investigated relationships between daily output of a solar still and solar radiation and found that distillate production would only begin once a certain threshold value for solar radiation had been reached (different values for different types of basin stills). Below this value, heat loss through conduction, convection and radiation exceed the energy absorbed through solar radiation. This happens during the first hours after sunrise, while fresh water production continues a few hours after sunset due to the energy stored in the water within the still. Belessiotis (1995) plotted the productivity behaviour of a basin solar still as follows (simplified and reproduced as Figure 3.6):

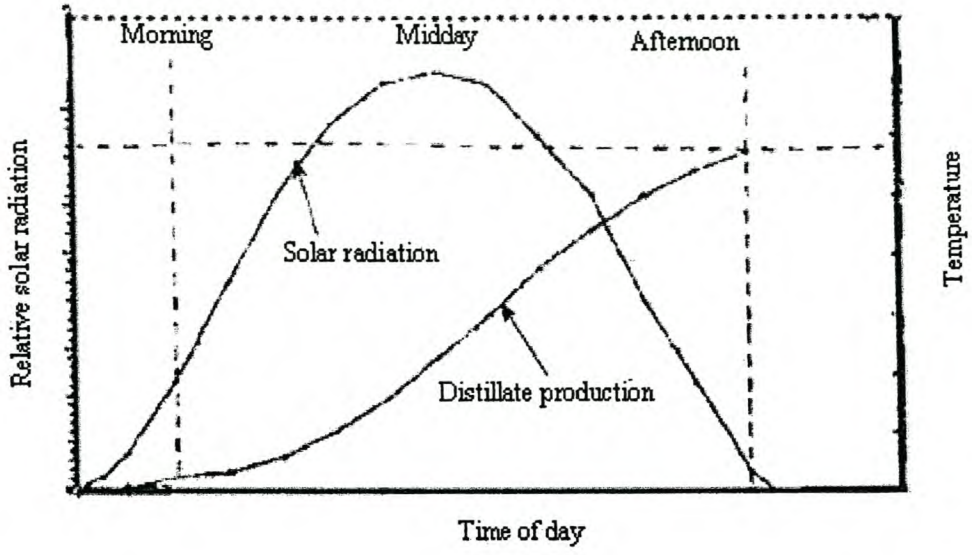

Figure 3.6: Typical productivity behaviour of a solar still (from Belessiotis 1995).

3.2.3 Efficiency

The efficiency of a solar still (η) is the amount of energy utilised for water evaporation divided by the amount of incident solar radiation energy, normally expressed as a percentage. The operating efficiency of a solar still increases exponentially with increasing basin water temperature, but unfortunately heat loss increase in the same way. Thus single-effect solar stills have the serious disadvantage of low efficiency. Under extreme favourable solar radiation and design conditions, efficiencies up to only 50% are reported (Maalej 1991).

Efficiency calculations provide real relative performance comparison information, they represent the ability of a still to distill water according to the input radiation energy. It is expressed as a percentage, and can be calculated as follows: $\eta = (m_e.h_w)/H_s$ (dimensionless, where h_w is the heat of evaporation of water at the feed temperature, m_e is the mass of water evaporated and H_s is the radiation on the horizontal water surface). For given values of h_w, lines of constant efficiency will be straight and passing through the origin (see Figure 3.5). These lines intersect the clear-day performance curve and indicate that the

solar still operates with increasing efficiency as the solar radiation increases. The average temperature of the water in the still basin increases with the radiation intensity and produces an exponential increase in the vapour pressure within the enclosure. The higher pressure is accompanied by more evaporation per unit of heat input, thereby increasing the efficiency.

The amount of heat required to increase the water temperature to the temperature of vapour formation plus the heat needed for vapour formation is given by in the above equation. Arif Ileri (1997) used this equation to calculate efficiencies for a set of different basin stills. The value h_w was assumed to be 2.43 MJ/kg. One of his interesting findings was that increasing the glass thickness lowered the efficiency much more than the change in transmittance alone implies (e.g. 15.5% efficiency loss versus 6.1% transmittance loss).

3.3 Experimental properties of locally-built basin solar still

A number of basin stills were built locally for evaluation purposes. In order to facilitate future data comparison, the chosen design was similar in general dimensions to the only commercial basin solar still that was available at the time (designs were obtained from Mr H McCracken in the USA). The stills had marine plywood frames, 20 mm polyurethane insulation and glass covers of varying thicknesses with silicone sealant waterproofing and linings. The horizontal basin area was typically 1,6 m^2. The sloped angle of the glass cover was 3 °. Figure 3.7 shows a picture of one such still.

These stills were used to formulate an understanding of the numerous parameters that influence the performance of such stills, i.e. construction materials, basin dimensions, geographical position of application, prevailing climate, aspects of solar radiation, productivity, efficiency and operating temperature. This was needed as reference data to set up and execute in-house experimental investigations to improve still productivity (see Chapters 7 to 12).

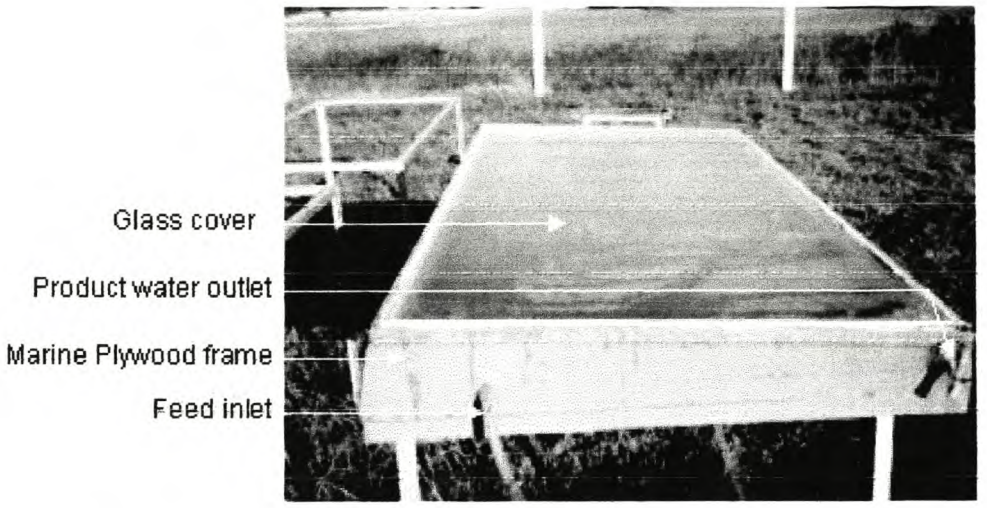

Figure 3.7: Experimental solar still constructed locally.

3.3.1 Geographical position, climate and aspects of solar radiation

The evaluation of the locally manufactured solar stills was carried out at the University of Stellenbosch in the Western Cape Province of South Africa, which has the geographical position longitude 18 ° 50' E and latitude 33 ° 58 ' S. The region has a Mediterranean winter rainfall climate with mild winters and hot summers. The test site itself has an open sky view, apart from early morning interference from nearby buildings on the eastern horizon.

The stills were positioned with the sloped cover facing north i.e. along the E/W axis. Figure 3.8 shows the monthly angle of maximum solar radiation incidence at the test site on a horizontal surface and on the still cover. Figure 3.9 shows maximum-recorded radiation values for the test site recorded over the one-year test period. Figure 3.10 shows the % transmittance of the window glass cover for different angles of incidence as measured at 600 nm wavelength.

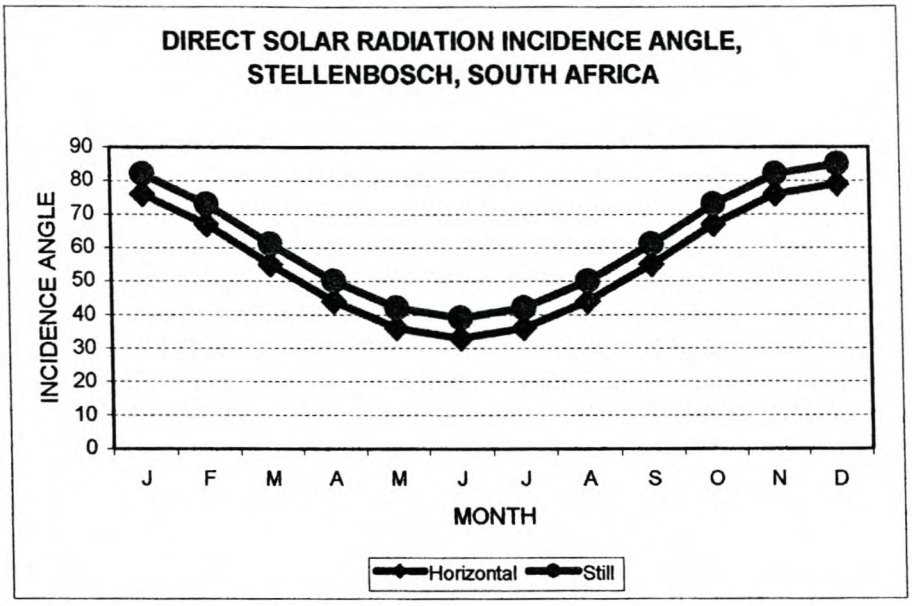

Figure 3.8: Solar radiation incidence angle at Stellenbosch test site.

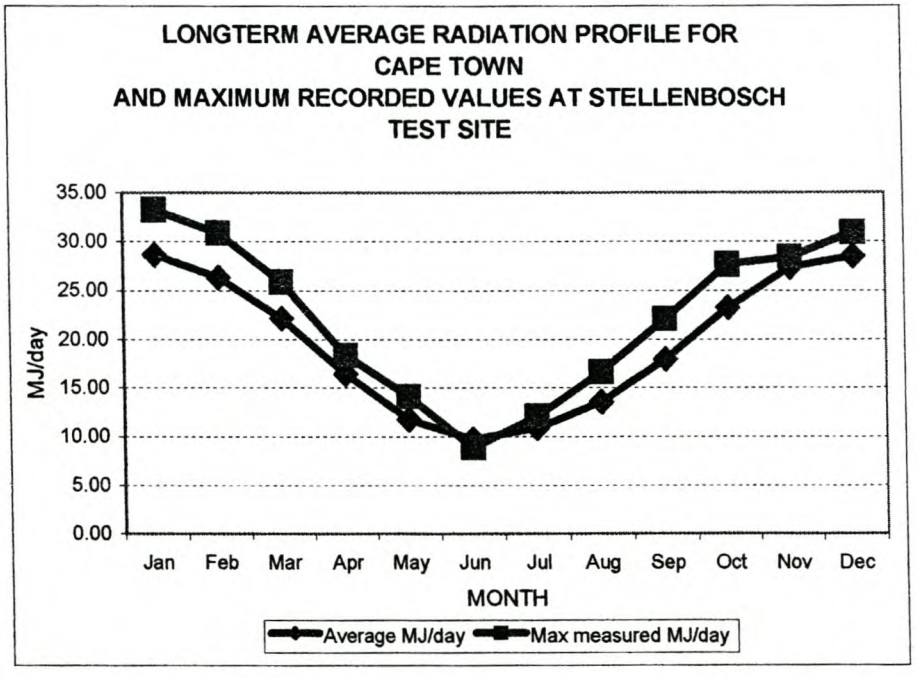

Figure 3.9: Radiation profiles for Cape Town (long term average) and Stellenbosch test site (recorded monthly maximum over test period) (Cape Town and Stellenbosch are located within 50 km of each other).

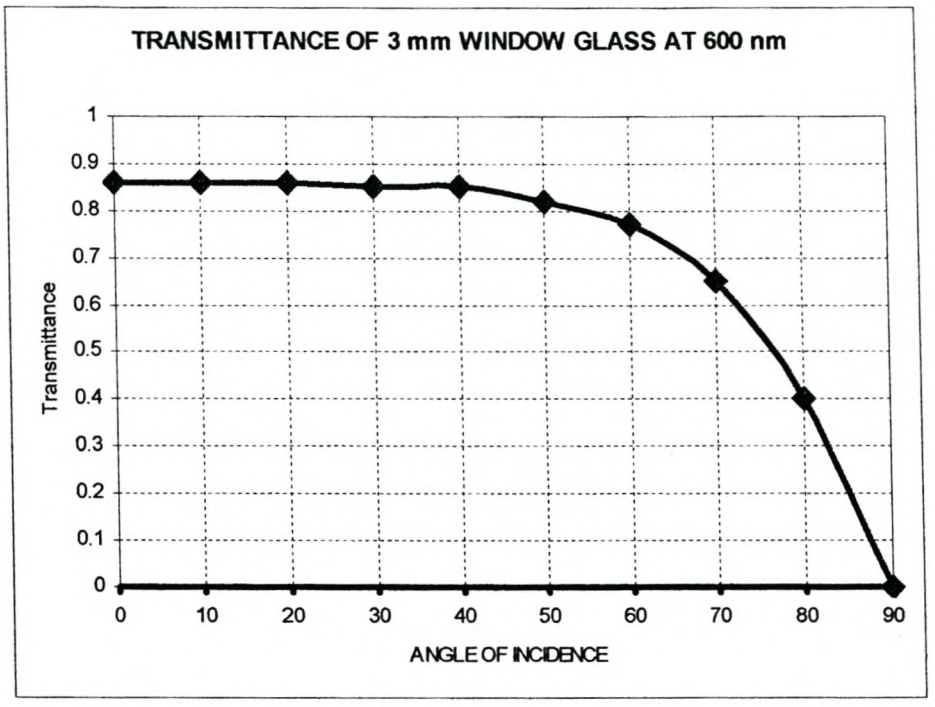

Figure 3.10: Transmittance of glass cover of locally built solar still.

3.3.2 Productivity

The daily output of one still was monitored intermittently over the period October 1999 to September 2000. This was carried out by collecting the distillate in a calibrated container. Figure 3.11 shows the productivity of the still over the entire test period, while Figure 3.12 shows the productivity on selected cloudless days.

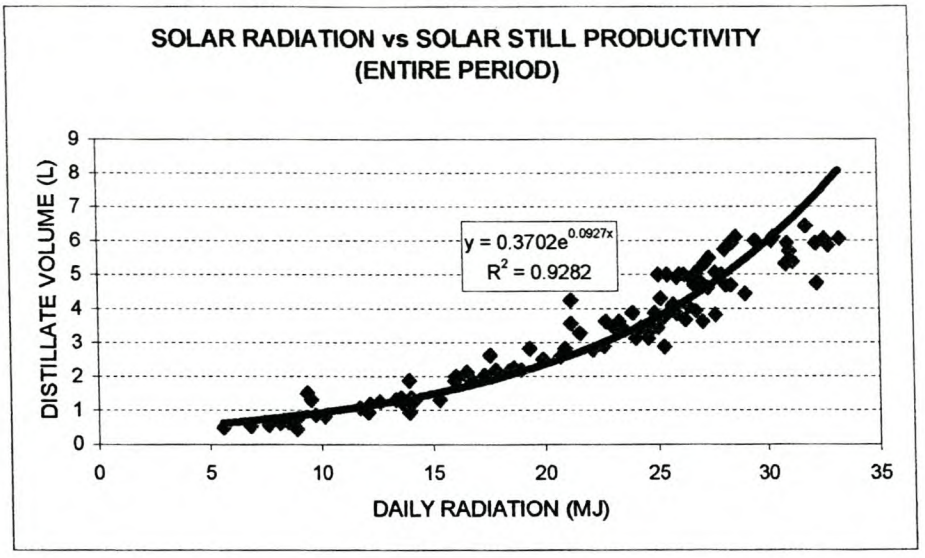

Figure 3.11: Production rate of experimental solar still.

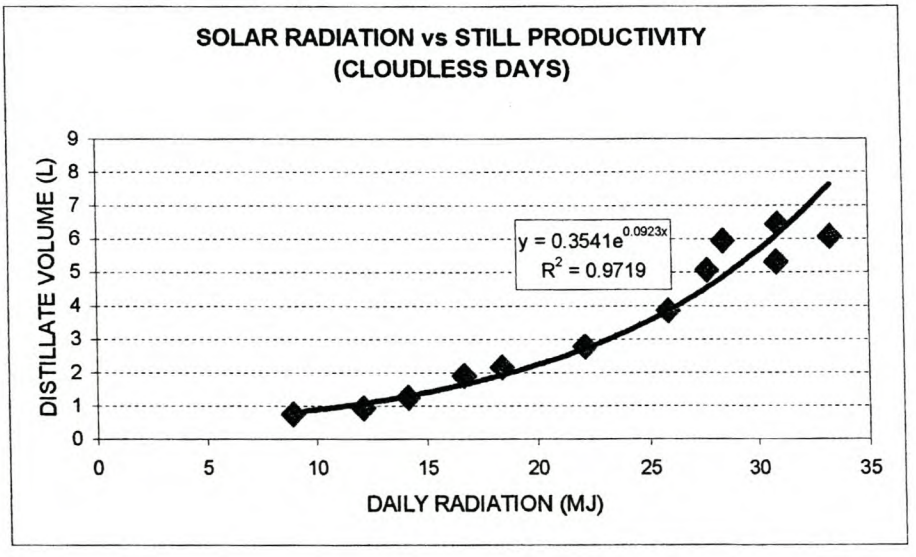

Figure 3.12: Production rate of experimental solar still on cloudless days.

Exponential equations best fit the data of both Figures 3.11 and 3.12, with the productivity of the still being best described by the exponential equation:

$$P = 0.3451e^{0.0923R} \quad \text{--------} \quad 3.1$$

where P is the production rate (L/m ^{2}.d) and R is the total daily solar radiation (MJ). When the values obtained from Equation 3.1 are compared with those of

Howe and Madani (Section 3.2.2), it can be seen that the correlation is good, especially with higher solar radiation intensities (see Figure 3.13). Equation 3.1 will therefore be used in the following Sections and chapters to predict the productivity of similar stills in the same environment.

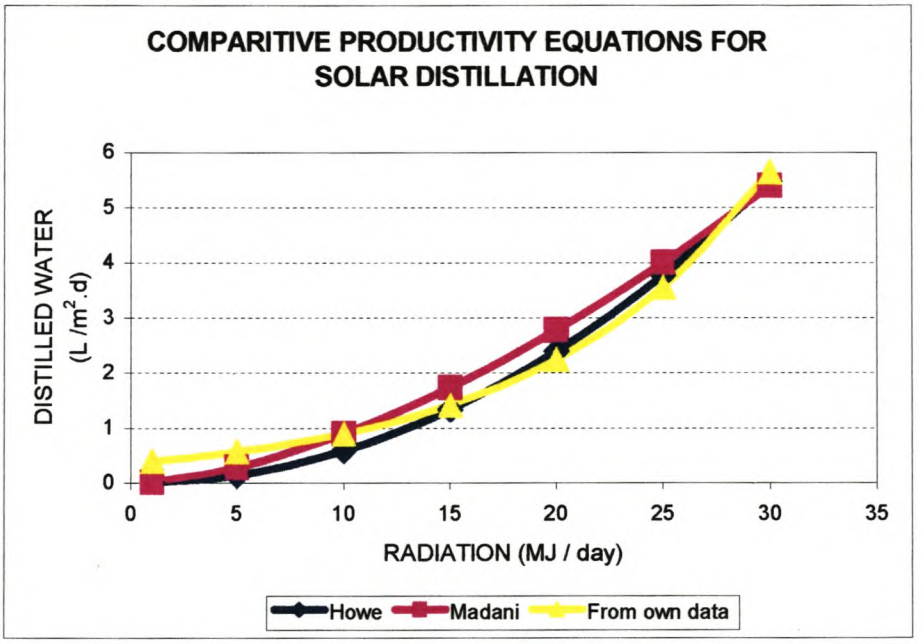

Figure 3.13: Comparative equations for solar still productivities (Howe – reference, Madani - reference and author's own data).

3.3.3 Efficiency

The average monthly efficiencies of the solar still presented in Figure 3.11 were calculated using the equation $\eta = (m_e.h_w)/H_s$ given in Section 3.2.3, and are presented in Figure 3.14.

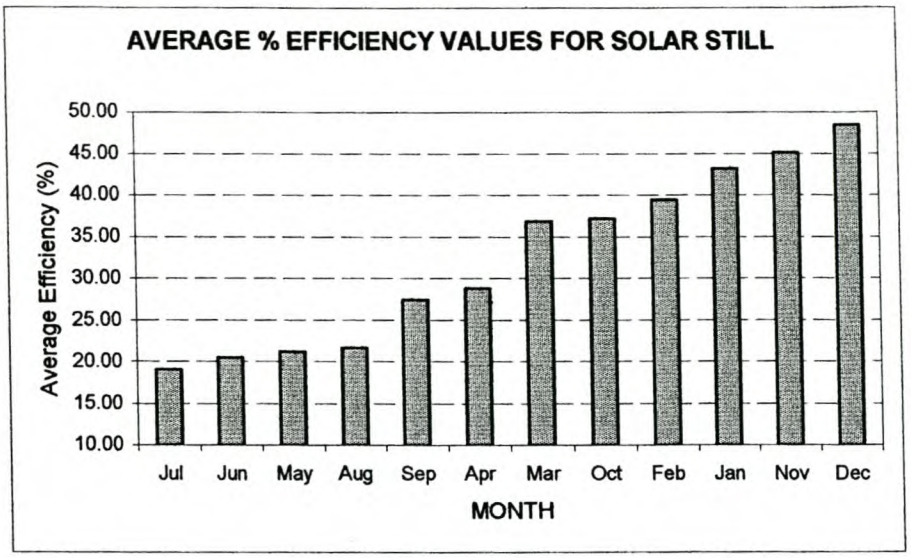

Figure 3.14: Efficiency values for experimental solar still.

When the efficiency / radiation graph is studied (Figure 3.15), it confirms that, for these specific still designs, increased solar radiation leads to improved efficiencies. It also exposes their inherent economic drawback, namely, their seasonal changes in efficiency, i.e. more than 50% lower efficiency during the winter months than during summer.

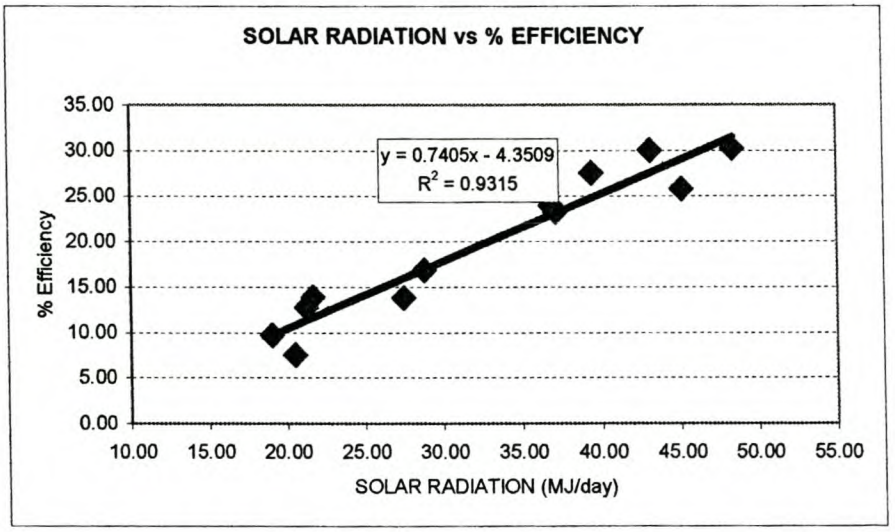

Figure 3.15: Efficiency versus solar radiation profile for experimental solar still.

Apart from there being fewer sunshine hours during winter, there is also a reduction in direct solar radiation transmitted through the glass cover due to the

change in the inclination angle of direct solar radiation. (Diffuse component of global radiation for the Cape Town area is being accepted as being between 15% and 25% of the global radiation (Still 1991)). From Figure 3.10 it can be seen that with 3-mm window glass, at inclination angles of more than 60 ° relative to the vertical, the % transmission falls below 80%. Figure 3.16 presents the maximum number of direct radiation hours recorded on the 21st of each month as well as the maximum number of hours when more than 80% of direct solar radiation will reach the still basin, assuming a two-dimensional sun trajectory relative to the cover.

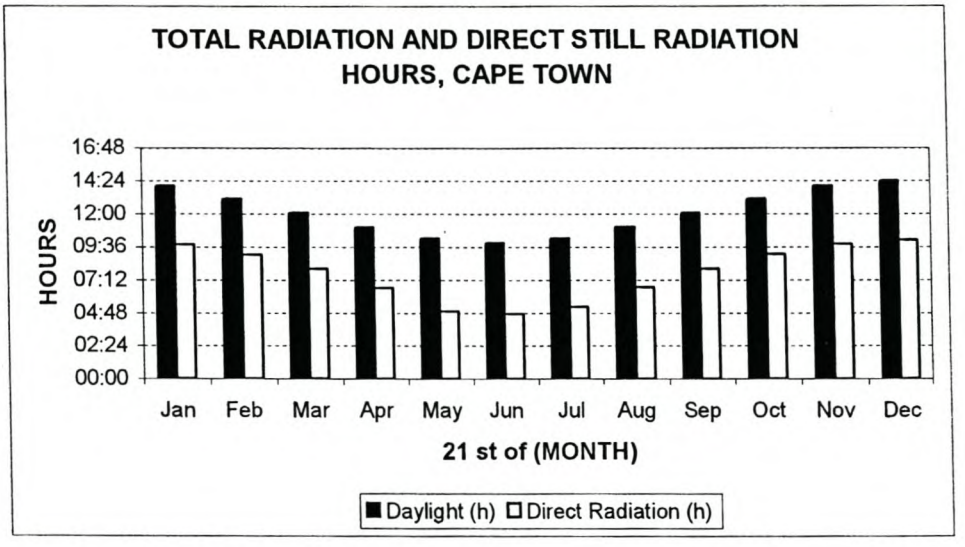

Figure 3.16: Total direct radiation and direct basin radiation hours.

Exponential equations are found when the radiation periods are plotted against average monthly efficiencies (Figure 3.17).

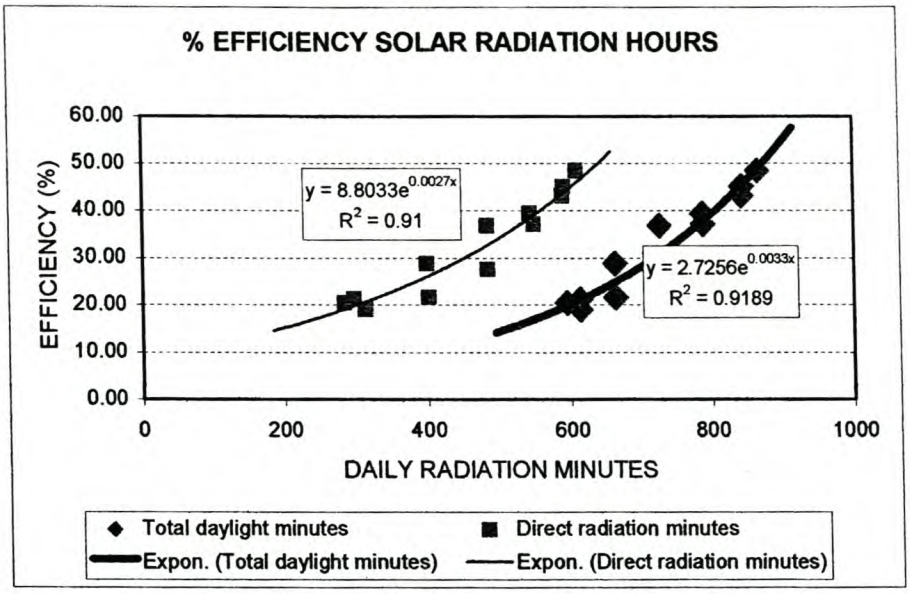

Figure 3.17: Correlation between average monthly efficiency and global and direct radiation hours.

From Figure 3.17 it can be seen that nearly the same efficiency value will be obtained irrespective whether the total direct radiation equation or the direct basin radiation formula is applied. Since it is easy to obtain the time between sunrise and sunset, the equation:

$$\eta\,(\%) = 2.7256\, e^{\,0.0033\, t} \text{ ------- } 3.2,$$

together with equation 3.1 of Section 3.3.2, provide helpful means of making first-order predictions of the performance of the experimental solar stills. Table 3.1 shows the correlation of calculations carried out on randomly chosen days using these equations versus values calculated from actual measurements. Both equations can be used to predict a solar still's performance in a 'calibrated' environment and reasonable predictions of water production can be made. For example, by using equation 3.2 the calculated efficiency for the period 1 to 20 October 2000 (with 755 daylight hours) was 32.3%. Calculations based on actual average values were 31.5% (within 2%). The average daily radiation over the period was 22.59 MJ/day and the average daily water production was 4826 mL. The calculated daily production is 4438 (-8%). Although these equations still do not provide very accurate results, the results are within the same margin of error

as those obtained using much more complicated simulation calculations (Tiwari 1998).

Table 3.1: Correlation between actual and calculated values for productivity (*P)* and efficiency (η) *of* a single solar still

DATE	P mL / still / day (measured)	P mL / still / day (calculated)	P % difference	% EFFICIENCY (actual values)	% EFFICIENCY (Calculated)	% difference
20-10-99	8000	5779	-28	47.8	36.5	-11.33
2-11-99	7400	6861	-7	41.2	39.7	-1.46
3-12-99	9600	8390	-13	29.48	46.1	16.62
25-1-00	9600	7615	-21	51.33	43.0	-8.32
13-2-00	7900	6013	-24	46.42	38.6	-7.85
8-3-00	6600	5930	-10	39	32.7	-6.29
11-4-00	3450	3015	-13	28.52	25.9	-2.64
7-5-00	2050	2040	0,5	21.98	22.0	0.03
25-6-00	1015	1251	23	18.17	19.4	1.18
26-7-00	1300	1405	8	18.86	21.1	2.23
18-8-00	1500	2001	33	16.34	23.8	7.49
22-9-00	4450	4246	-5	30.61	30.1	-0.49
		Ave:	-5		Ave:	-0.90

From equations 3.1 and 3.2, as well as from similar characterisation attempts made by other researchers (Madani 1989, Delyannis 1981), the following conclusions can be made for the specific basin still design:

- Productivity will increase exponentially as solar radiation increases, irrespective of season;
- Efficiency will increase linearly as solar radiation increases;
- Efficiency will increase exponentially as the duration of solar radiation increases i.e. seasonal influences are significant;
- The above implies that, during the summer months, not only productivity but also efficiency will be significantly higher than during winter, i.e. the efficiency of a solar still is a seasonal characteristic and can only be used to compare stills under similar environmental conditions;
- It is also clear that comparative experimental evaluations to increase productivity (in order to lower distilled water cost) will have to be carried out under identical

test conditions. This means either parallel field characterisation of a number of test stills or in-house testing under controlled conditions. The latter option is preferred due to the more reproducible test environment. The results are discussed in Chapters 7 to 11.

3.3.4 Temperature profiles inside the still

The temperature profiles inside a test still were recorded over 24-hour intervals at a data collection rate of 15 minutes in order to have a reference framework for further in-house characterisation. Calibrated thermocouples coupled to a datalogger were used to measure temperatures at positions above the basin floor indicated in Figure 3.18. Figures 3.19 and 3.20 show temperature profiles on a cloud-free day and an overcast day respectively.

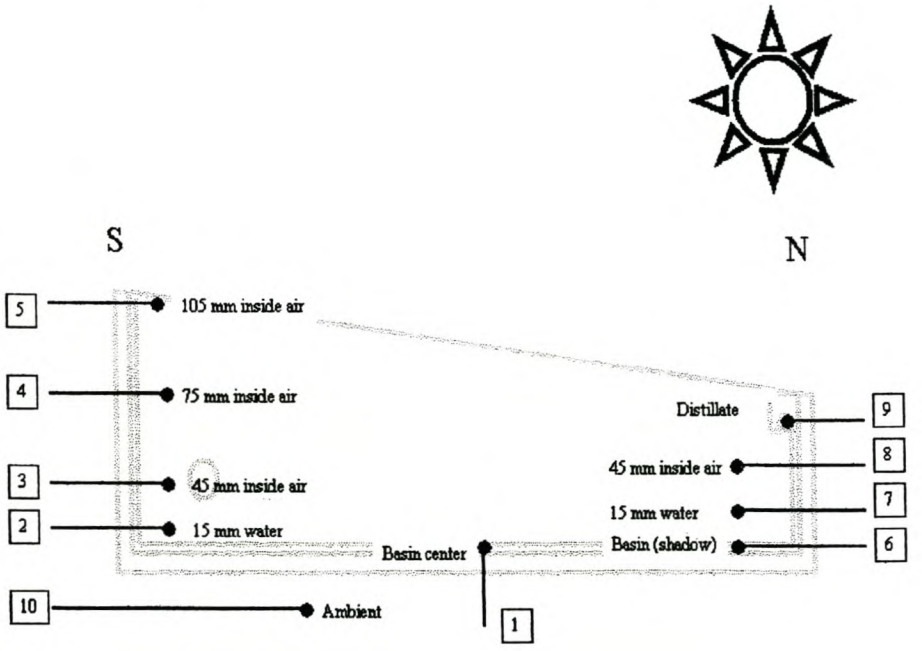

Figure 3.18: Positions of thermocouples inside solar still.

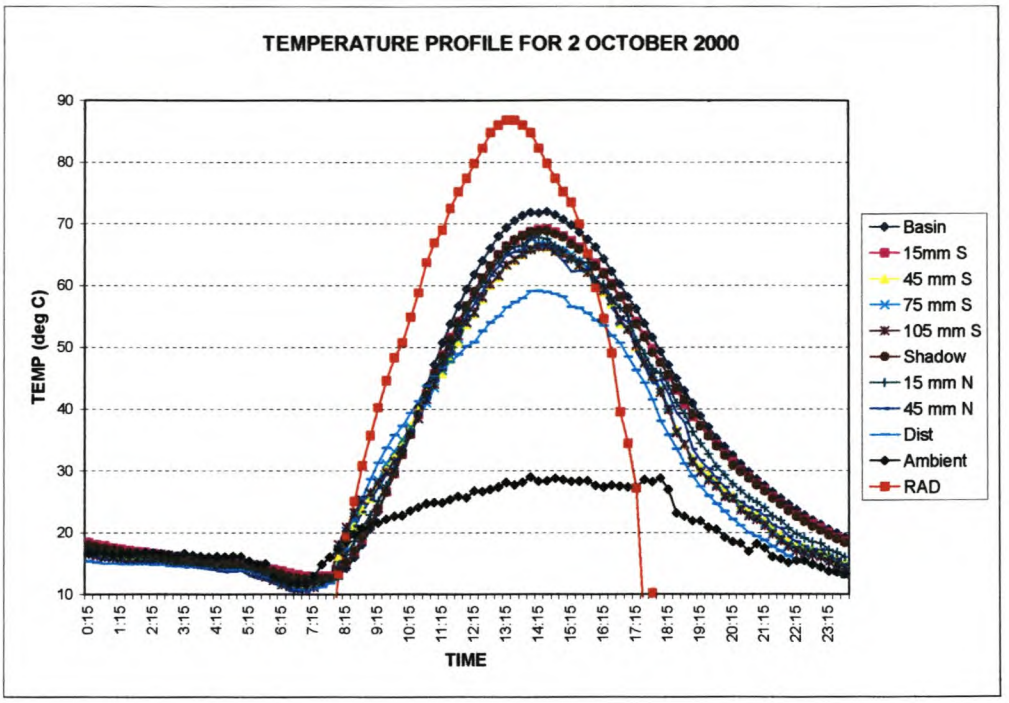

Figure 3.19: Temperature profiles inside solar still on a cloudless day. The relative global radiation profile over the same period is also shown (RAD).

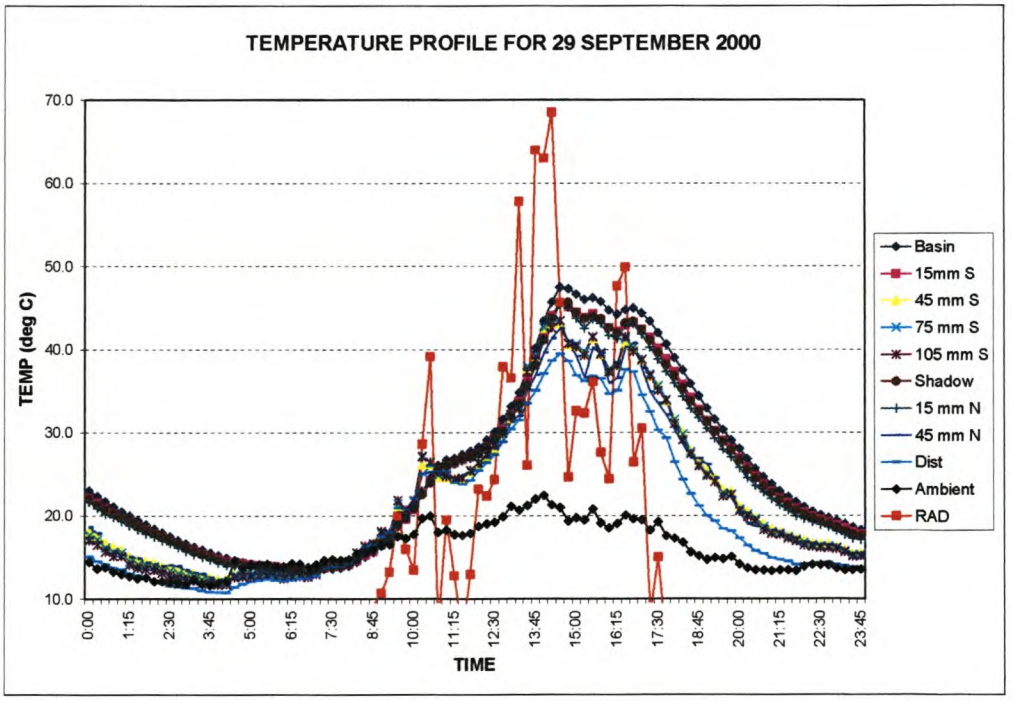

Figure 3.20: Temperature profiles inside solar still on a cloudy day. The relative global radiation profile over the same period is also shown (RAD).

These thermal profiles are in agreement with Figure 3.7. It can be seen that the maximum still temperatures lag the solar radiation peak by approximately one hour. Better insight into the heating behaviour can be obtained when analysing the thermal profiles of Figure 3.19 during early morning (Figure 3.21), over midday (Figure 3.22) and late afternoon (Figure 3.23). Radiation was measured using a solar cell behind 3 mm window glass.

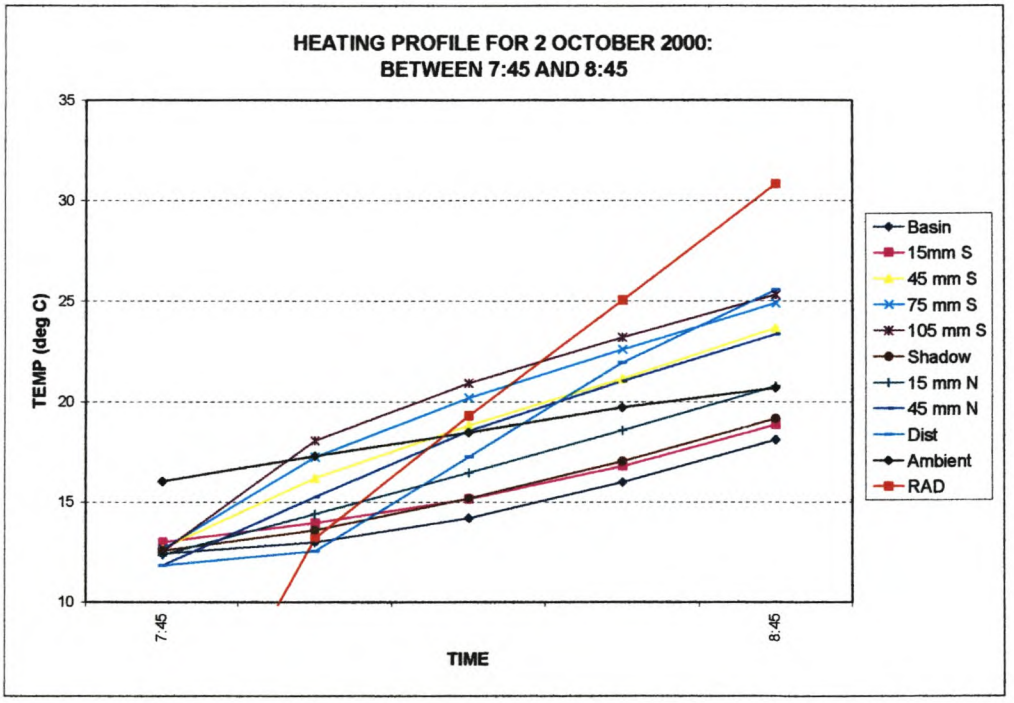

Figure 3.21: Heating profile of test still during early morning.

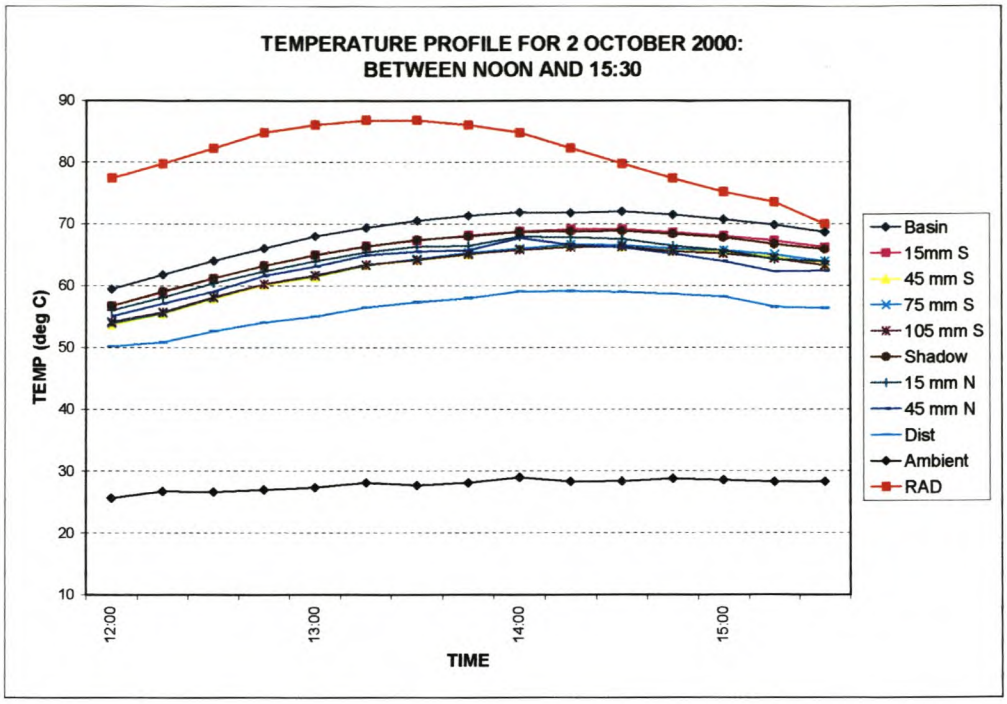

Figure 3.22: Thermal profile of test still over noon.

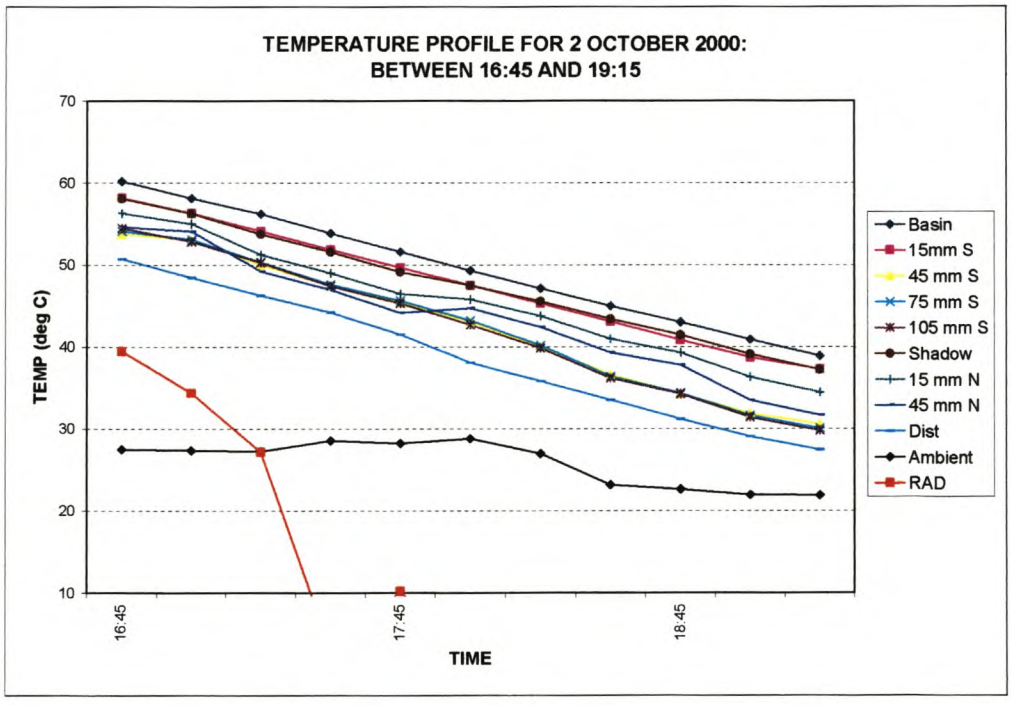

Figure 3.23: Cooling profile of solar still.

From the above three Figures it is now possible to characterise the typical

heating and cooling behaviour of a still on a cloudless day (2 October 2000). Figure 3.24 summarises this thermal behaviour of the experimental still. A good correlation with the results obtained by Belessiotis (Figure 3.6) can be seen.

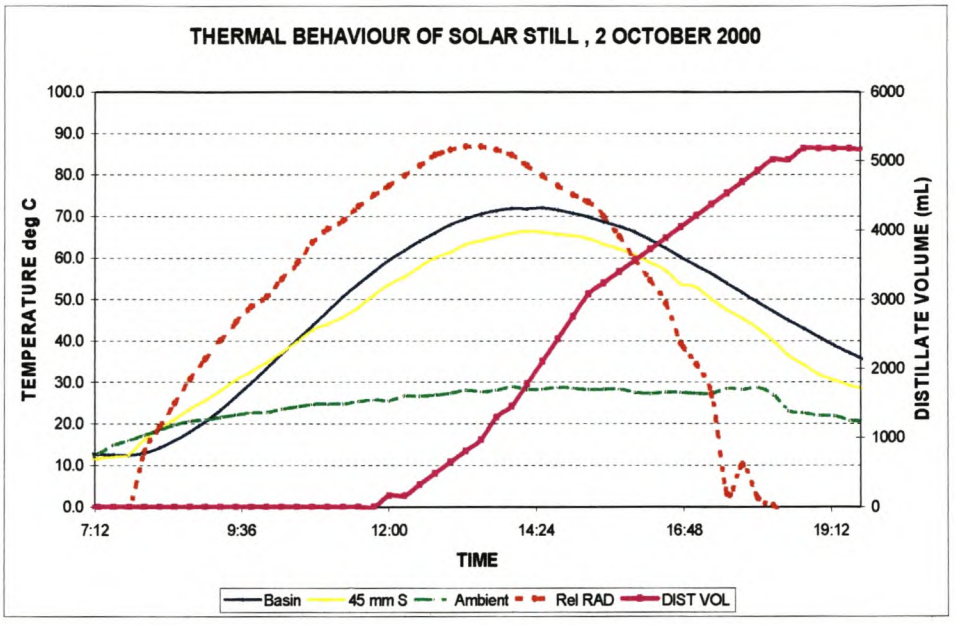

Figure 3.24: Thermal and distillation behaviour of experimental test still.

The above Figure shows that the maximum rate of distillation coincides with the peaks in internal and ambient temperatures (dotted line). Figure 3.25 shows the distillation rate relative to the solar energy distribution on a clear day.

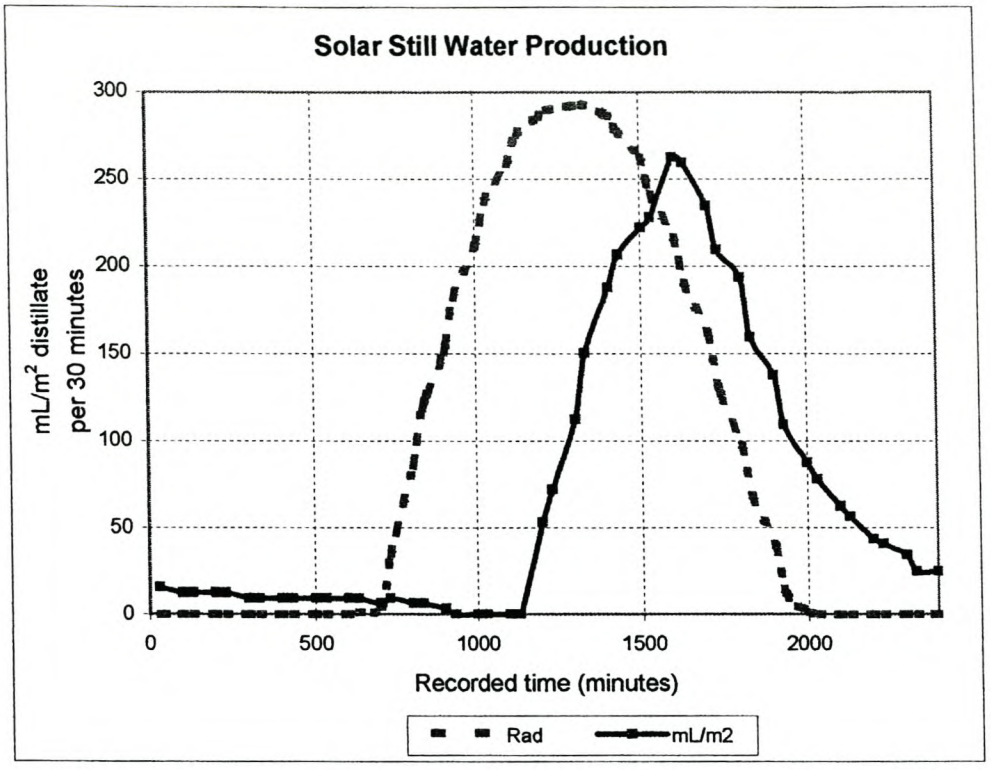

Figure 3.25: Distillation rates versus relative solar energy spectrum recorded on 9 September 2002.

The field data obtained was used to set up and execute in-house experimental investigations aimed at increasing still productivity. It is also now possible to position the experimental still onto Figure 2.10, assuming the experimentally-measured daily average distillate production of 3,3 $L/m^{-2}.d$, measured over a one-year period (Table 3.1).

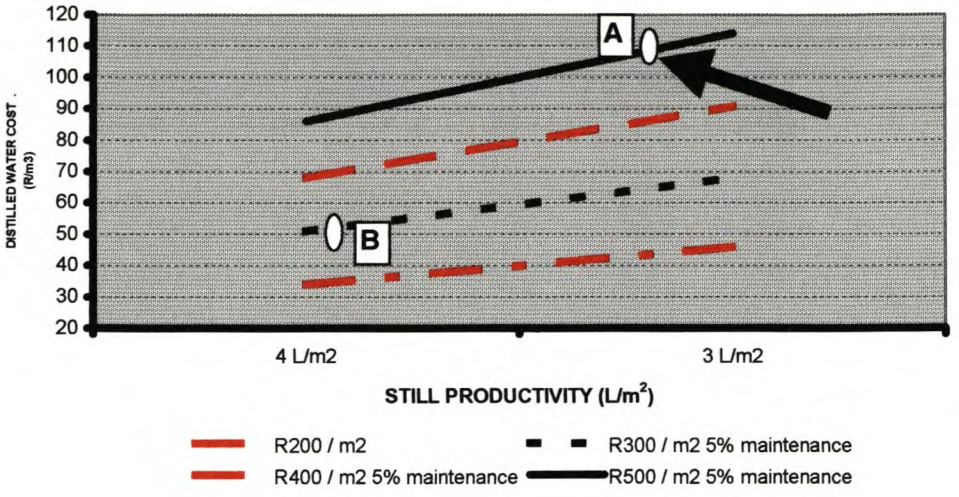

Figure 3.26: Position of experimental still on economic evaluation graph ([A]: current position, [B]: research goal)

CHAPTER 4

SOLAR STILL WATER QUALITY

4.1 Background

It is estimated that 60% of rural families in developing countries are without safe and clean household water (Andreatta 1994). In many areas the groundwater has too high a TDS (total dissolved solids) content, while the presence of specific contaminants may have additional negative effects for human use, for example (Natu 1979):

- the presence of high fluorine concentrations can lead to dental fluorosis,
- high sulphate concentrations can lead to gastro-intestinal irritation,
- some ions, like copper and iron, can negatively affect the taste of drinking water, and
- high chloride concentrations can be corrosive.

Solar still technology can be used to supply potable water to small rural communities in specific geographical areas (e.g. as described in Chapter 1), as it will not only desalinate brackish water but may destroy water borne pathogens as well (EPSEA project, 1999).

4.2 Feed water

The quality of the feed water can impact on the operational procedure of a solar still, for example:

- turbid (unfiltered) water containing physical particles can block feeding pipes and pumps,

- feed water containing volatile organics may not be suitable for solar still desalination as the organic compounds may distil over into the product water,
- algae growth can be experienced as a problem in basin stills (Natu 1979) (preventative measures include the use of copper sulphate or the use of alternate construction materials), and
- scale deposit can occur in hard waters (AA Delyannis 1983) [A].

4.3 Recommended potable water specification

The maximum acceptable TDS value of drinking water recommended by the World Health Organization (Jamieson 1986) is less than 500 mg/L, with the maximum allowable limit being 1500 mg/L. This means that blending of distilled water from a solar still with the saline feed water can be considered to increase the water production capacity.

In the literature, references are often made to the applicable water standards of the United States of America, and specifically those laid down by the EPA (Environmental Protection Agency, http://www.epa.gov/). The EPA is responsible for the National Primary Drinking Water Regulations of the USA, which are health-related standards that establish law-enforceable Maximum

[A] The degree of *hardness* can be expressed in terms of the standards developed by the US Water Quality Association, which categorises water in terms of milligram per liter (mg/L) of calcium carbonate equivalent (see the following Table).

DESCRIPTION	Milligram per liter (mg/L)
Soft	Less than 17.1
Slightly hard	17.1 to 60
Moderately hard	60 to 120
Hard	120 to 180
Very hard	180 and above

The *Langelier Saturation Index* (LSI) is a calculated number that is used to predict the calcium carbonate stability of water. The LSI is expressed as the difference between the actual system pH and the saturation pH. The formula takes the following into account, namely: alkalinity (mg/L as $CaCO_3$), calcium hardness (mg/L as Ca^{++}), TDS (mg/L), actual pH and the water temperature ($^{\circ}$C). Negative LSI values indicate no scale formation potential, while positive values indicate that scale will form. Higher concentrations of Ca, TDS and alkalinity all promote a greater tendency for scale.

Contaminant Levels (MCLs). The EPA also sets non-enforceable MCL Goals (MCLGs) at which no or known or anticipated adverse health effects in humans are expected. National Secondary Drinking water Regulations are also laid down by the EPA. These are also non-enforceable, and are guidelines regulating contaminants that may cause cosmetic or aesthetic effects in drinking water. In India the recommended safe limit for TDS in drinking water in arid regions is only 1500 ppm, while each person should have access to 40 liters of water per day of which 10 liters are meant for cooking and drinking. In Egypt the suggested minimum volume of hygienic water for drinking and cooking purposes is 5 liters per day per individual (Abulnour 1983). For South Africa, an amount of drinking and cooking water of 3 to 4 liters per day per capita is recommended (van Schalkwyk 1996).

Useful guidelines for assessing South African domestic water supplies exist, and these address the quality of water for drinking (health and aesthetic), food preparation, bathing and laundry (Quality of Domestic Water Supplies, (Second Edition) Volume 1: Assessment Guide, WRC report TT 101/98, 1998). This provides a handy tool for water management planning in areas where solar stills can be applied, as the bulk of household water can be of a higher TDS content than is required for drinking and cooking purposes only. Of particular importance are the fluoride and nitrate concentrations in rural water supplies, where absolutely safe maximum levels of 0,7 ppm and 26 ppm respectively, were recommended (Workshop Report, Water Research Commission, March 1999). Some relevant South African household water quality requirements are presented and compared to EPA standards in Table 4.1.

Table 4.1: Typical household water quality standards

RSA guidelines for Domestic Water use *(not all parameters included)*					EPA Drinking Water Standards				WHO[71] Standards (mg/L)	
Test	Min	Max	Units	Target/ ntbe [1]	MCLG [2]	MCL [3]	Units	P/S [4]	Acceptable	Allowable
Al	0	0.15	mg/L	T	0.05 - 0.2		mg/L	S		
Ca	0	32	mg/L	T	*as per ec*			*Ref 69*	*75*	100
Cd	0	0.005	mg/L	ntbe	0.005	0.005	mg/L	P		
Cl	0	100	mg/L	T	250		mg/L	S	200	600
Cr	0	0.05	mg/L	ntbe	0.1	0.1	mg/L	P		
Cu	0	1	mg/L	T	1.3	1.3	mg/L	P	0.05	1.5
ec	0	70	ms/m	T	4.7 - 5.8	4.7 - 5.8	uS/cm	USP 23		
F	0	1	mg/L	T	4	4	mg/L	P	0.7	1.7
F	0	8	mg/L	ntbe	2		mg/L	S		
Fe	0	0.1	mg/L	T	0.3		mg/L	S	0.1	1
K	0	50	mg/L	T						
Mg	0	30	mg/L	T					30	150
Mn	0	0.05	mg/L	T	0.05		mg/L	S		
Na	0	100	mg/L	T						
NO_3^-, NO_2^-	0	6	mg/L	ntbe	10, 1	10, 1	mg/L	P	< 50	100
Pb	0	0.01	mg/L	ntbe	0	0.015	mg/L	P		
pH	6	9	phu	T	6.5	8.5		S	7.0 - 8.5	6.5 - 9.2
SO_4^{2-}	0	200	mg/L	T	250		mg/L	S	200	400
TDS	0	450	mg/L	T	500		mg/L	S	500	1500
Turbidity	0	1	ntu	ntbe						
V	0	0.1	mg/L	ntbe						
Zn	0	3	mg/L	T	5		mg/L	S		

1: ntbe: not to be exceeded
2: MCLG: Maximum contaminant level goal
3: MCL: Maximum contaminant level
4: P/S: Primary / secondary

4.4 Product water

4.4.1 Quality assurance

Routine testing to determine the distilled water quality is an essential part of the running of a solar still unit or plant, especially when the distilled water is blended with source water to increase production capacity and/or to lower water cost. These tests may include the following:

- electrical testing, which gives an indication of the concentration of dissolved, ionised solutes. This can be related to salt content (TDS),
- turbidity (good drinking water should have no discernible turbidity),
- bacterial contamination, especially through counts to indicate the presence of pathogens,
- residual chemicals from water pre-treatment (chlorine, copper sulphate)
- chemical analysis (e.g. specific elements such as Cl, SO42-, Ca, Mg, F, NO3-, Cu, Fe, NaCl, alkalinity, hardness),
- other tests, such as for organic compounds and heavy metals need only be carried out routinely if contamination is suspected and/or if initial feed water testing have indicated such contamination.

4.4.2 Total Dissolved Solids

Total dissolved solids (TDS, temperature dependant) traditionally include dissolved sub-micron particles smaller than 0.45 μm. A rough approximation is that the TDS of a fresh-water source (in ppm or mg/L) can be obtained by multiplying the specific conductance (in μΩ/cm) by 0.65 (Kirk–Othmer). This relationship follows mainly from the ionic mobility of Na^+ and Cl^-. Typically, solar distilled water at a pH of 7,3 has a conductivity of 7.6 μΩ/cm (or TDS less than 5 ppm, Murasse 1989).

As has been highlighted in the literature study in Chapter 2, solar distillation is primarily a desalination technology with all the demineralisation advantages associated with a distillation process. Tables 4.2 (own research, feed water taken near Elands Bay along RSA West Coast) and 4.3 (Tiwari 1986) illustrate this by comparing the quality of solar distilled water with that of a tap water source.

Table 4.2: Chemical quality of solar distilled water (feed water source: seepage water near coast at Elands Bay, RSA West Coast)

Characteristic (mg/L)	Feed water	Product Water
Colour	Yellow	Colourless
Sodium	1576	0.7
Calcium	157	1.4
Magnesium	233	0.1
Chloride	2809	< 1
Fluoride	1.3	< 0.1
TDS	5888	8
$CaCO_3$	1350	3.9

Table 4.3: Typical analysis of solar distilled water and tap water

Physical Analysis	Tap water	Solar distilled water
Appearance	Clear	Clear
Odour	None	None
pH	7.0	7.0
Total dissolved solids at 105 °C (mg/L)	1109	18
Chemical analysis		
Chlorides as Cl	310	6
Phenolphthalein as $CaCO_3$	0	0
Total alkalinity as $CaCO_3$	332	4
Total hardness as $CaCO_3$	440	4
Calcium hardness as $CaCO_3$	220	2
Magnesium hardness as $CaCO_3$	220	2
Dissolved solids as SiO_2	10	2
Dissolved iron as Fe	0	0
Total sulphates as SO_4	150	neglible

4.4.3 Microbiological water quality

4.4.3.1 *Contaminants and testing*

It is practically impossible to keep water passing through any piping system totally free of pathogens (protozoa, bacteria and viruses). There are a number of water quality tests that can be used to determine the level of bacterial contamination. The coliform bacteria test is a reliable indicator of pathogens; and is measured in coliforms/ 100 mL. Total Plate Counts or the Heterotrophic Plate Count provides an estimate of the total number of bacteria that will develop into colonies during a period of incubation in a nutrient (measured in colony-forming-units or cfu/mL). Other tests include identification of specific bacteria such as *Pseudomonas aeruginosa*, viruses and pathogenic protozoans.

Because of the complexity and cost of testing for water-borne microorganisms, routine examination of water for pathogens is not always feasible. It is furthermore important to keep in mind that a 'safe' water indication at the moment of sampling does not necessarily guarantee safe water an hour before or after testing.

4.4.3.2 *Microbiological quality of solar distilled water*

It is generally accepted that the distilled water produced by solar distillation is sterile (coliform density equal to nil) due to the relatively high evaporation temperatures inside the still (Tiwari 1986). Heating water to 65 ° C for 6 minutes will normally kill all germs, parasites and viruses. The hepatitis virus, which is one of the most resistant intestinal pathogens, is killed within 10 minutes at 70 ° C and within 1 minute at 75 ° C. Such temperatures can easily be obtained inside solar stills (Tiwari 1998).

It is, however, the quality of solar distilled water produced at lower operating temperatures (e.g. during long overcast periods or during winter months) that

is of concern. This uncertainty motivated an experimental investigation into the microbiological cross-contamination potential inside a solar still, under thermal conditions where the basin water temperature did not exceed pasteurisation temperature.

4.4.3.3 *Determination of microbiological cross-contamination potential inside a solar still*

Due to practical constraints such as ease of cleaning and disinfection, full-sized stills were deemed unsuitable for the investigations. Two similar solar still units, each about $1/40^{th}$ of actual size (1500 mL capacity), were therefore built with the same construction materials identified in Chapter 5, namely polyurethane foam (frame and insulation), black flexible polypropylene (lining), aluminium (gutter) and glass (removable cover). The experimental set-up described in Chapter 7 was used to simulate daylight (see Figure 4.1, second still used as control not shown).

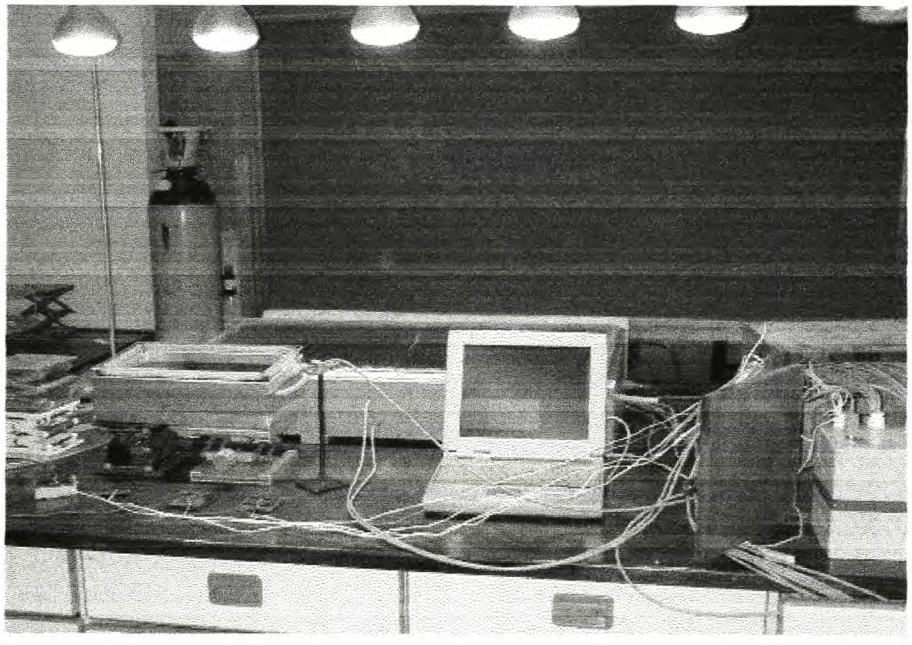

Figure 4.1: Experimental set-up used to study microbiological water quality, showing output controllable lamps (top), small solar still (below left) and temperature / radiation data logger (below right).

The microorganism used as indicators was *Escherichia coli*, which are typical microbial contaminants containing a green fluorescent protein from jellyfish for distinguishing purposes. Cells were grown overnight at 30 °C to a concentration of ca. 10^8 cells per mL.

100 µl of the *E. coli* solution was added to a saline water solution (TDS = 5000 mg/L) in both the experimental stills. The first (test) still was then exposed to constant radiation for a period of 24 hours, while the second (control) still was covered and kept at room temperature for the same period. A data logger was used to measure the water temperature in the test still. The concentration of microorganisms in the basin water of both stills, as well as in the distillate of the test still, was measured at 8-hour intervals for up to 24 hours. This analyses was done on 2 mL duplicate water samples at the required intervals. The experiment was repeated at different radiation levels (to reach different temperatures). Figure 4.2 shows the results for the different experiments.

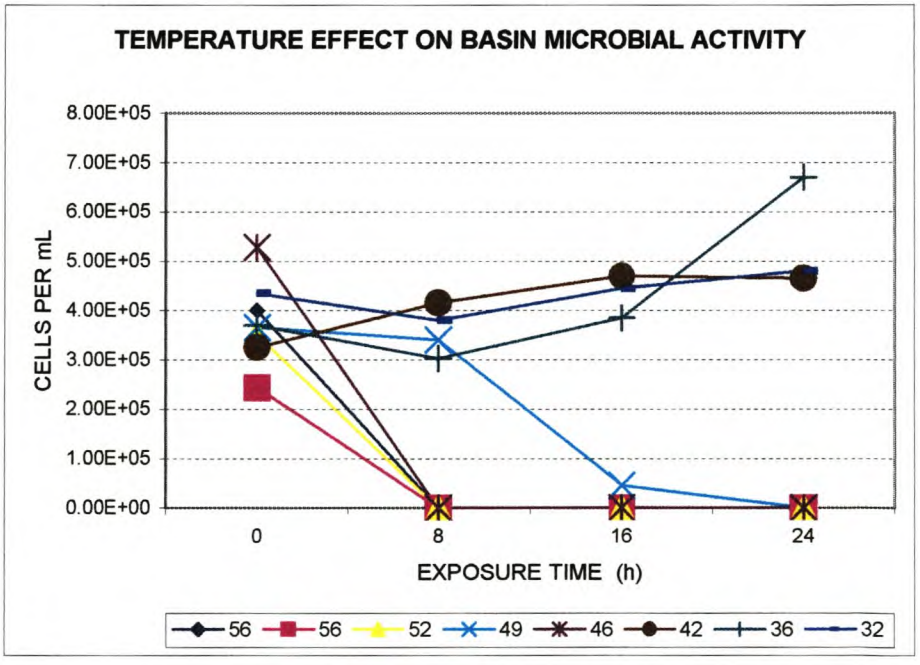

Figure 4.2: Pasteurisation effect in the still basin at different radiation levels (as measured against effective still temperature).

In all cases where distillation occurred, no microbiological contamination of the distillate was measurable. It was further shown that the pasteurisation efficiency inside the still basin decreased at temperatures lower than 50 °C. It is however important to note that distillation will also not normally take place under these conditions (see Figure 3.24). Under conditions of low basin temperatures (< 42 ° C), microbial activity increased with time. This means that under environmental conditions where internal still temperatures are relatively low (e.g. heavy overcast or rainy weather), complete pasteurisation of the feed water will not be achieved.

Solar distilled product water will however normally be free of microbiological contaminants during periods of low radiation. This should however be further verified through a study that includes different types of microbiological contaminants such as viruses and parasites. Brine disposal in cases where the feed water contains microbiological contaminants should also be addressed, specifically during conditions of relatively low solar radiation.

4.5 Recommendations

From the literature overview and experimental investigations into solar distilled water, the following recommendations regarding specifications related to a solar still plant are made (also see Addendum):

- national health standards must be conformed to,
- identify relevant additional standards set by other facilities and institutions (both national and international),
- from the above, draw up a set of limits for individual cases,
- monitor the water produced by solar distillation by testing according to the above specification,
- further studies should be undertaken to determine the potential of microbial contamination of solar distilled water produced by the basin solar still, i.e. at different temperature profiles (simulating different environmental

conditions) and different types of contaminants (i.e. parasites, bacteria, viruses and fungi / algae), and

- the following diagram of water analyses is recommended for use with solar still units and plants:

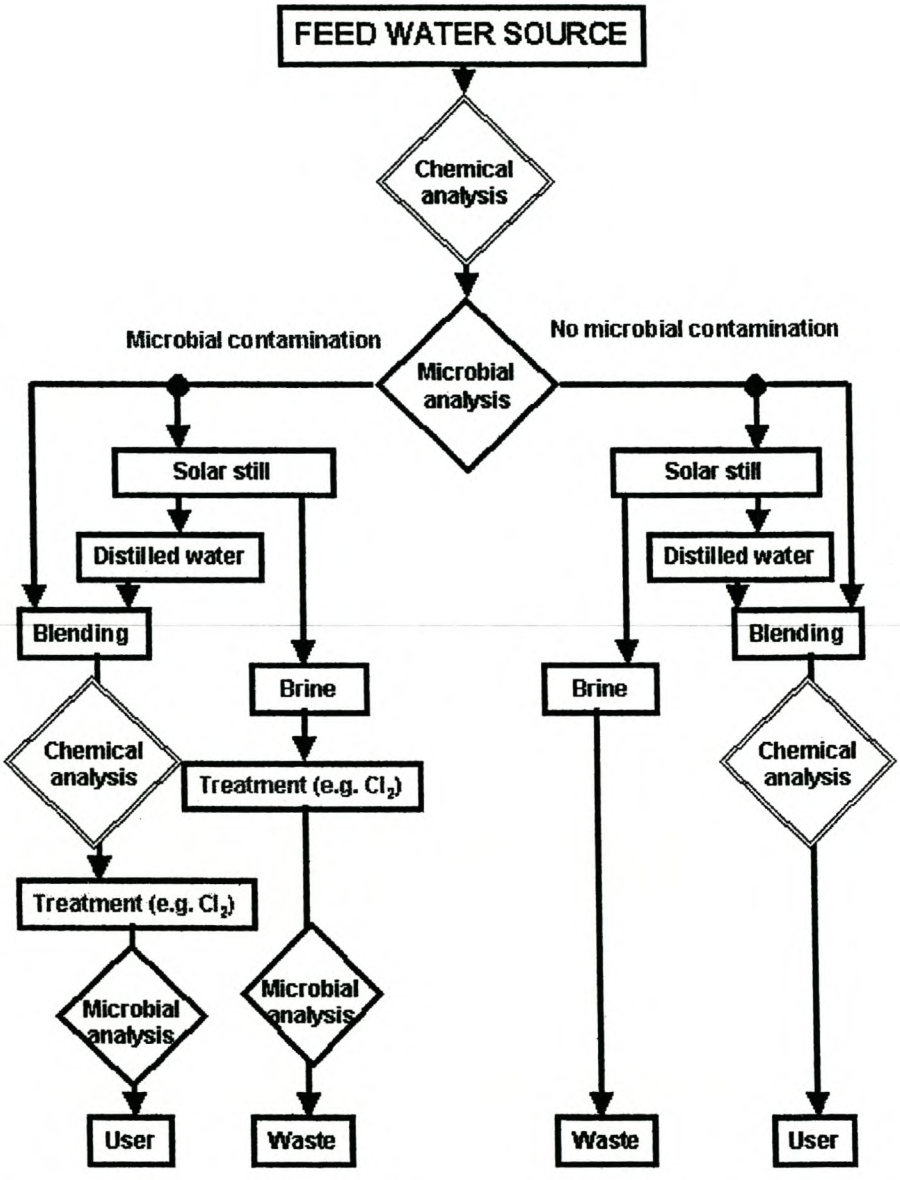

Figure 4.3: Recommended solar still water analysis layout.

CHAPTER 5

IMPORTANT PROPERTIES OF SOLAR STILL CONSTRUCTIONS MATERIALS

5.1 Background

The construction cost of a solar still consists of two main contributing factors, namely the labour and the material costs. As both these costs are however dependant on a number of uncontrollable and time dependant factors, the identification of the material qualities and the subsequent evaluation of potential substitute materials within a cost framework is better suited to this study. For the purposes of examples used in this study, labour costs will be expressed in South African Rands, and material costs at the time of evaluation will be used.

At the start of this research project in 1999, the local construction cost of a basin still was about R500/m ^{2}. Figure 5.1 shows the relative contribution of each still component at the time.

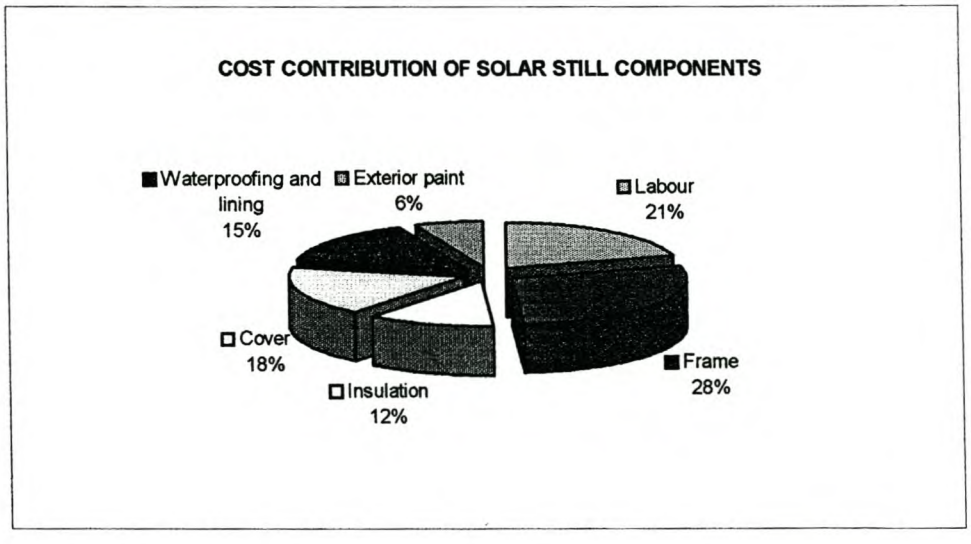

Figure 5.1: Relative cost contribution of solar still components.

5.2 Requirements for different solar still components

Figures 3.24 and 5.1 show that halving the still construction cost can halve the cost of solar distilled water. In order to identify cheaper construction materials it was first necessary to identify the specifications for each component (frame, cover, waterproofing lining, exterior and insulation). The impact on labour was evaluated in terms of the increase/decrease in costs (Rands) resulting from the use of substitute materials.

5.2.1 Frame

A suitable solar still frame must be lightweight, structurally strong enough to support the basin with saline water, rigid without a tendency to deform, environmentally durable and resistant to chemical and physical degradation. The insulation can form part of the frame, and serves to limit heat loss from the basin to the environment. Table 5.1 summarises typical frame materials from the literature. Other materials include polycarbonate and plywood.

Table 5.1: Solar still frame materials

Frame	Description / example	Reference
Brick / cement	Brick masonry with cement plaster	Natu 1979
Ferro cement	Cement sidewalls reinforced with chicken-wire	Kuhla 1998
Wood	Insulated with 5 cm glass wool	Tiwari 1991
Fibre reinforced plastic	Poly-ester composite with uv retardant / glass	Tiwari 1986
Concrete	Sidewalls and partition walls	Lof 1961
Galvanised iron	1 mm GI with 5 cm glass-wool insulation	Madani 1989
Aluminium	3 mm frame with fibreglass insulation	Rahim 1995
Polyurethane	Rigid one-piece foam frame	Geddes 1982

5.2.2 Cover

The solar still cover material must allow good transmission (low absorbance) of solar radiation over the widest possible wavelength band. The material must be rigid, have good wettability, must be resistant to photochemical degradation and have physical stability over the application temperature range. Table 5.2 lists typical cover materials.

Table 5.2: Solar still cover materials

Cover	Description / example	Reference
Glass	2,6 to 6 mm window glass	El Haggar 1993
Treated glass	Improved wettability; reduced horizontal	Arif Ileri 1997
Tempered glass	plane	McCracken 1985
Glass / plastic	Standard patio glass	Lof 1961
Plastic film	2,5 mm window glass	Murase 1989
Plastics	1 mm polyethylene film	Geddes 1982
	CA, PC, GRP, polyester-acrylic laminate, PVF, FEP film	

5.2.3 Lining

The basin lining absorbs transmitted solar energy; it heats up, and then conducts the heat to the water in the basin. Normally it serves the additional purpose of waterproofing. The requirements of the lining are good heat absorbance (black surface), thermal stability over the application temperature range (no degradation), chemical stability (no saline water corrosion) and chemical inertness (no volatile components). Table 5.3 summarises typical lining materials.

Table 5.3: Solar still lining materials

Lining	Description / example	Reference
Paint	Ordinary black paint	Maalej 1991
	Black polyvinyl spray	Madani 1989
Plastic / rubber	0,5 mm black Mylar liner	Kulha 1998
	Black poly-ethylene	Yadav 1987
	Polypropylene, PVC, black ABS, 1 mm black butyl rubber	
Asphalt	Impervious material for basin liner	Lof 1961
	Together with GI still basin	Tiwari 1991
Fibre reinforced plastic	Blackened FRP	Tiwari 1996
Aluminium	0,1 black anodised aluminium	Ouahes 1987

5.2.4 Other materials

The exterior of a solar still provides protection against its physical environment. This environment is typically hot and dry, although conditions such as rain, frost and saline mist spray can also occur. The requirements of the exterior surface are quite similar to those for the coating of buildings, and therefore good quality exterior paint can be used.

Collection channels inside a still must be inert so as to not contaminate the distilled water. Typical materials include aluminium (Natu 1979) and PVC (El-Haggar 1993).

The piping costs of a still are normally insignificant, but care must still be taken to use materials that do not degrade over the application temperature range.

5.3 Material evaluation

Evaluation of construction materials involved identifying relevant characteristics for each of the still components presented in Section 5.2, evaluating different alternative materials, and then integrating economically feasible combinations of components conforming to these characteristics into prototype stills for further evaluation.

5.3.1 Frame

The frame of the reference still was an aluminium framework with 25 mm high-density polyurethane foam insulation for the basin floor and sidewalls (thermal transmittance 0,74 W/m ^{2}). This framework conforms to the requirements of Section 5.1.1. It does however contribute significantly to the total still cost (about 40% or R200/m ^{2}). Table 5.4 summarises commercially available frame alternatives with cost comparisons.

Table 5.4: Comparison of solar still frame materials

Material	Cost R /m	Thermal Conductivity W/m°C
Aluminium	Reference	160.00
Brick / cement / ferro cement	+	0.950
Marine plywood	o	0.144
Galvanised iron	+	50.00
Wood	+	0.042
Fibre-reinforced plastic	o	0.035
Polyurethane foam (no support frame)	+	0.026

(+: cheaper than reference; o: similar or more expensive than reference).

Thermal conductivity from http://www.public.lastate.edu/~greenhouse/unit2.html

Stills built on-site (cement, concrete, etc), galvanised iron (GI) stills, wooden stills and polyurethane stills will generally cost less than aluminium frame stills. In the case of cement stills, however, the increased number of man-hours needed for on-

site construction will probably offset the material savings.

The lifetime and technical suitability of the remaining frameworks were also evaluated. Such an experimental investigation was carried out over a one-year period: five stills with different frameworks: cement, FRP, painted wooden, marine ply and GI frames were constructed and exposed to the environment. All stills had black silicone linings and 3 mm glass covers. The cement and FRP stills did not have polyurethane insulation. For most of the test period the stills were empty. Figure 5.2 shows some of the stills at the environmental test site.

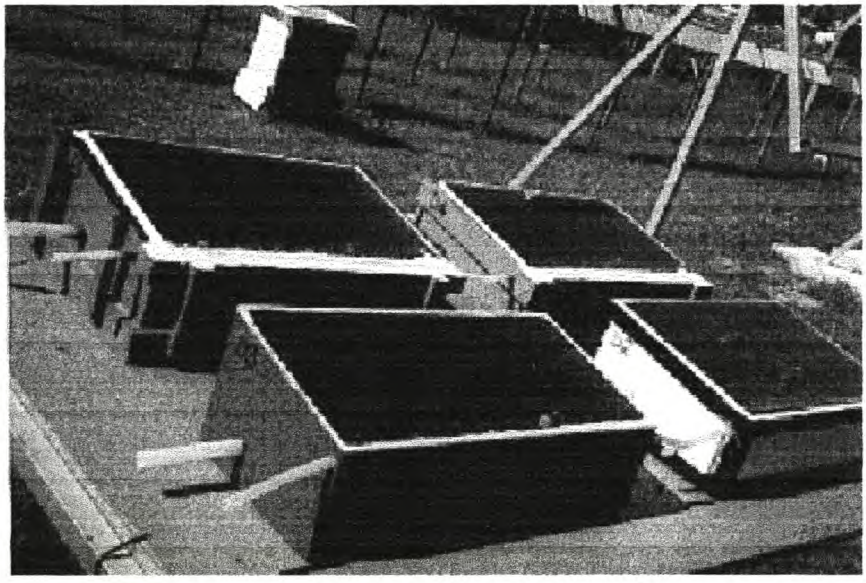

Figure 5.2: Testing of still frames constructed from different materials.

After the test period both the FRP and marine plywood frames showed no signs of physical degradation and maintained their functionality, confirming their suitability as alternative frameworks. The wood-framed still was visibly deformed, and it was leaking. The GI still rusted despite its pre-treatment, and consequently contaminated the distillate. Furthermore, its glass cover cracked three times over the test period, which indicated that the difference in expansion coefficients between the glass and the frame was too great. The cement still also started cracking and leaking soon after the experiment commenced. This part of the evaluation was subsequently aborted after only two months because of the high maintenance inputs.

From the experimental results and results tabulated in Table 5.4 it was concluded that the use of an aluminium framework together with polyurethane insulation remained a preferable functional option, especially if a light-weight unit is preferred (e.g. if the units are to be moved regularly). The use of FRP or marine plywood offered no real cost advantage. A cost reduction of about 40 % on aluminium frame stills could be achieved through the use of a thinner aluminium frame and treated wooden support barriers on the exterior. Different types of insulation materials were not evaluated due to the suitability (lowest thermal conductivity, Table 5.4) and low cost of 'Structalite'. A further 10% cost saving was possible through the use of 20 mm isolation foam (0,87 W/m ^{2} thermal transmittance). The importance of the insulation material has been discussed in Section 5.1.

5.3.2 Cover

Glass is by far the most common option for solar still cover material, and the reference still was fitted with ordinary 4-mm window glass (18% of the told cost, Figure 5.1). The economic benefit of using glass becomes apparent when a comparison is made between it and other alternatives (Table 5.5). In addition, window glass is freely available in rural areas.

Table 5.5: Comparison of solar still cover materials

Material	Cost R/m^2
4 mm window glass	Reference
6 mm tempered glass	-
3 mm window glass	+
3 mm polycarbonate	-
PVC	-
'Perspex' ®	-
Polyethylene film	+
Fluoropolymer film	o

(+: cheaper than reference; o: similar to reference; -: more expensive than reference).

5.3.2.1 Solar energy transmittance

A presentation of the solar energy spectrum is given in Figure 5.3. The 90 ° incident % transmittance measured for different cover materials over the solar spectrum is given in Figure 5.4.

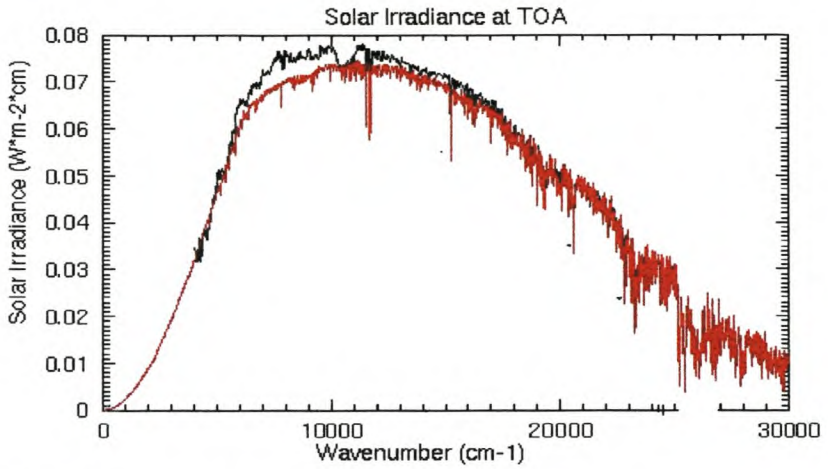

Figure 5.3: Solar energy spectrum

(Top of Atmosphere [TOA]: black line; solar irradiance at sea level: red line).

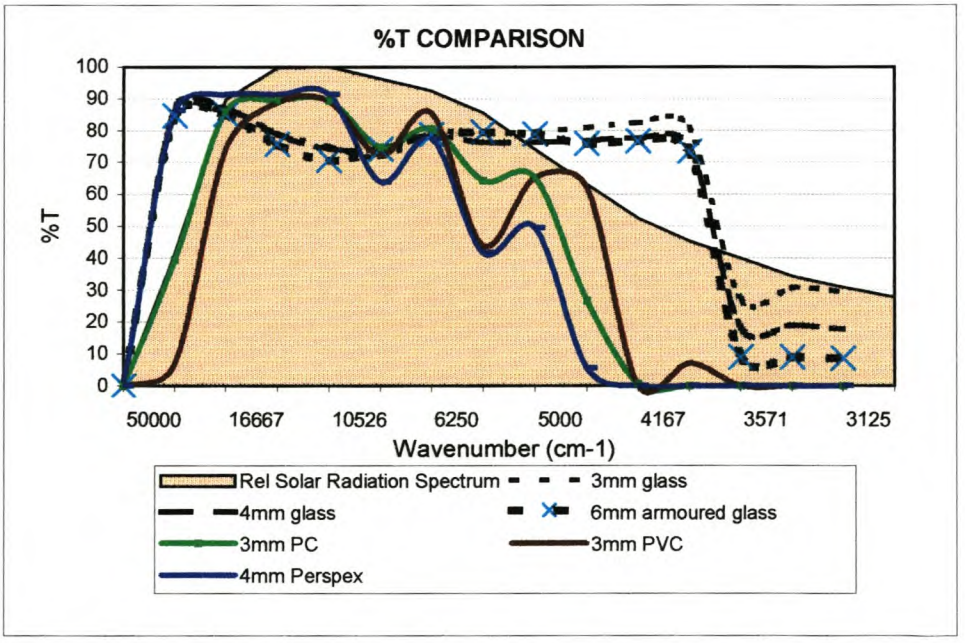

Figure 5.4: Comparison of % solar energy transmittance for different solar still cover materials.

McCracken (1985) reported the following wavelength-independent transmittance values for different cover materials (Table 5.6).

Table 5.6: % Transmittance of common solar still cover materials.

Material	% solar transmittance	% infrared transmittance
Low-iron glass	91	< 2
Ordinary window glass	86	2
Polycarbonate (PC)	86	6
Polyethylene	90	80
Polymethylmethacrylate (PMMA)	89	6
Polyvinylfluoride (PVF)	90	58

In Section 3.2.1 the importance of the cover transmitting the maximum amount of solar radiation (mainly visible and near infrared spectrum) was stated. Figure 5.4 and Table 5.6 show that glass, PMMA, PC and PVF perform well in this respect, with 3 mm window glass having the broadest average transmittance. The useful solar transmittance 'window' through glass is approximately between 350 and 2550 nm. Low infrared transmittance of glass is also important, as this will 'trap' the heat radiated from the basin inside the still.

5.3.2.2 Impact resistance

Glass has a notably lower impact resistance than PC, acrylic and PVC panels of equivalent thickness (http://www.public.lastate.edu/~greenhouse/unit2.html). Glass, also having the highest specific gravity of these materials, can thus be regarded as least suitable from a handling viewpoint.

Plastic films in general have the drawback that, although their impact resistance may be high, the use of such films would have a design impact necessitating the use of additional hardware to keep the film tightly stretched over the basin (Wilkerson 1992).

5.3.2.3 Wettability

It is known that untreated plastic materials often have poor wetting properties (Maalej 1991). McCracken (1985) categorised alternative cover materials in terms of wettability as excellent (glass), treatable (PVF, PMMA, PC) and possibly treatable (PE). Cover treatment, being temporary, is non-ideal from a practical viewpoint and therefore glass is preferable.

Determining the positive wetting ability of window glass by distilled water was carried out at room temperature with a Cahn Dynamic Contact Angle Model 322 instrument. Results were compared to those of two other cover materials, PC and PMMA). The following θ_R-values were recorded: 41° for glass, 55° for PC and 42 ° for PMMA. None of the surfaces displayed complete or thorough wetting with distilled water with regard to advancing as well as receding contact angles.

5.3.2.4 Photochemical stability

The uv-stability of the cover material is important as degradation of the cover can lead to malfunction of the still. Glass and PMMA are regarded as having excellent uv resistance (life span 20 years +) (McCracken 1985), while PVF, PVC and PC must be treated to make them less susceptible to uv degradation and to achieve life spans in excess of 10 years. PE is not uv resistant and such films will normally have to be replaced every three years or less.

5.3.2.5 Physical stability

Important physical properties of the still cover material are: thermal transmittance (preferably high, see Section 3.2.1), thermal expansion (preferably low due to sealed joint with frame, see Section 5.3.1) and maximum application temperature (should be higher than maximum expected operational temperature of up to 100 ° C). Table 5.7 compares these properties for selected cover materials.

Table 5.7: Physical properties of cover materials

Material	%- Thermal transmittance	Thermal expansion (10^{-6} cm/cm °C)	Maximum operational Temperature (°C)
Glass	3	0,45	204
Polycarbonate	< 3	6,5	127
Polyethylene film	50	13 (sheet)	71
Polymethylmethacrylate	5	6,8	93
Polyvinylchloride	25	-	80
Polyvinylfluoride	20	13 (sheet)	107

(from http://www.cisti.nrc.ca/ , http://www.edlrine.com/ and http://www.tangram.co.uk)

Although glass exhibits poor thermal transmittance properties, it has a low thermal expansion coefficient and high operational maximum temperature. PE, PMMA and PVC have favourable thermal transmittance, but are unsuitable for interfacing with the expected maximum temperatures inside the solar still.

5.3.2.6 Conclusions and recommendations

The recommended cover for further investigation was 3-mm window glass because:

- it has the lowest cost per m^2 of the candidate materials;
- it is commercially freely available and a well known commodity;
- glass exhibits good solar energy transmittance over the widest wavelength range;
- it has excellent uv–stability;
- it has a low coefficient of thermal expansion; and
- it has a high operational temperature ceiling.

Negative properties of glass are its low impact strength and low thermal transmittance. Its wettability is acceptable although not displaying complete or thorough wetting with distilled water (θ_R-value of 41°).

The use of 3 mm window glass rather than 4-mm window glass resulted in a cost saving of 33% on the cover.

5.3.3 Lining

The lining covers the interior base and sidewalls of the still. The preferential use of a black lining for maximum heat emissivity ($e \propto T^4$) has been discussed in Section 3.2.1. The lining of the reference still was acetic acid-cured black silicone ('Bostik 2550') and contributed 15 % to the still cost (Figure 5.1). Table 5.8 compares the unit costs of typical black lining options.

Table 5.8: Price comparison of candidate lining materials.

Material	Cost R/m^2
Black silicone RTV sealant ('Bostik 2550)	Reference
Nitrile rubber mats	-
Laminated 'Neoprene' rubber	-
Polyethylene sheets	+
High density polyethylene	(+)
Polyurethane adhesive ('Genkem BAW 536')	o
Polyurethane waterproofing paint ('Durapond')	+
Polypropylene (PP), vacuum formed	(+)
Polypropylene sheets ('Correx')	+
Black ceramic tiles	((+))

(+: cheaper than reference; (+): only available in mass produced quantities; ((+)): additional waterproofing materials required; o: similar to reference; -: more expensive than reference)

5.3.3.1 Thermal stability

While the temperature inside an operational still will probably never exceed 90 ° C, temperatures in excess of 120 ° C have been measured inside dry stills exposed to direct solar radiation. Hence, as a precaution the lining should therefore be thermally stable i.e. not undergo any phase transitions (measured by Differential Scanning Calorimeter) or chemical degradation (weight loss measured by Thermal Gravimetric Analysis) from ambient temperatures

(minimum 0 ° C) to up to 130 ° C. The thermal properties of the candidate materials are as listed in Table 5.9.

Table 5.9: DSC and TGA results for lining alternatives.

Material	DSC (onset of first phase transition)	TGA (% weight loss up to 100 °C (left) and 130 °C (right)	
Black silicone RTV sealant ('Bostik 2550)	> 160	0,3	1,0
Nitrile rubber mats	>180	0,2	0,4
Laminated 'Neoprene' rubber	133	0,3	0,6
Polyethylene sheets	118	-	softened
High density polyethylene	116	-	softened
Polyurethane adhesive ('Genkem BAW 536')	< 140	0,1	0,3
Polyurethane waterproofing paint ('Durapond')	> 140	0,4	1,5
Polypropylene (PP), vacuum formed	146	-	-
Polypropylene sheets ('Correx')	141	< 0,1	< 0,1
Black ceramic tiles	>200	< 0,1	< 0,1

The above DSC results show that polyethylene linings cannot be used up to 130 ° C as weight losses of more than 1% were measured at 130 ° C for the polyurethane-based paint.

5.3.3.2 Chemical stability

The lining must be resistant to hot, saline water. A first order go / no go test was designed whereby 7 X 7 cm ^{2} squares of the different lining materials were subjected to a 24 hour reflux period in one liter of a 33% NaCl solution, whereafter 500 mL of distillate was collected. This test was carried out in order to determine lining degradation through (i) visual colour changes in the saline water over the test period and (ii) sensible detection of contaminants in the distillate. The results are presented in Table 5.10. Paint and PE testing was not completed due to their thermal unsuitability (Section 5.3.3).

Table 5.10: First-order degradation studies on lining materials.

Material	Saline water discolouring	Smell / taste in distillate
Black silicone RTV sealant ('Bostik 2550)	No	Detectable
Nitrile rubber mats	Intense	Strong
Laminated 'Neoprene' rubber	Intense	Strong
Polyethylene sheets	No	No
High density polyethylene	No	No
Polyurethane adhesive ('Genkem BAW 536')	No	Strong
Polyurethane waterproofing paint ('Durapond')	-	-
Polypropylene (PP), vacuum formed	No	No
Polypropylene sheets ('Correx')	No	No
Black ceramic tiles	No	No

Although subjective to a degree, Table 5.10 confirms the good corrosive resistance of PE and PP, while also indicating the potential problem of volatile contaminants associated with multi-component rubbers.

5.3.3.3 Environmental exposure

Experimental stills with different lining materials (Silicone sealant, PE, vacuum formed PP, hollow PP sheets and ceramic tiles) were exposed to natural solar radiation over a one-year period at the environmental test site. The stills were dry i.e. maximum temperature exposure was obtained. The stills were routinely visually inspected and also after test completion. The silicone sealant and tile linings seemed relatively intact, although the presence of air bubbles in the silicone lining suggested that the bond between the silicone sealant and the insulation foil was deteriorating. The vacuum-formed PP showed signs of discolouring, while the Correx also showed distinct surface cracks. The PE lining had completely disintegrated.

5.3.3.4 Conclusions and recommendations

It was determined that the existing use of black silicone sealant was not preferred

due to the negative taste effect it transfers into the distilled water.

Black PP lining was recommended for further investigation because it provides a cheaper alternative to silicone sealant (the use of hollow 6 mm 'Correx' PP sheets instead of silicone sealant reduced the lining costs by 48%), it requires less labour hours to assemble and it appears physically and chemically stable in a corrosive environment over the desired temperature range.

Potential long-term uv and hot water exposure stability problems associated with the use of the different types of PP need to be addressed to determine the lifetime of the lining. The use of other types of black PP (e.g. flexible PP) should also be investigated.

5.3.4 Other components

Due to the relatively small impact other components such as exterior paint and piping have on the still costs (~ 6%), they were not addressed as part of the investigation. The suitability of commercially available exterior PVA paint was confirmed over a three-year solar still plant trial run under harsh conditions in Bushmanland, South Africa (Goldie *et al* 2003). Silicone tubing remained preferable as distillate piping due to its inertness over a wide temperature range. Silicone sealant was used to fix the cover panes to the frame.

5.4 Substitute material screening model

From the requirements for the different still components (Section 5.2) and following the material evaluation tests, it is now possible to evaluate substitute materials for the different components for the specific still design. This evaluation must be carried out in cost context i.e. it must eventually have an economic benefit (cheaper still). Table 5.11 summarises these screening tests, and provides criteria for future evaluation.

Table 5.11: Screening matrix for alternative still components

Component	Criteria	Test / measurement	Relevance
Frame / insulation	Weight	Frame mass	Low
	Support strength	Design calculation	Critical
	Durability	Environmental exposure	Critical
	Thermal insulation	Thermal conductivity	High
Cover	Solar energy	% transmittance	Critical
	Rigidity	Impact resistance	High
	Wettability	Receding contact angle	Critical
	Photochemical stability	Uv degradation	High
	Physical properties	Thermal transmittance,	Low
		Coefficient of thermal expansion,	Low
		Max application temp	Critical
Lining	Thermal stability	DSC	Critical
		TGA	Critical
	Chemical stability	Saline water boil / discolouring	Critical
		AFM	
		Taste / smell,	Critical
	Distilled water quality	Chemical analysis	High
			Critical

(*Low*: normally acceptable for use; *High*: only acceptable if superior in other respects; *Critical*: Failure to conform excludes the use of the component)

From the above screening matrix it was possible to propose a component design, which had a cost reduction impact of 34% on the reference still (conservatively assuming the same number of man-hours to construct the still). The proposed redesigned still consisted of polyurethane insulation supported by an aluminium / wood frame, 3 mm window glass cover and a PP lining.

From Figure 5.6 the positive economic impact of the use of these proposed materials in still construction can be seen (the arrow indicates the reduction of distilled water cost from R110/m^2 [A] to R70/m^2 [C].

With the material evaluation model now in place, the emphasis of the research was on improving the overall still productivity through in-house (laboratory) studies, as described in the following chapters.

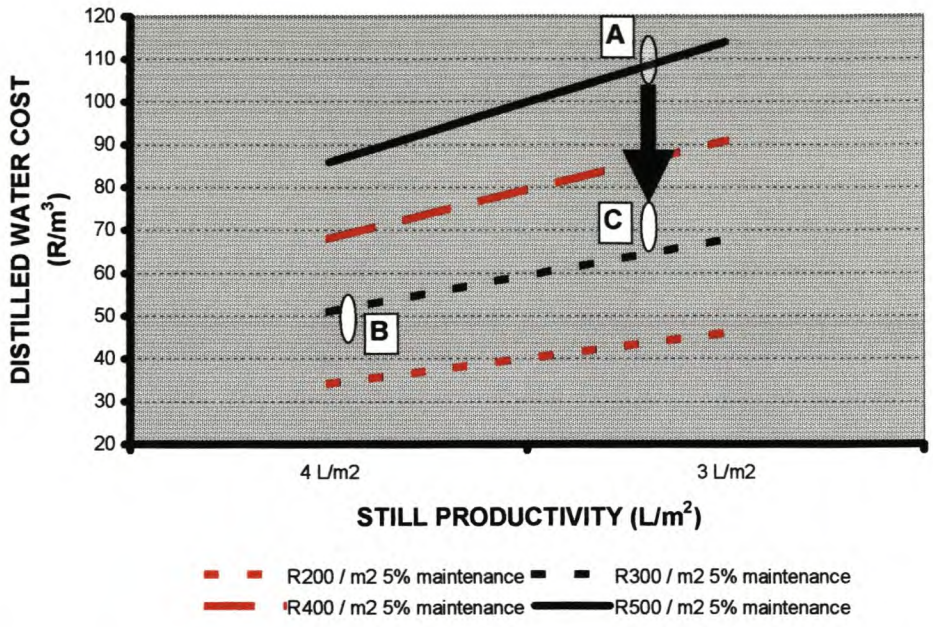

Figure 5.5: Distilled water cost improvement through the use of proposed cheaper construction materials

(A: distilled water cost of reference still; B: research goal; C: distilled water cost after design improvements).

CHAPTER 6

IMPORTANT PHYSICAL PROPERTIES OF SOLAR RADIATION, GLASS COVER AND FEED WATER

6.1 Background

The importance of maximum transmittance of solar radiation into the feed water inside a solar still, in order to achieve maximum yield, has been discussed in Chapter 3.

The transmittance depends on:

a. Wavelength of solar radiation.
b. Thickness and type of cover (in this case glass).
c. Angle of incidence of solar radiation.

The wavelength of the solar spectrum falls within certain limits. The thickness of the glass cover used in this study varied from 3 to 6 mm (ordinary window glass was selected for economic reasons). The angle of incidence varies according to the season (Figure 3.8). Hence it was decided to investigate the relationship between these three variables in order to establish a useful solar radiation bandwidth for the solar still cover.

6.2 Solar radiation spectrum

6.2.1 Wavelengths of solar radiation

Figures 5.3, 6.1 and 6.2 give presentations of the solar energy spectrum. The solar spectrum has a peak close to 500 nm and consists roughly of 10% ultraviolet, 45% visible, 45% infrared radiation (Osram technical brochure).

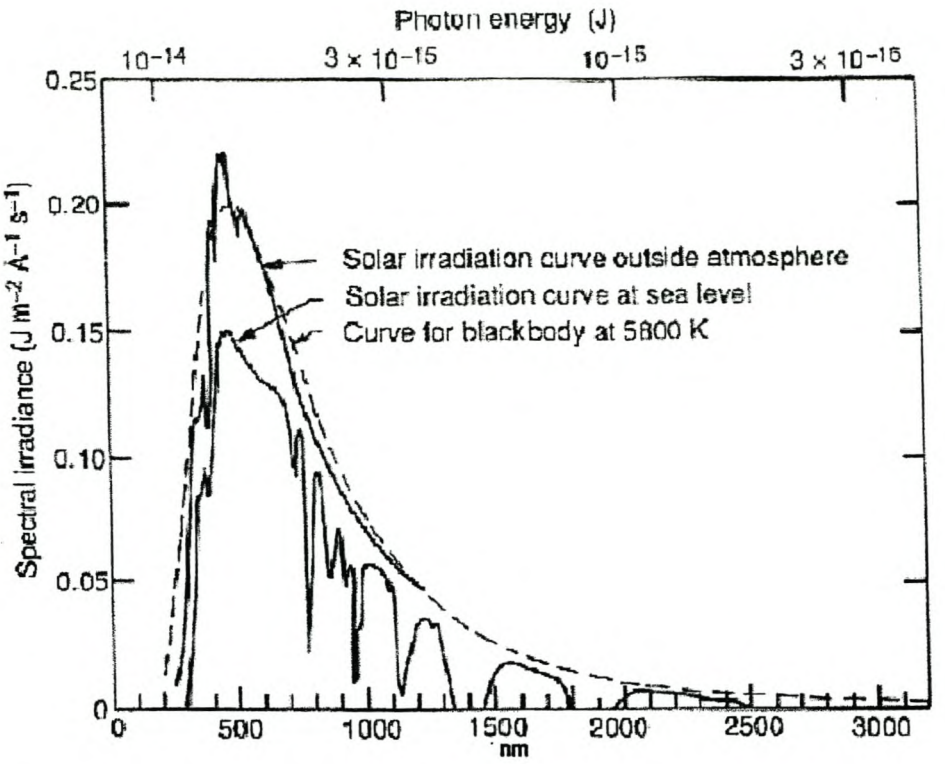

Figure 6.1: Solar radiation spectrum.

The peaks recorded at sea level are attributed to absorption by atmospheric carbon dioxide and water vapour and can be related to the combination tones and overtones of the fundamental vibrations of the CO_2 and H_2O molecules.

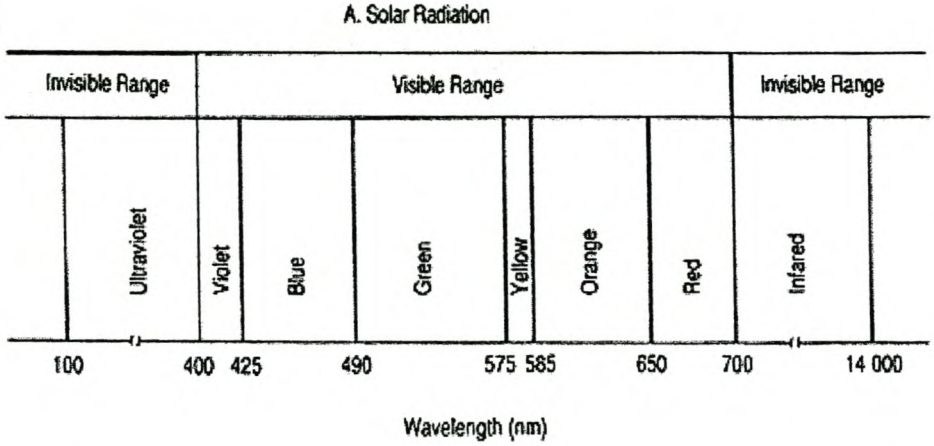

Figure 6.2: Solar radiation spectrum relative to visible light .

6.2.2 Thickness and type of glass

Ordinary glass of the soda-lime-silica type (window or plate glass) can transmit more than 90% of the incident radiation in the UV-A and visible regions of the spectrum, provided the Fe_2O_3 content is lower than 0.035%. If this content is higher then the transmittance is somewhat decreased.

6.2.3 Angle of incidence of solar radiation

The maximum angle of incidence (relative to the horizontal) on the glass cover of the still in Stellenbosch varies between 30 ° in winter to 76 ° in summer.

6.3 Determination of transmission properties of glass

An attachment (see Figure 6.3) was constructed to vary the angle of incidence with respect to the main beam of the spectrometers. This attachment was used to position a glass square in the sample compartments of a GBC UV/VIS 920 and Perkin Elmer 1600 FTIR spectrometers. The % transmission was then recorded over the relevant wavelength region.

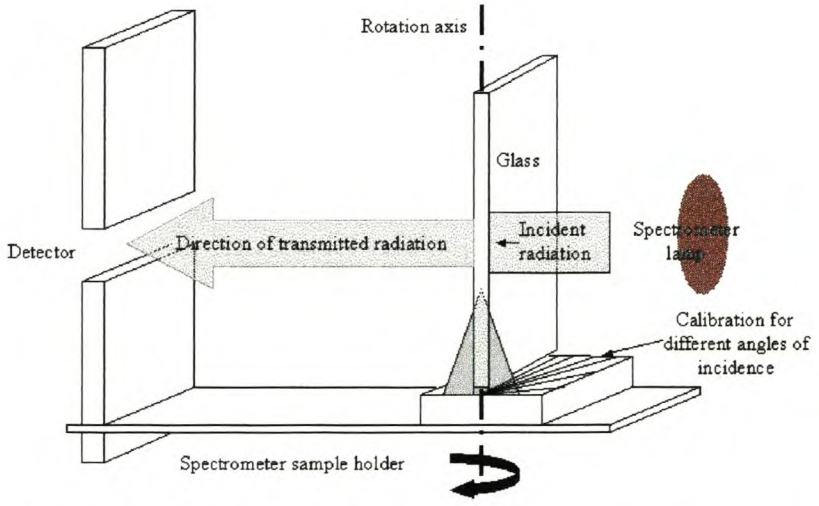

Figure 6.3: Attachment placed in UV/VIS and FTIR spectrometer sample compartments for recording % transmission of glass at varying angles of incidence.

6.4 Experimental results

The results of these investigations are presented in Figures 6.4 and 6.5.

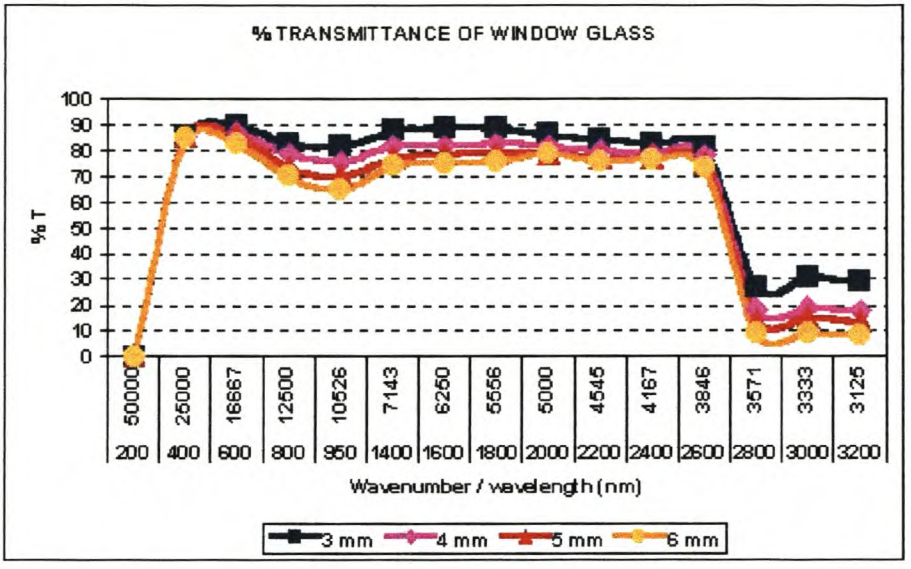

Figure 6.4: Influence of glass thickness on transmittance of window glass.

The transmittance is uniform at a high level for angles of incidence ranging from 0 to 40° and drops sharply as the angle approaches 90° (Figures 6.5 and 3.8).

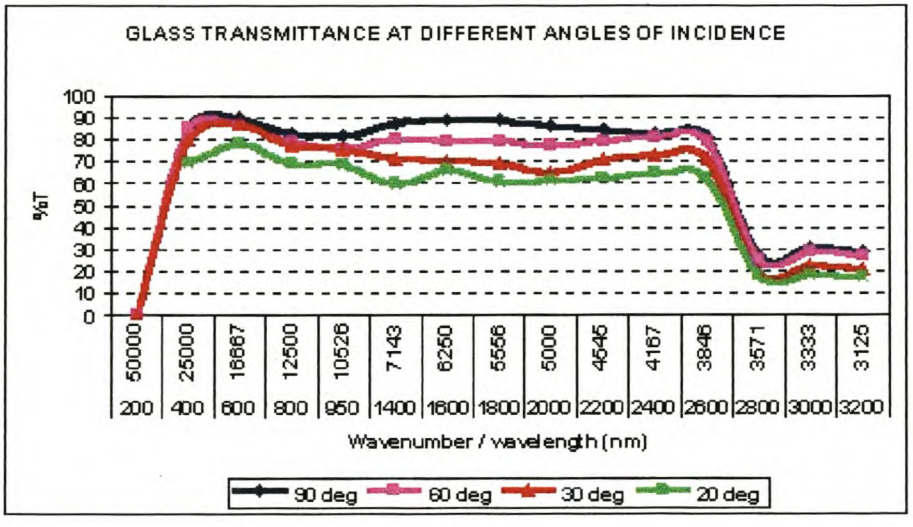

Figure 6.5: Influence of angle of incidence on radiation transmitted through 3-mm window glass.

From Figures 6.5 and 6.6 it can be seen that even at low angles of incidence, more than 50 % of direct radiation will pass through the 3 mm glass cover between 330 nm (30303 cm^{-1}) and 2740 nm (3650 cm^{-1}).

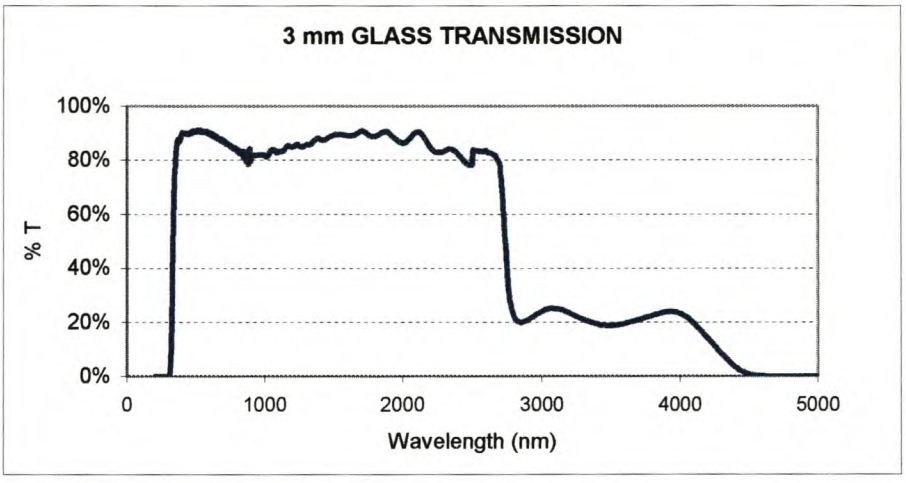

Figure 6.6: Transmittance of 3-mm window glass.

6.5 Useful solar radiation bandwidth for solar still cover

From Figures 6.4, 6.5 and 6.6 a useful radiation bandwidth for the solar still cover could be extracted. This is presented in Figure 6.7.

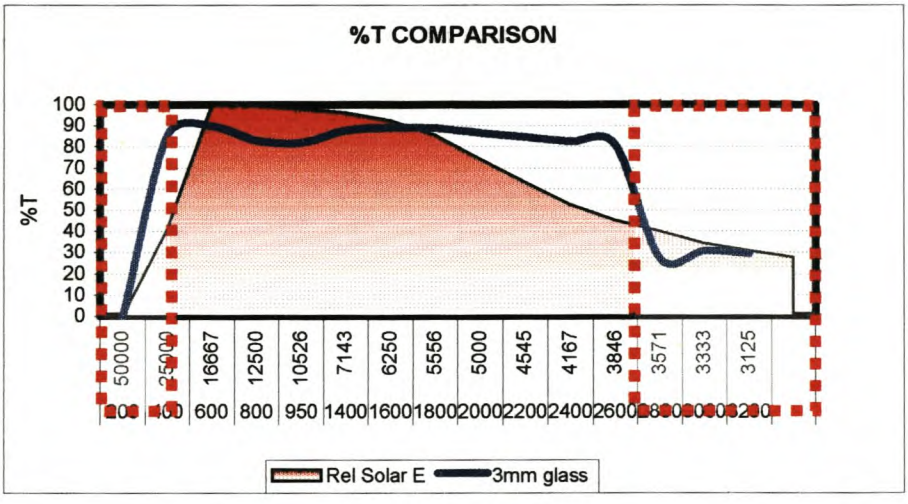

Figure 6.7: Useful solar radiation window.

The useful solar bandwidth is thus between 3 600 cm $^{-1}$ (2 775 nm) and 28 000 cm $^{-1}$ (357 nm) for the specific solar still used in this investigation.

6.6 Absorbance of water

The absorbance spectrum of distilled water over a broad spectral range is presented in Figure 6.8.

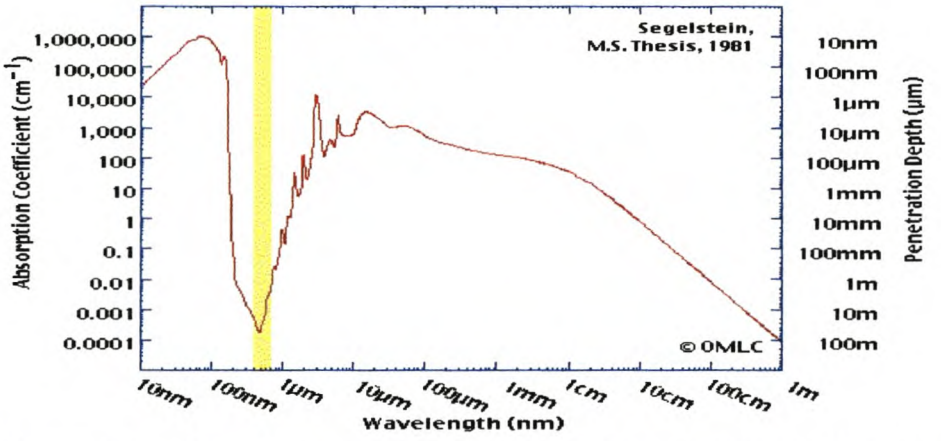

Figure 6.8: Absorption spectrum of distilled water (visible light range highlighted).

The large peak on the left of Figure 6.8 is due to the electronic excitation of the water molecule. This is followed by a region of no absorption in the visible region (highlighted) and therefore maximum radiation penetration depth.

The peaks at longer wavelengths are due to vibrational excitation of the water molecule. These peaks appear as the result of overtones and combination tones of the fundamental vibrations of the water molecule. They appear in the near infrared region.

Behind the glass cover the effective absorption range is limited by the useful solar bandwidth (Figure 6.7). The absorbance of water in this region is given in Figure 6.9.

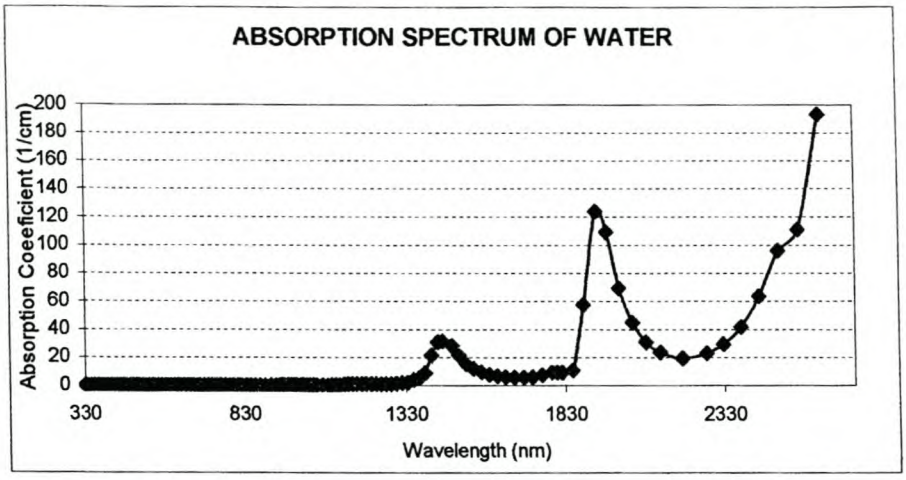

Figure 6.9: Absorption spectrum of water over effective solar radiation range behind glass cover.

6.7 Conclusions and recommendations

Figures 6.8 and 6.9 provide valuable insight into the radiation absorption behaviour of the water inside the still:

- The visible radiation transmitted through the cover will also be transmitted through the water and absorbed only by the basin lining,
- The water depth in the basin will determine to what degree near infrared radiation will be absorbed by the water. In the test set-up, the maximum basin water depth was 32 mm. This means that radiation with wavelengths from 1 000 nm and upwards will also be absorbed by the water, while from wavelengths 2 000 nm and upwards, nearly all radiation will be absorbed by the water (radiation penetration depth less than 1 mm),
- The shallower the water depth in the basin, the greater the bandwidth of the radiation transmitted to the liner – see Figure 6.8. (At wavelengths longer than about 1 000 nm the intensity of solar radiation decreases dramatically, refer Figure 6.1, due to the solar radiation characteristics and the modification thereof by the water vapour in the atmosphere.)
- These facts dictate that the liner must be able to absorb the greater bandwidth of radiation transmitted to it and to convert it into heat. Consequently the liner must be black, therefore absorbing all wavelengths

in the visible and near infrared region. This is due to electronic excitation of the dye molecules normally used in the lining material. The electronic energy is converted through internal conversion to vibrational energy of the liner matrix. This vibrational energy is transferred to the water molecules in the basin by collision and radiation and thereby causes it to be heated.

- With the above understanding of the properties of the incoming radiation, the still cover and the feed water, it is now possible to design a laboratory test setup to study productivity enhancement in greater detail (Chapter 7).

CHAPTER 7

DESIGN OF EQUIPMENT USED TO EVALUATE THE EFFICIENCY OF SOLAR STILLS IN-HOUSE

7.1 Background

Important literature and experimental properties of operational basin solar stills were discussed in Chapter 3. It however becomes apparent that the theoretical insight necessary to design and execute still efficiency improvements based on field trials will be almost impossible because of the number and complexity of seasonal, site and meteorological dependant variables (best illustrated by Figures 3.5 and 3.20). An in-house test facility, in which the number of variables could be limited and controlled, was therefore designed and used. This test facility had to the following features:

- spacious enough to allow experiments to be carried out on solar still prototype units resembling the basin design configuration including inlet, outlet and distillate piping as well as measuring equipment,
- equipped with a radiation source which at least simulates the solar spectrum through the glass transmittance window (Figure 6.7),
- a controlled environment in terms of ambient temperature and air flow, and
- should initial characterisation show positive results, the facility be able to be upgradeable to allow more sophisticated testing.

A laboratory facility that adequately conformed to the above requirements was consequently identified and equipped for the in-house tests on solar stills described in this Chapter and also in Chapters 8 to 11.

7.2 Experimental set-up

The initial experimental set-up consisted of two experimental basin stills, an overhead adjustable framework onto which six light bulbs could be fitted, piping

for feeding and flushing the stills with municipal tap water, and piping from the stills to calibrated distillate containers. Thermocouples were used to record temperature profiles, and distillate production was measured volumetrically. Figure 7.1 shows the experimental layout.

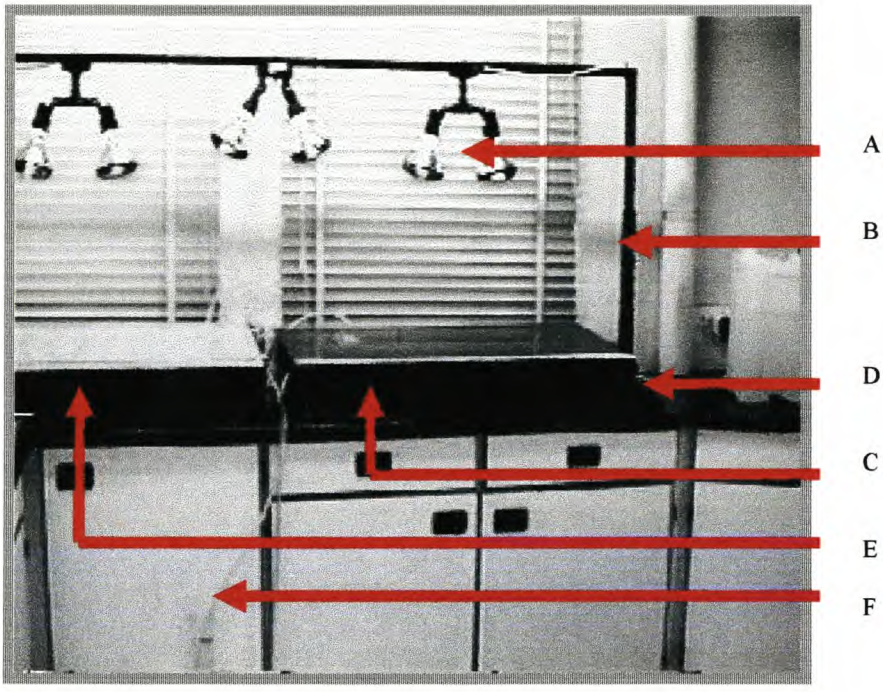

Figure 7.1: Arrangement for in-house solar still testing (A: Light source, B: Height adjustable frame, C: Solar still # 1, D: Feed water piping, E: Solar still # 2, F: Distillate piping to volumetric measurement container).

7.2.1 Radiation source

One of the first problems was the choice of a radiation source that would satisfactorily simulate the useful part of the solar spectrum. So-called daylight lamps exist, but these are of the fluorescent types, they are lengthy in size but have very low (< 30 W) output. A number of commercial light suppliers were approached, and eventually Osram 'SICCATHERM' lamps (250 W) were recommended. These lamps are commercially available as 'red' or 'clear, which is best illustrated by their radiation profiles (Osram Technical brochure) as presented in Figure 7.2, which also compares the radiation profiles of the lamps

relative to the solar energy spectrum.

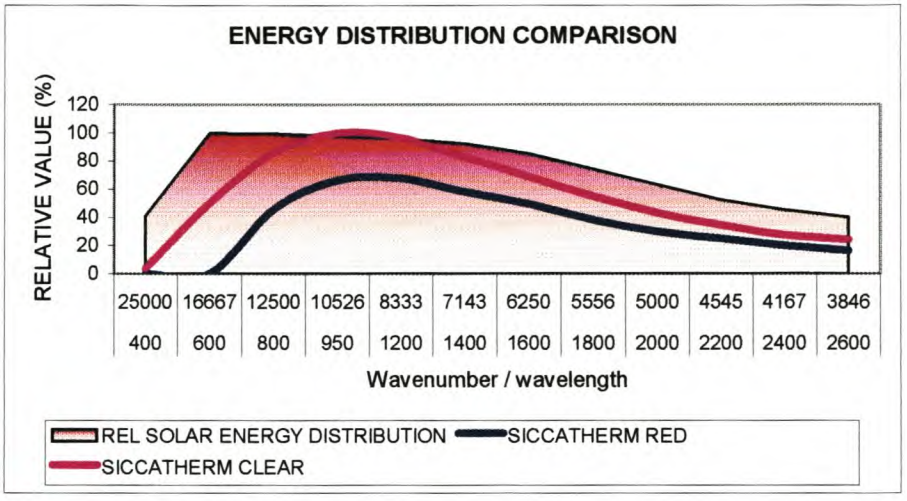

Figure 7.2: Relative energy distributions of OSRAM Siccatherm lamps and solar energy spectrum.

Figure 7.2 shows that the clear lamp spectrum simulates the solar spectrum to a reasonable degree. The red lamp is of lower intensity and excludes the visible radiation spectrum < 600 nm. Both lamps have a radiation peak at about 1000 nm, which is about 500 nm higher than that of the solar spectrum.

7.2.2 Solar still description

Two similar solar stills, each 12,5 liter in capacity, were constructed for the experimental test runs. The still designs were scaled-down versions of the commercially available basin still referred to in Section 2.3. The frames were made of marine plywood exterior (able to support instrumentation probes firmly) with 20-mm polyurethane foam insulation on the interior base and sidewalls. Ordinary 3-mm window glass, with transmittance properties described in Section 6.1.1, was used as cover material. Bostik 2550-silicone sealant was used as lining material as it was convenient for the installation and removal of recording probes. One of the stills (C1) was completely lined with black silicone, simulating the stills used for field characterisation (Section 3.3), and was used as reference. The other still (C4) was lined with white silicone sealant (Figure 7.1)

in order to study the performance difference between the stills due to lining colour differences. Both stills had silicone tubing for feed water inlets and distillate outlets. The distillate production of the stills was gravitated from the stills and collected separately. The stills were positioned underneath the lamps in such a manner that the radiation distribution on the covers was evenly spread and optimal. The angle of incidence onto the covers was fixed (97 °).

7.2.3 Instrumentation for recording of heating profiles inside stills

At first the temperature profiles inside the stills were recorded with temperature probes (± 0.15 °C accuracy) connected to a four-channel Pace Scientific XR440 pocket data logger. Using this configuration it was possible to record combinations of temperatures of the water inside the basin, at different heights in the air mass above the water, at both sides of the cover and of the immediate surroundings. After completion of an experiment the data was transferred to MS-Excel for interpretation. Figure 7.3 shows typical temperature profiles obtained from initial in-house characterisation.

In later experiments it became clear that more simultaneous data collection points were necessary. An analogue data logger capable of recording up to sixteen channels of temperature, pressure, radiation and other voltage-induced signals was the custom designed and built by the Department of Physics, University of Stellenbosch. Data accuracy resolution was specified and tested to be better than 99%. This data logger could be operated from a solar cell, and was also used for the field experiments described in Section 3.3. Figure 7.3 also shows typical temperature profiles obtained with this data logger.

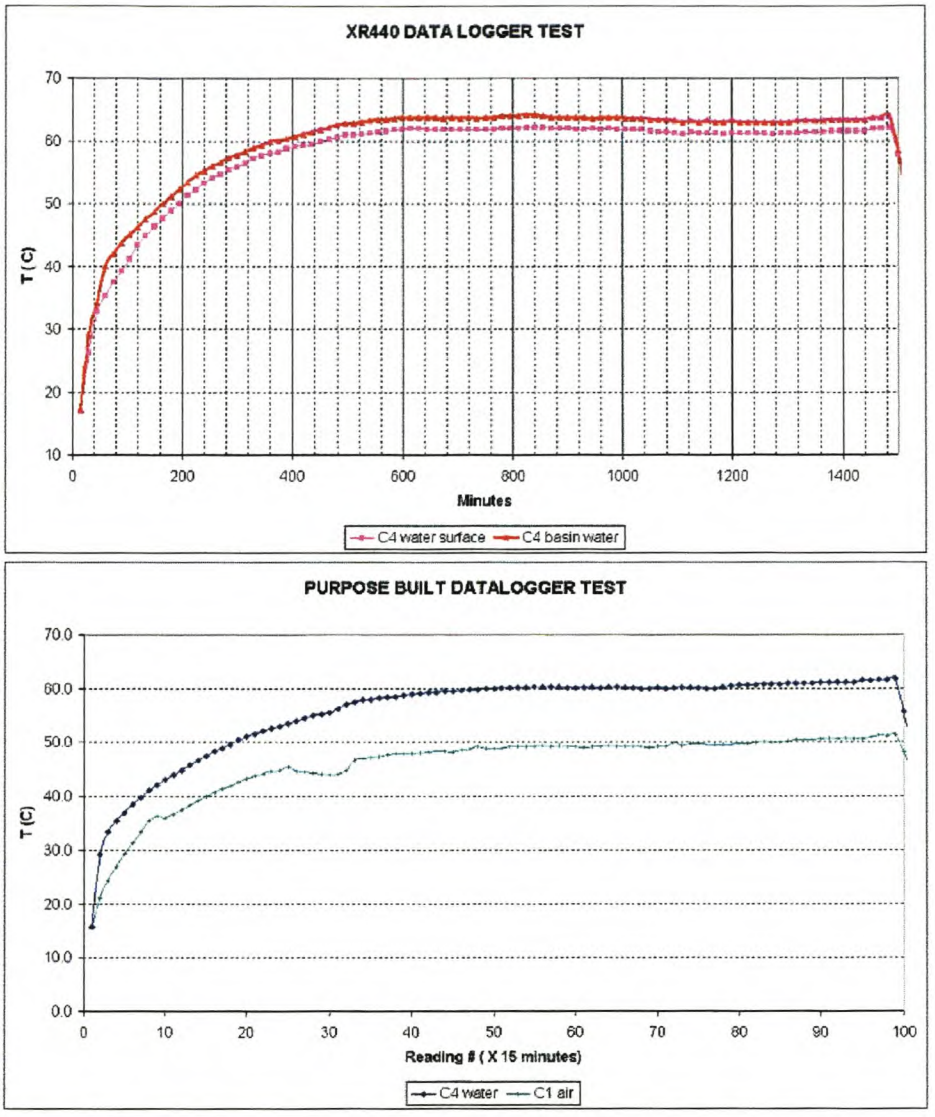

Figure 7.3: Typical temperature profiles obtained with Pace Scientific (top) and custom built (bottom) data logger.

Distillation rates and volumes were measured volumetrically by placing a calibrated siphon discharge, modified from a GC fraction counter, in the distillate piping. The occurrence and time of discharge of a fixed volume of distillate were counted and recorded electronically by electrodes measuring the current loss on discharge. Figure 7.4 presents a diagram of the apparatus, while Figure 7.5 shows typical results.

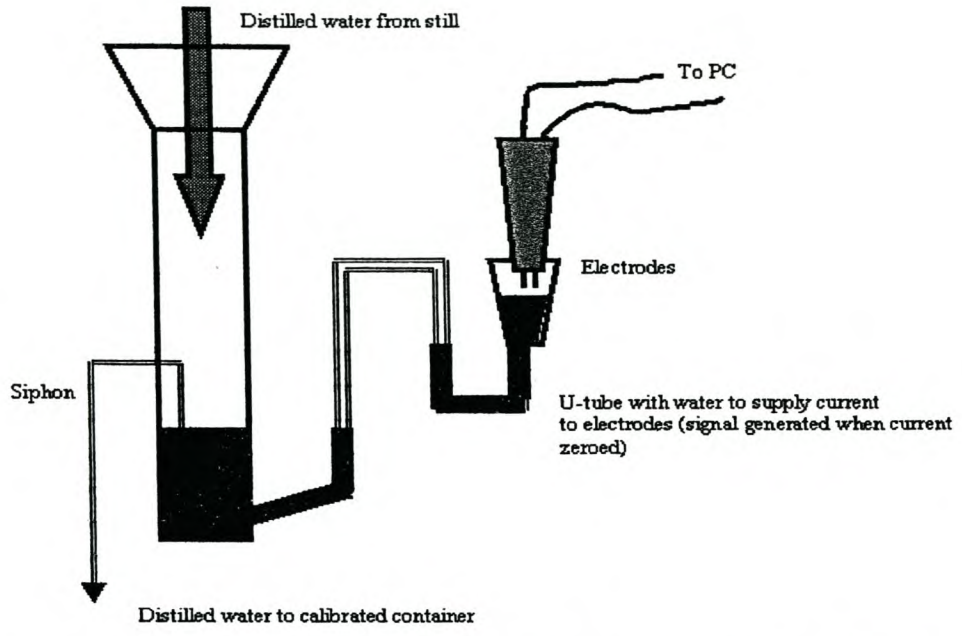

Figure 7.4: Volumetric discharge container used for measurement of distillation rates and volumes.

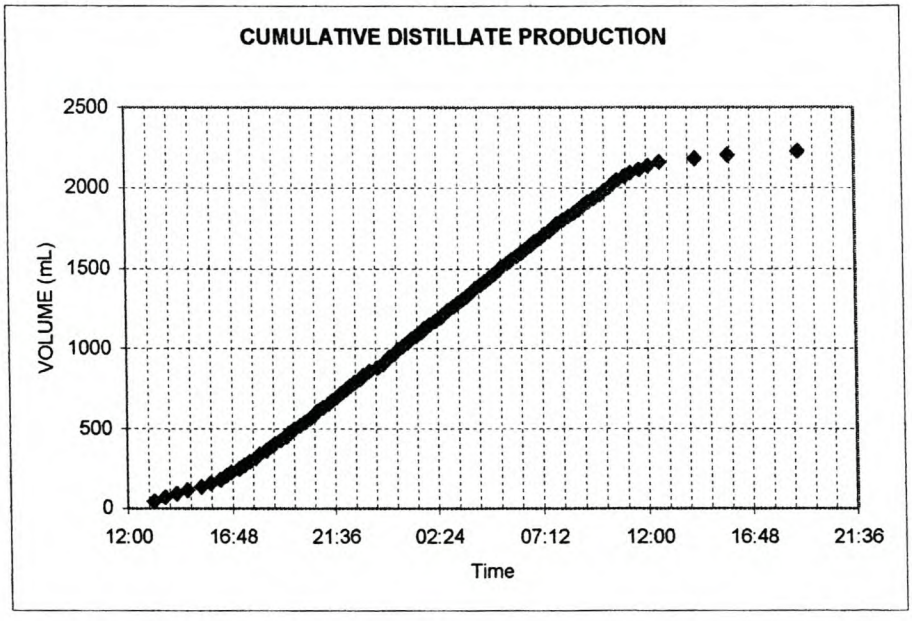

Figure 7.5: Format of results from siphon volume counter.

Radiation distribution from the incandescent lamps onto the still covers was measured qualitatively with a Macken Instruments P20Y calorimeter-type power probe. This was done by first zeroing the probe inside a dark container and then

exposing the absorbing head for one minute to the light source. With the experimental set-up pictured in Figure 7.1, the radiation deviation measured at random over the still covers was less than 15% (between 1,9 and 2,2 W).

A calibrated solar cell was used to determine the approximate radiation intensity onto the still covers. This solar cell was first calibrated externally through correlation with solar radiation data on a number of cloudless days, as received from the nearby Nietvoorbij meteorological station (Figure 7.6).

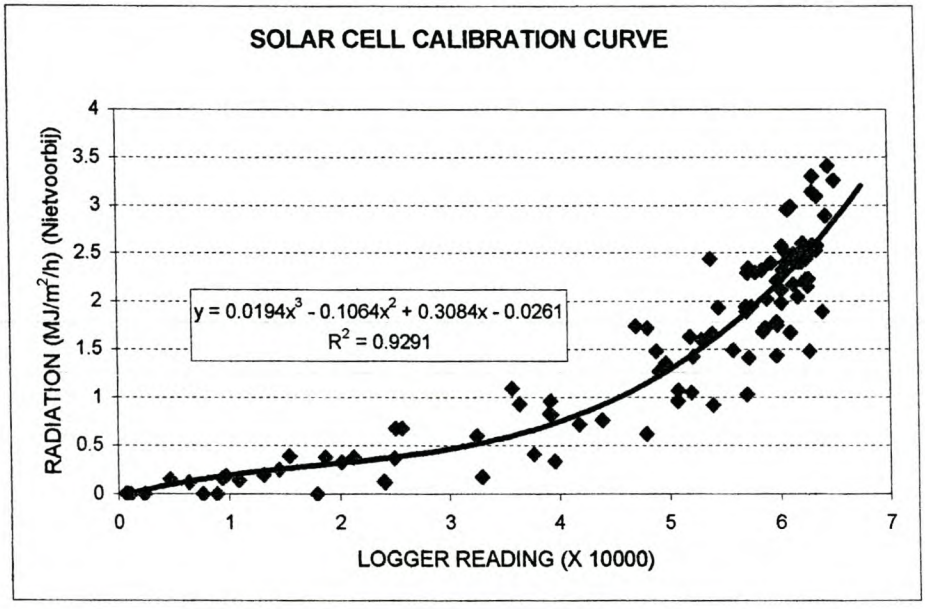

Figure 7.6: Calibration curve for solar cell used for indoor characterisation tests (hourly values measured on cloudless days).

Using the above curve, it was possible to correlate the indoor radiation intensity under clear lamps with solar radiation (Figure 7.7).

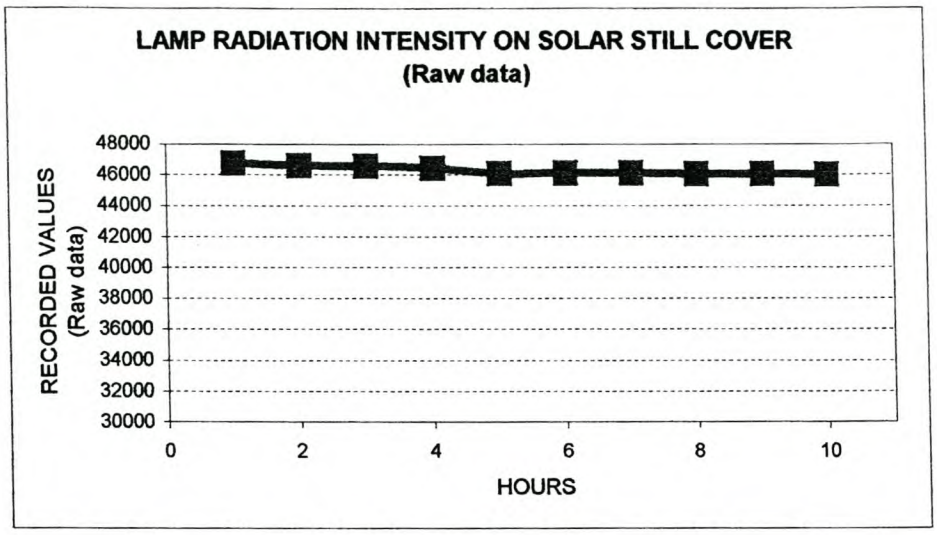

Figure 7.7: Radiation intensity from Siccatherm lamps on still covers (raw data).

Using the calibration curve established in Figure 7.6 and the productivity equation $P = 0.3541e^{0.09923\,R}$ (Equation 3.1) as determined for the still C1 (see Section 3.3.2), a productivity correlation graph for different in-house radiation exposure periods was drawn up (Figure 7.8).

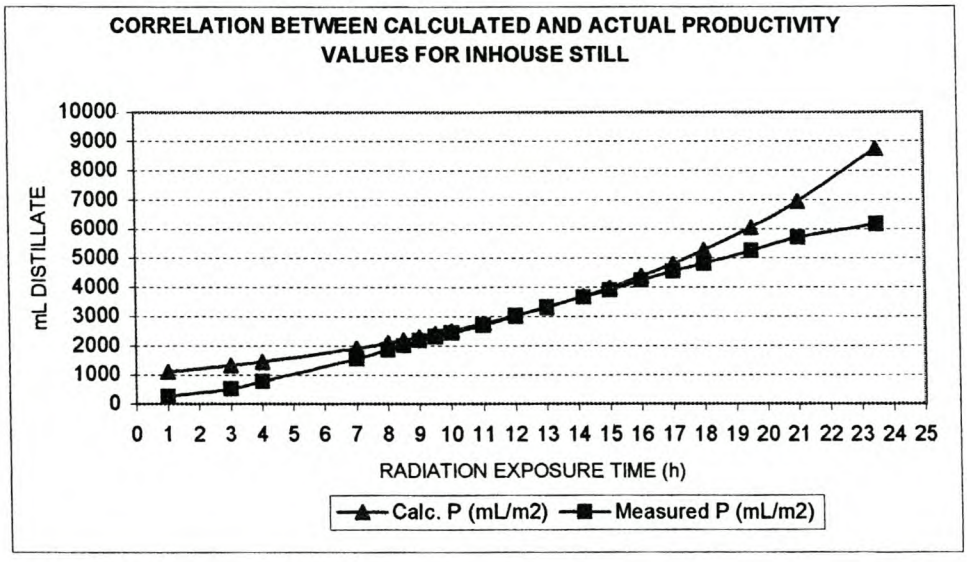

Figure 7.8: Correlation between measured and calculated distillate volumes for in-house still (still C1, clear lamps, radiation intensity as per Figure 7.7).

7.3 Conclusions and recommendations

From Figure 7.8 it can be seen that under the specific experimental conditions, the best productivity correlation with expected field values will be obtained between 8 and 18 hours (equal to total radiation of between 8 and 18 MJ/m^2). This means that this particular experimental test arrangement is particularly well suited for simulating conditions corresponding to low solar radiation, such as can be expected with low daily direct sunshine hours (e.g. winter and cloudy days, see Figure 3.11). These are also the conditions that affect efficiency negatively (Figure 3.14), and therefore this configuration was deemed suitable for investigating efficiency improvement (following Chapters).

CHAPTER 8

IN-HOUSE TESTING OF SOLAR STILLS: FIXED POSITION RADIATION

8.1 Introduction

Using the experimental set-up and measuring equipment described in Chapter 7, simulation experiments were conducted to characterise and explain solar still behaviour under conditions of low radiation.

8.2 Experimental and results

Clear and red SICCATHERM lamps were used throughout (Figure 7. 9). The radiation cycles were 24 hours (from lamps switch-on to lamps switch-off). Distillation volumes and rates (where possible) were recorded as the main experimental responses.

8.2.1 Standardisation

First it was necessary to standardise C1 (still with black liner, see Section 7.2.2) in terms of productivity relative to the specific experimental conditions. This was carried out in duplicate under clear lamps by placing C1 first in the left-hand position and then in the right-hand position (see Figure 7.1). Figure 8.1 shows the good repeatability of the volumes distilled water produced in the two different positions.

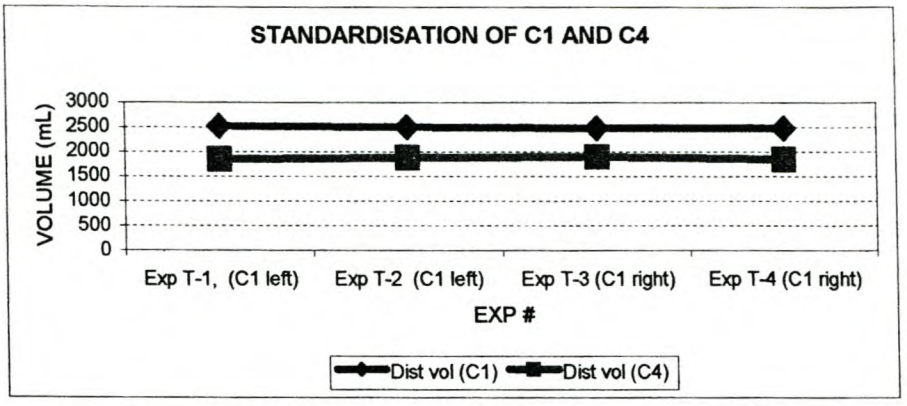

Figure 8.1: Comparison of the distillation volumes of C1 (still with black liner) and C4 (still with white liner).

Figure 8.1 shows that the productivity of C1 is about 34% better than C4. This relationship was used as a control throughout the rest of the experiment. C1 was kept in the right-hand position for the duration of the subsequent test runs.

8.2.2 Clear lamps vs. red lamps

The experiments described in Section 8.2.1 were repeated with red lamps instead of the clear lamps to investigate the influence of a lower radiation intensity and a narrower but longer wavelength band on the stills' productivity (Figure 8.2).

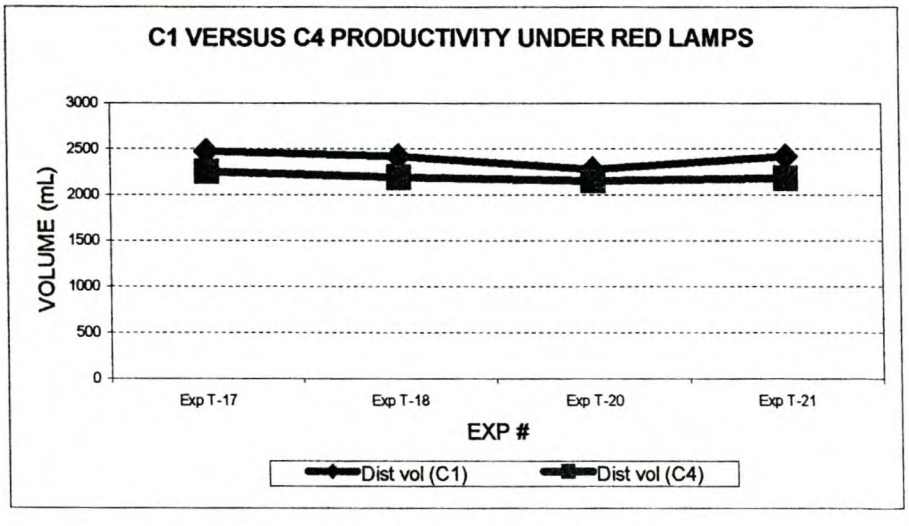

Figure 8.2: Productivity of C1 and C4 under red lamps.

A comparison of the average productivity values from Figures 8.1 and 8.2 expressed as a percentage of C4 productivity under clear lamps shows the trend:

C4 (clear, 100%) < C4 (red, 117%) < C1 (red, 128%) < C1 (clear, 134%).

Actual values are given in Figure 8.3.

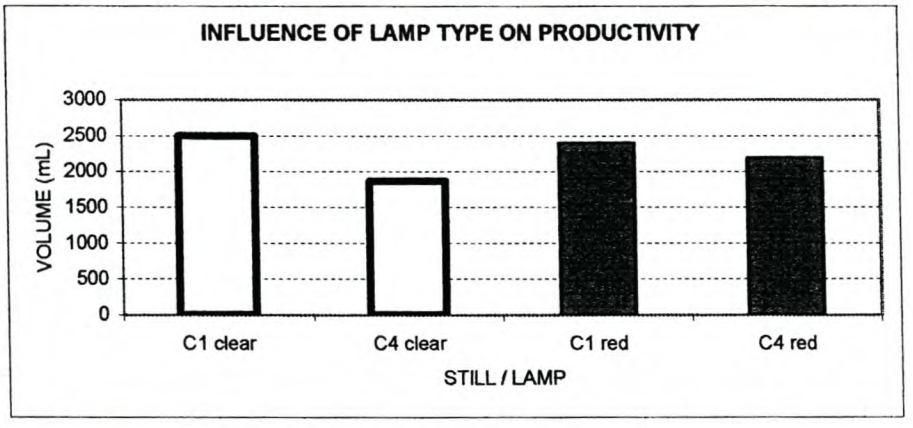

Figure 8.3: Productivity comparison of C1 and C4 under clear and red lamps.

8.2.3 Temperature profiles inside the still

The temperature profiles inside a still exposed to atmospheric conditions have been presented in Section 3.3.4. It was seen that so many variables exist because of the dynamic non-steady state of the environmental conditions. Should each and every one be taken into account, it would make optimisation studies practically impossible. For the purpose of this part of the in-house simulation, the number of variables has been reduced to the type of radiation (i.e. from clear or red lamps). This was purposefully done so that the responses discussed in Section 8.1 could be related to changes to the still.

Figure 7.3 presented typical temperature readings that were recorded during test runs. The temperature profiles comprised three parts, namely an initial heating curve followed by constant temperature, and then a cooling down curve once the lamps were switched off. Experiments were consequently conducted where the

air temperatures (20 mm above water surface) and basin temperatures (basin floor) were recorded for the different arrangements presented in Figure 8.3. Figure 8.4 shows typical recorded temperature profiles for C1 under red and clear lamps.

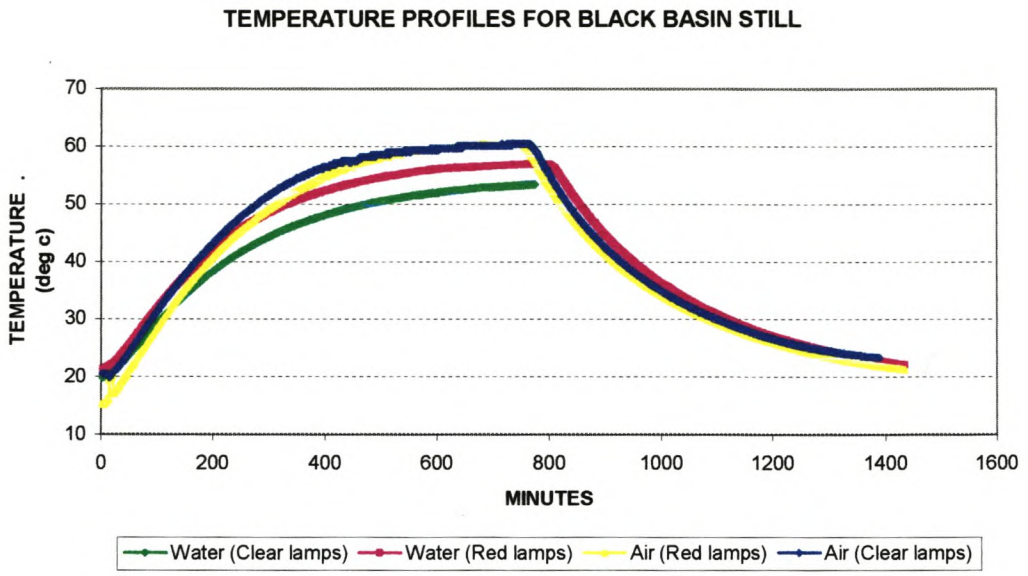

Figure 8.4: Temperature profiles for black-lined stills under red and clear lamps.

Figure 8.5 compares the water and air temperatures for all experiments, presented as the increase from start temperature, i.e.

$$T_{plot} = T_t - T_0.$$

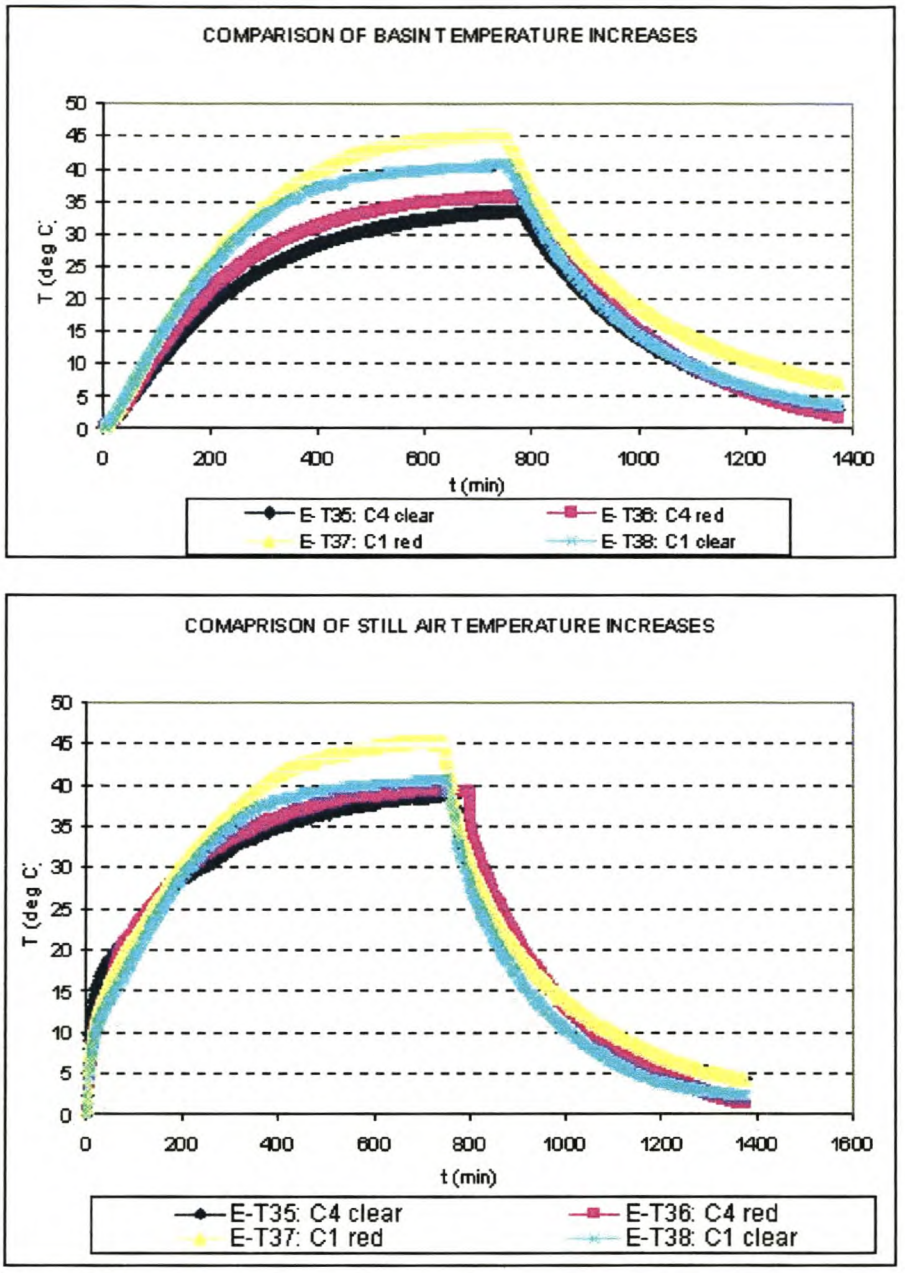

Figure 8.5: Comparison of water and air temperature increase profiles for black- and white-lined stills under red and clear lamps.

8.2.4 Effect of still colour

The importance of having a black radiation-absorbing surface in contact with the water in the still basin has been discussed in Section 3.2.1 and implemented in Section 7.2.2. It has been experimentally demonstrated for the specific test

conditions in Section 8.2.1 and Section 8.2.2. In practise, however, factors such as scale formation and salt deposits occur, which can cause the 'degree of blackness' of a still to decrease. Two sets of simulations with respect to the degree of 'blackness' were conducted, first by precipitating $CaCO_3$ on the basin of C1, and the second by varying the degree of 'blackness' of C4.

8.2.4.1 *Scaling*

C1 was filled with hard water with known high scale-forming potential (TDS 7552 mg/L, calculated Langelier Saturation Index of 1.986, see Section 4.2) sampled from a well near Brandvlei, Northern Cape. The still was subjected to repeated radiation cycles as described in Section 8.1. It was flushed and filled with well water between cycles to maintain the same storing volume.

Sedimentation began soon after the first radiation cycle had commenced, and increased noticeably during each cycle despite the flushing. A thin sediment layer evenly covered the still basin after completion of the fifth cycle. (This layer was collected through filtration, air-dried and analysed by X-ray diffraction spectroscopy as being a mixture of Calcite and Aragonite). The rate of water production per cycle is given in Figure 8.6.

8.2.4.2 *Blackening of basin*

Commercial polyethylene shadow netting of different mesh sizes was fixed to the still basin and used to obtain different degrees of blackness (0%, 20%, 40%, 85% and 99%). Each experiment to determine the 'blackening effect' on productivity of the still was carried out in triplicate. The total distillate ratios C1:C4 are given in Figure 8.7.

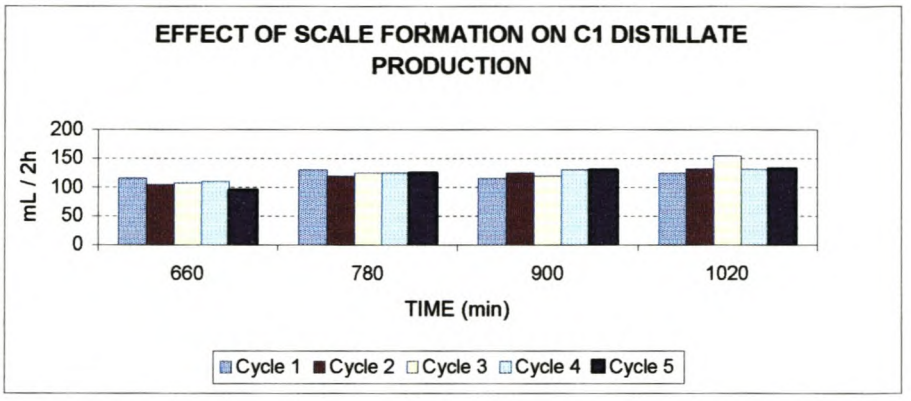

Figure 8.6: Influence of scale formation on C1 productivity.

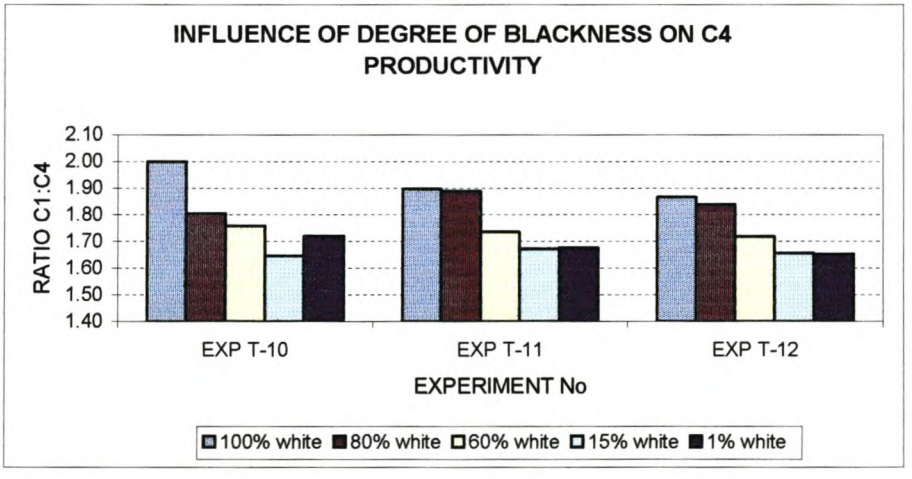

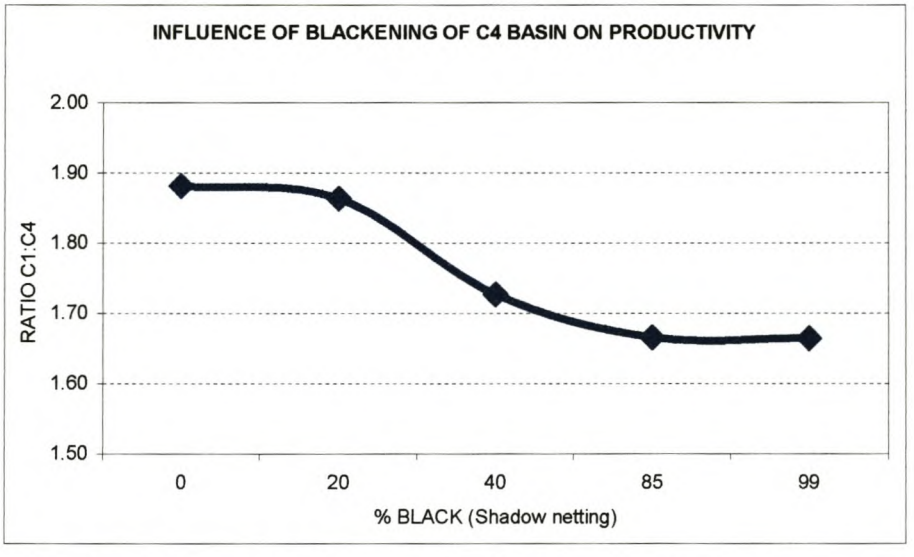

Figure 8.7: Influence of blackening of C4 basin on distillate ratio C1:C4.

8.2.5 Influence of lining

The required properties of suitable lining materials were discussed in Section 5.2.3. Two commercial materials were recommended for further investigation, namely silicone sealant ('Bostik 2550') and hollow polypropylene sheets ('Correx'). Experiments were subsequently carried out with the basin floor of the white C4 still covered with the respective lining materials, and the effects thereof on the productivity of C4 were monitored with C1 as reference. Due to the suitability of the experimental set-up, further experiments were also conducted using floating medium density black polyurethane foam and with glazed black ceramic tiles placed on the basin floor.

To determine any productivity shifts, experiments were again conducted in triplicate, and repeated under red lamps. The results are summarised in Figure 8.8 in order of increasing productivity.

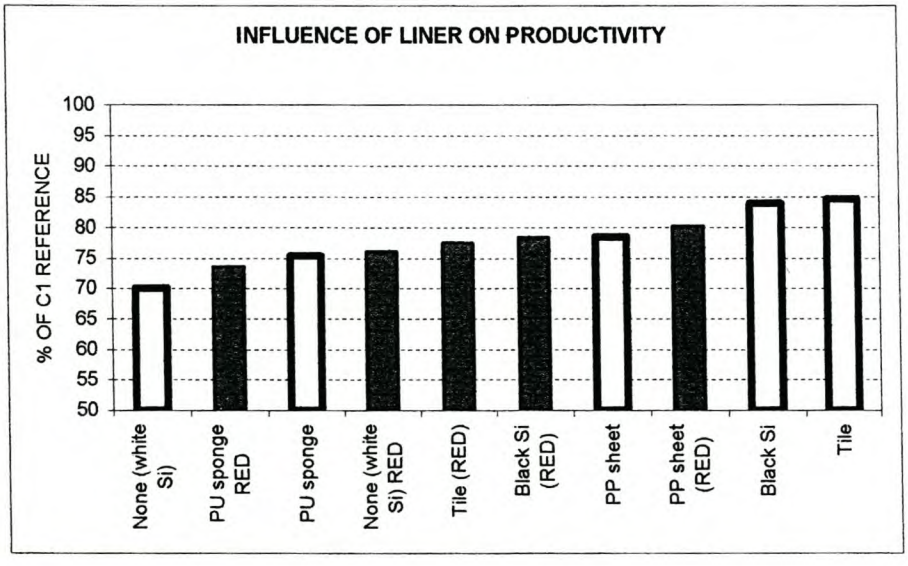

Figure 8.8: Influence of lining on C4 productivity.

8.2.6 Influence of water depth

The influence of the water depth (i.e. water volume) on the distillation rate was

investigated by radiating C1 until all the water had evaporated. The radiation cycles were 12 hours, followed by a 12-hour cooling down period. The still air and basin temperatures, as well as the distillation volume per day, were recorded. The results are given in Figure 8.9.

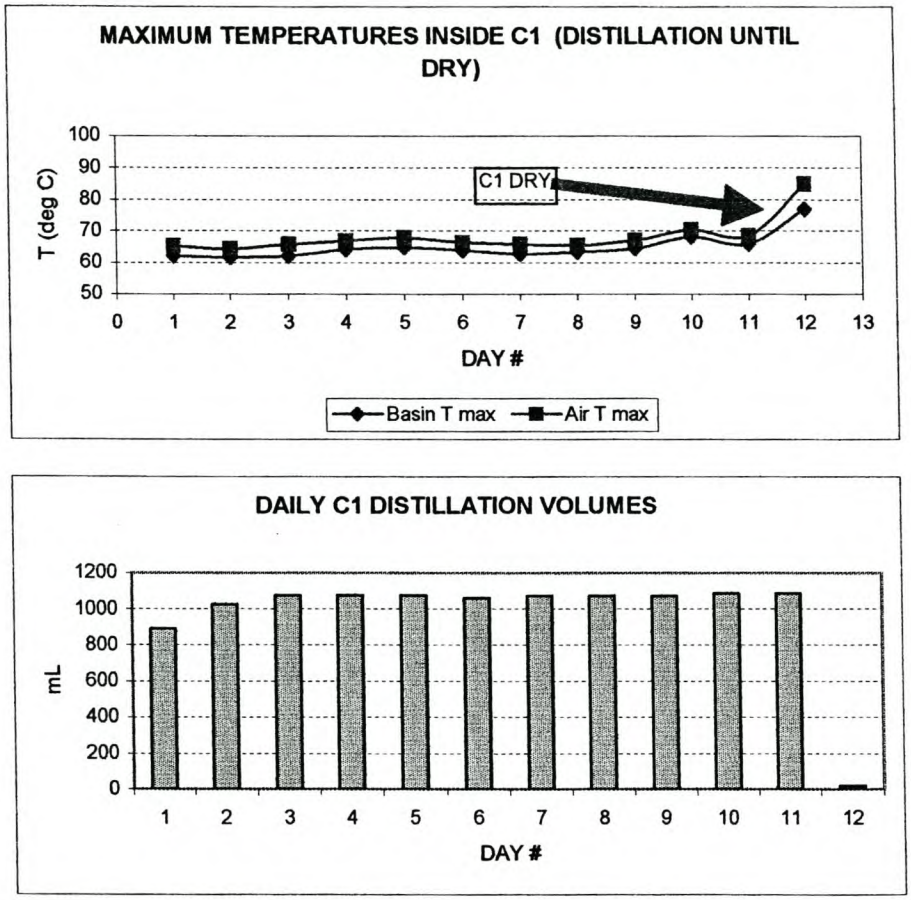

Figure 8.9: Thermal and productivity behaviour of C1 during distillation until dry.

8.3 Discussion

After completion of the experimental investigations described in Section 8.2, the results were analysed to determine the suitability of the test configuration for continued simulation testing, as well as to implement possible improvements.

8.3.1 Operation

Figure 8.1 showed that under the clear lamps the productivity of the black still (C1, lining containing carbon black) was consistently about 34% higher than that of the white still (C4, lining containing TiO_2). As both stills were similar in construction (Section 7.2.2) and had similar water depths (30 mm) and volumes (12500 mL) at the start of the radiation cycle, the difference in productivity could only be attributed to the lining. It was therefore necessary to review the heat flows presented in Figures 3.2 and 3.3 for the two different stills.

Direct radiation from the SICCATHERM lamps (H_{lamp}) will be partially reflected ($H_{ref\text{-}glass}$) and absorbed ($H_{abs\text{-}glass}$) by the glass cover. More than 80% of the radiation with wavelengths between 330 and 2470 nm will however be transmitted through the glass (H_{trans}), as with solar radiation (Figures 6.7 and 7.2). A fraction of H_{trans} is then reflected from the water surface ($H_{refl\text{-}water}$), while the remainder passes into the water. According to Figure 6.9, radiation with wavelengths between 330 and 1330 nm (i.e. including the full visible portion of the lamp spectrum) will pass through the water and onto the lining ($H_{trans\text{-}water}$). Longer wavelengths in the near-infrared region up to 2740 nm will be also be absorbed by the water ($H_{abs\text{-}water}$).

Up to this point the heat flows for the two stills should theoretically have been the same. The main difference from here onwards was the high degree of heat absorption by the black lining of C1 ($H_{abs\text{-}lining}$), and of heat reflection by the white lining of C4 ($H_{refl\text{-}lining}$). In the case of C1, $H_{abs\text{-}lining}$ further enhanced the water heating process by conducting heat into the water. With C4, however, this contribution is negligible and the only advantage is possibly additional absorbance due to the longer path length of the scattered radiation inside the water. Further, heat absorbed by the black sidewalls of C1 will generate longer wavelength radiation, which will also be better absorbed by the surroundings (including the basin water) than in the case of C4.

A closer analysis of the different heating profile stages as presented in Figure 8.4 best illustrates the difference in temperature responses for the stills. Figure 8.10

presents the temperature changes of the water and the air during the first 20 minutes of the radiation cycle.

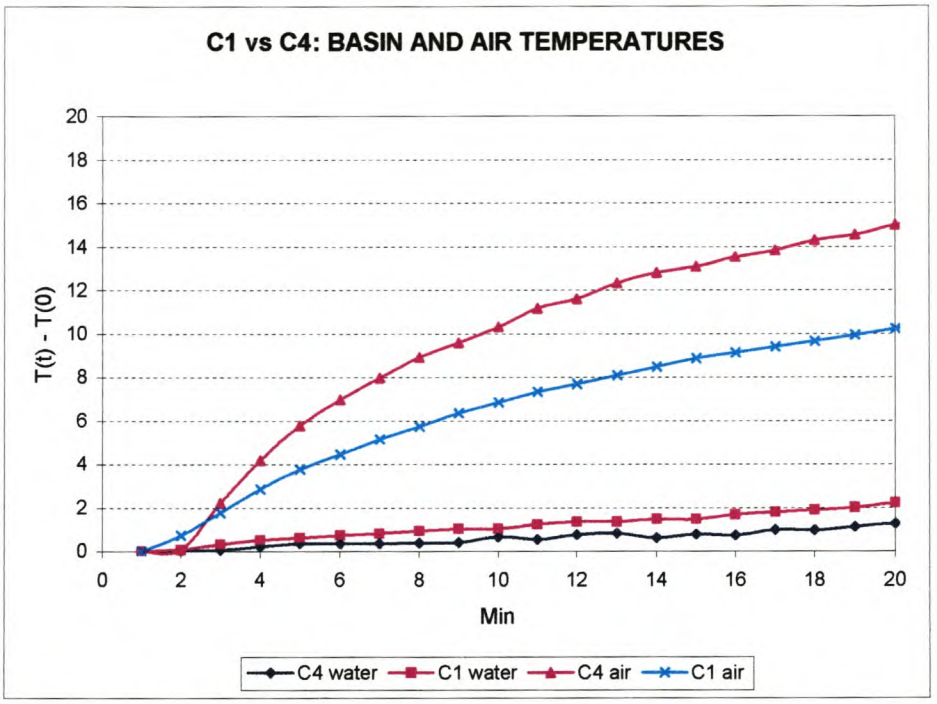

Figure 8.10: Temperature increases during first 20 minutes of radiation cycle.

Figure 8.10 shows that the air temperatures inside the stills increase quickly due to the low heat capacity of the enclosed air mass. More importantly, that of C4 air temperature increases faster than that of C1 because of $H_{refl\text{-}lining}$. However, the water temperature of C1 increases faster than that of C4 due to $H_{abs\text{-}lining}$. The increase in C4 water temperature can thus be attributed mainly to the absorption of radiation by the water, with a small contribution convected from the heated air mass above the water.

After the initial heating phase, a second phase of nearly linear heating can be distinguished between 40 and 200 minutes (Figure 8.11).

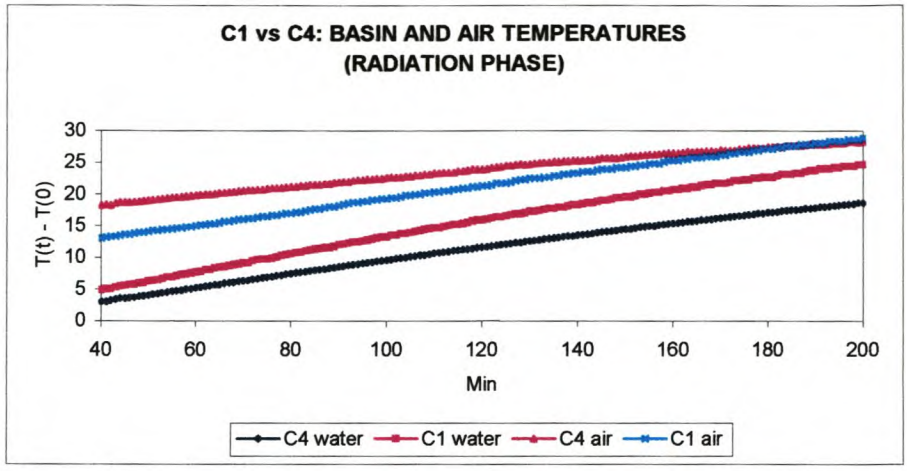

Figure 8.11: Temperature increases between 40 and 200 minutes of radiation cycle.

During the above period the temperature of the water in C1 increased faster than in C4 (C1 has a higher heating constant), which indicated the contribution of the heat generating black lining. C1 air temperature also increased faster than C4, as the cover absorbs longer wave radiation from the water *and* sidewalls. The last stage of the radiation cycle exhibited polynomial character (Figure 8.12), and it can be seen that the temperatures of C1 had practically stabilised while C4 temperatures were still marginally increasing.

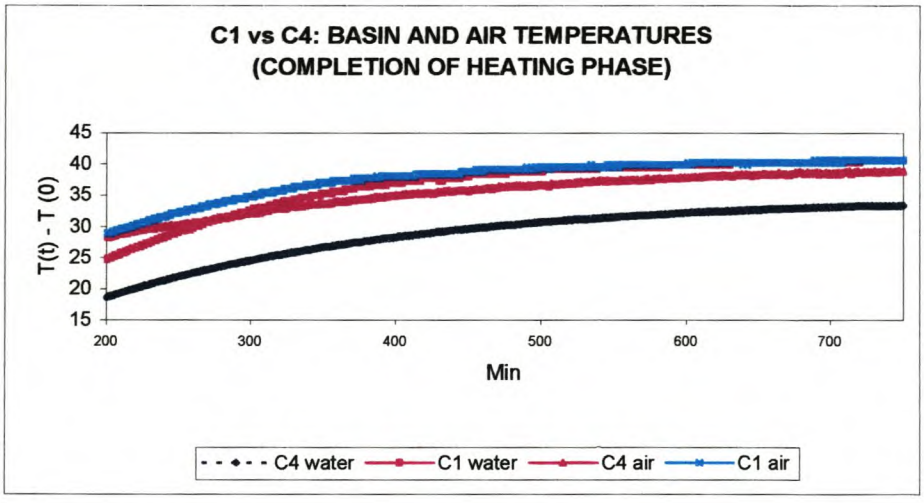

Figure 8.12: Final temperature profiles of radiation cycle (to switch-off of lamps).

Figure 8.12 also shows that the water and air temperatures inside C1 were nearly the same and higher than in C4, and that the maximum air temperature of C4 was distinctly higher than the water temperature, illustrating the heat deflecting nature of the white still.

It was also possible to calculate the expected temperature increases inside the stills by using the formulae presented in Figures 8.11 and 8.12. As an example, Figure 8.13 shows the correlation between calculated and actual C1 water temperatures during follow-up experiments. Productivity will be improved especially under conditions of limited radiation where (a) the basin water heats up fast and (b) high operational temperatures inside the still are achieved. These equations are therefore useful for comparative studies.

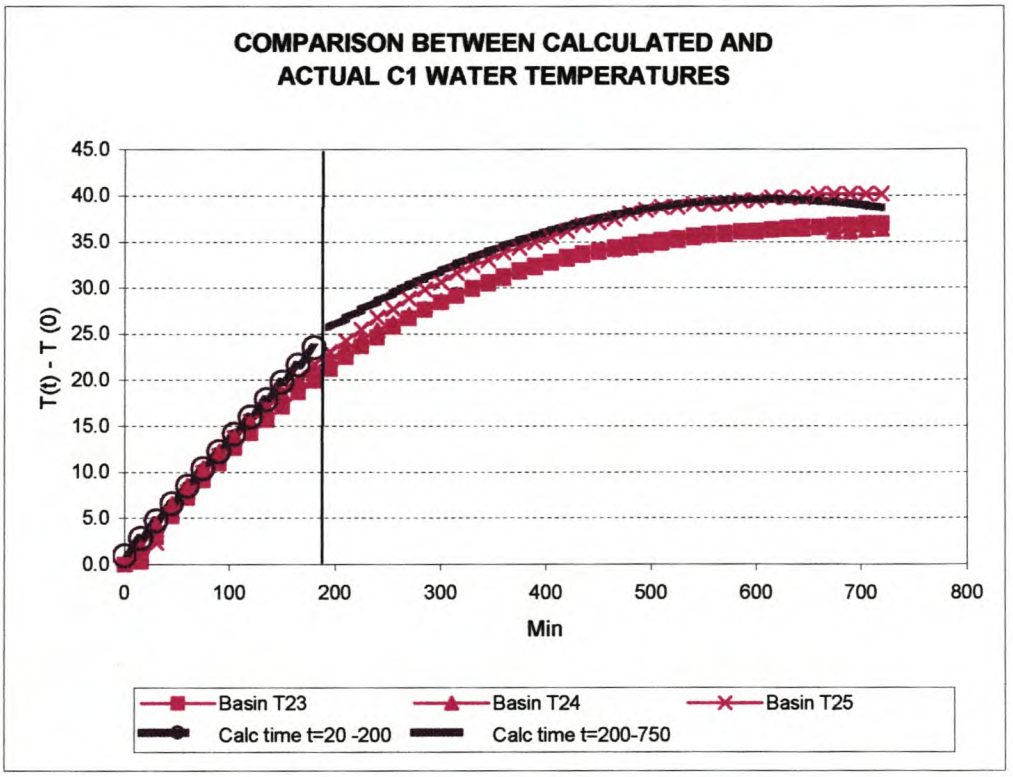

Figure 8.13: Calculated vs. actual C1 basin temperatures. Basins T23 to T25 refers to the numbers of the consecutive experiments.

The following conclusions are drawn from this part of the study, namely:

- A black absorbing surface on the inside of a basin still will improve the productivity (and efficiency) of the still. Under conditions of low radiation dosage (24 MJ or less) this increase can be up to 34%.
- The maximum water temperature inside a white still will be lower than in a black still due to heat being reflected away. Radiation absorption will mainly take place in the water (Figure 6.9). From the distillation data it can be seen that this component of the heat transfer into the water is however the most important, otherwise the productivity ratio C4:C1 would have been less than 0,5.
- The system's efficiency will be improved if more incoming radiation energy can be converted into longer wavelength internal radiation (Figure 6.9), which can also be absorbed by the water. Increased absorption under conditions of low external radiation dosages will maximize internal temperatures, which in turn will enhance the evaporation process and thus distillate production, resulting in higher productivity e.g. in winter months. Inspection of Figures 6.7 and 6.9 suggests that radiation with wavelengths between 357 and 1330 nm must be converted to wavelengths longer than 1330 nm. If this conversion can be effected below the glass, the maximum wavelength can go up to 6260 nm (1597 cm^{-1}). This represents the centre of the absorption band of the bending vibration of the water molecule.

8.3.2 Clear lamps vs. red lamps

The use of red lamps instead of clear SICCATHERM lamps resulted in little change in C1 productivity (-5%), but a more significant improvement in C4 productivity (+17%). The internal heating profiles were subsequently analysed, as described in the previous Section, to obtain mathematical heating equations. Results are shown in Figures 8.14 & 8.15.

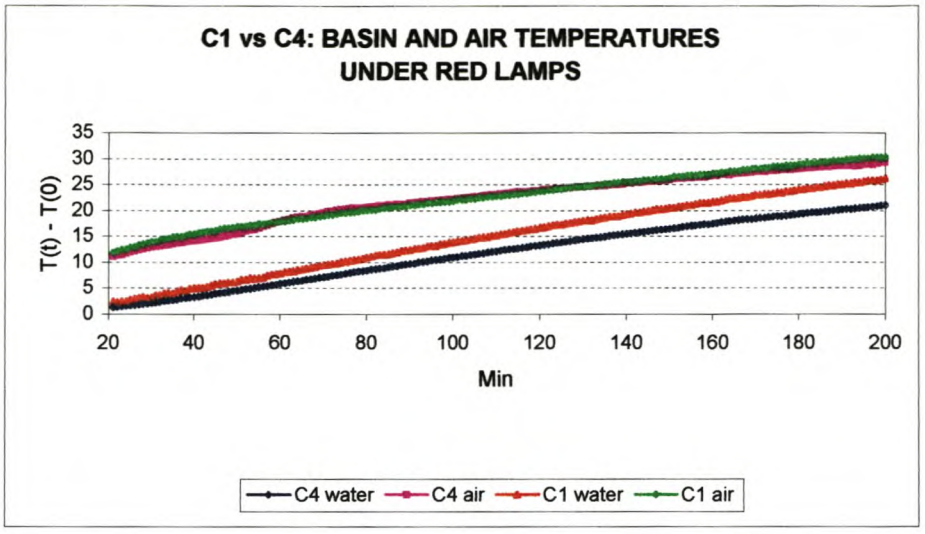

Figure 8.14: Temperature increases between 40 and 200 minutes of radiation under red lamps.

Comparing the heating constants obtained from Figure 8.11 and Figure 8.14, it can be seen that in the case of C4, both the rate of air heating,

$$k_{RED} = 0.095 \text{ vs. } k_{CLEAR} = 0.064 \ (\Delta = 0.031)$$

as well as the rate of water heating,

$$k_{RED} = 0.1139 \text{ vs. } k_{CLEAR} = 0.0987 \ (\Delta = 0.0152)$$

are higher under red lamps. For C1 the corresponding differences were –0.0042 (Δ_{AIR}) and 0.0106 (Δ_{WATER}) respectively, i.e. less of an influence. The order of productivity was the same as the order of the heating constants.

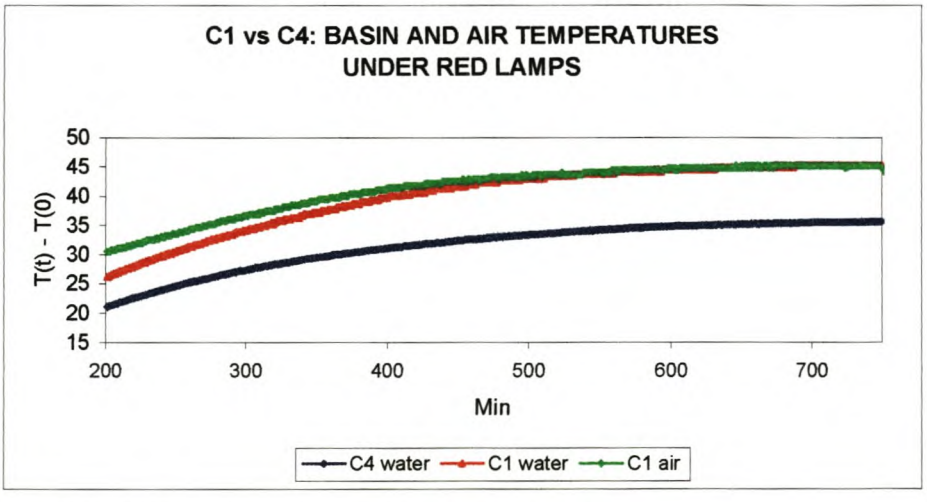

Figure 8.15: Temperature profiles under red lamps.

A comparison of Figures 8.12 and 8.15 shows that the heating profiles under red lamps were similar to those recorded under clear lamps, and (a) again the basin and water temperatures of C1 merged at the maximum, and (b) again the air temperature of C4 remained higher than the water temperature. The temperature increases were in both cases greater under the red lamps than under the clear lamps (also see Figure 8.5 for complete profiles).

The increase in productivity of C4 under red lamps could be explained by the shift of the radiation spectrum of the red lamps to higher wavelengths (Figure 7.2), i.e. relatively more energy was available for absorption by the water in the near-infra-red region in spite of the lower overall output of the red lamps. The slight decrease in C1 productivity could be explained similarly, as the absence of energy transferred into the black lining by shorter visible light wavelengths is offset by the increase in water absorption due to the above-mentioned radiation spectrum shift.

The results obtained with red lamps therefore support the suggestion that the conversion of radiation to longer wavelengths within the solar still will enhance productivity of a solar still.

8.3.3 Changes to basin colour

Sections 8.2.4 and 8.2.5 presented results for stills with different linings and / or varying degrees of blackness. In all cases the productivities were between those obtained with C4 and C1. The following conclusions are drawn from these results (for clear lamps):

- Scale or salt precipitation gradually forming on the basin of a black-lined still will not effect productivity drastically even if the basin floor is fully covered by the sedimentation. The black sidewalls still absorb and radiate enough heat into the basin to maintain a nearly constant distillation production rate.

- Gradual blackening of the basin floor of a white-lined still can increase the productivity by about 20%, which confirms the contribution made by lining heat absorption.
- Better performance improvement was obtained when a black lining was placed on the C4 basin floor than when a floating black foam sheet was submerged in the water. This can possibly be attributed to the very thin (even non-existing) water layer on the hot foam surface, a condition that will worsen in saline water if such a foam sheet is not optimised in terms of density and porosity.
- Under the experimental conditions of low and perpendicular radiation, the productivity of C1 did not change significantly as the water volume decreased. (As the radiation intensity increases, the lining will become relatively warmer and conduct more heat into the water, which then will heat up faster as its volume decreases, speeding up the evaporation process.)

- Solid black linings (silicone, polypropylene, ceramic tiles) placed on the bottom of the C4 basin improved performance by between 11% and 20%, again through the better utilisation of the wavelengths between below 1300 nm.

8.4 Conclusions and recommendations

The investigations and results described in the above Sections proved that under conditions of low radiation, the use of a black-lined still will yield the best productivity results, even if the basin of such a still is discoloured by physical contaminants such as scale. It was also qualitatively shown that absorption by the incoming radiation plays the primary role in water heating while heat transfer from the lining is secondary.

On the basis of the above, a new series of experiments was designed to:

- determine the influence of the angle of radiation inclination on productivity of the specific basin solar still design (see Chapter 9),

- improve productivity under low radiation conditions (Chapter 10),
- determine the influence of variation of radiation intensity on productivity (see Chapter 11), and
- determine the correlation between field and in-house results (Chapter 11).

CHAPTER 9

IN-HOUSE TESTING OF SOLAR STILLS: RADIATION FROM DIFFERENT ANGLES OF INCIDENCE

9.1 Introduction

Different parameters that influence solar still productivity were investigated in the previous Chapter, namely the effect of different wavelength bans of radiation, the colour of the solar still lining and the water depth inside the solar still basin. These investigations were all carried out with the radiation source placed directly above the still. In this Chapter, the productivity of the chosen solar still design is studied under conditions of radiation from different angles i.e. the angles of radiation incidence onto the still cover is varied.

9.2 Experimental and results

9.2.1 Experimental

The experimental set-up presented in Figure 7.1 was modified to allow adjustable radiation onto a test still. Eight clear Osram SICCATHERM lamps, described in Section 7.2.1, were fixed to an adjustable overhead beam. The test still was placed on laboratory jacks to allow the distance between the lamps and the still cover to remain constant irrespective of the incidence angle (see Figure 9.1). The 'black' test still, C1, described in Section 7.2.2, was used for this part of the investigation. The 16-channel analogue data logger described in Section 7.2.3 was used to record temperatures and light intensities at different positions in and around the still (see Figure 9.2). A volumetric discharge unit, similar to that shown in Figure 7.4, measured productivity over a 24-hour period. The actual radiation period per experiment was 12 hours, and angles of incidence (relative to the horizontal) were varied in 10-degree intervals from 97 ^{o} to 17 ^{o}. All experiments were carried out in duplicate.

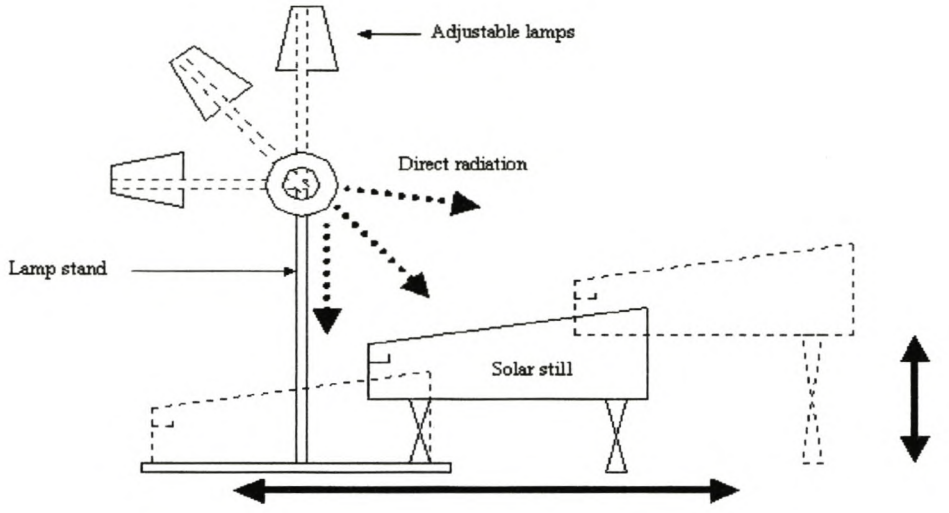

Figure 9.1: Experimental used set-up to determine the effect of different radiation angles on solar still productivity.

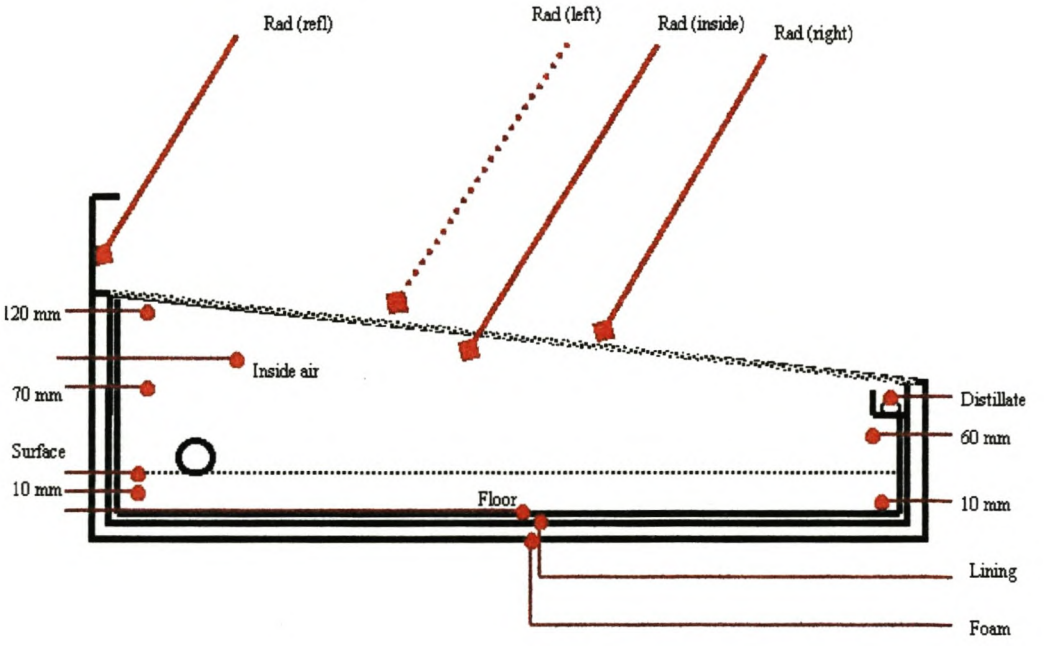

Figure 9.2: Position of temperature probes and light measurement panels on test still in experimental setup to determine influence of radiation angle on solar still productivity.

9.2.2 Radiation measurement

Three solar cells, similar to the one described in Section 7.2.3, were used to obtain *approximate* radiation values at the different measurement points shown in Figure 9.2. Solar cells were placed on the *left* side of the exterior cover perpendicular to the incidence radiation, on the *inside* of the glass cover (simulated by placing 3-mm window glass over a solar cell placed on the cover), and one cell placed *perpendicular* to the glass cover (but protected from direct radiation) to measure reflected radiation. All three cells were calibrated against a reference solar cell, and the calibration diagrams are given in Figure 9.3.

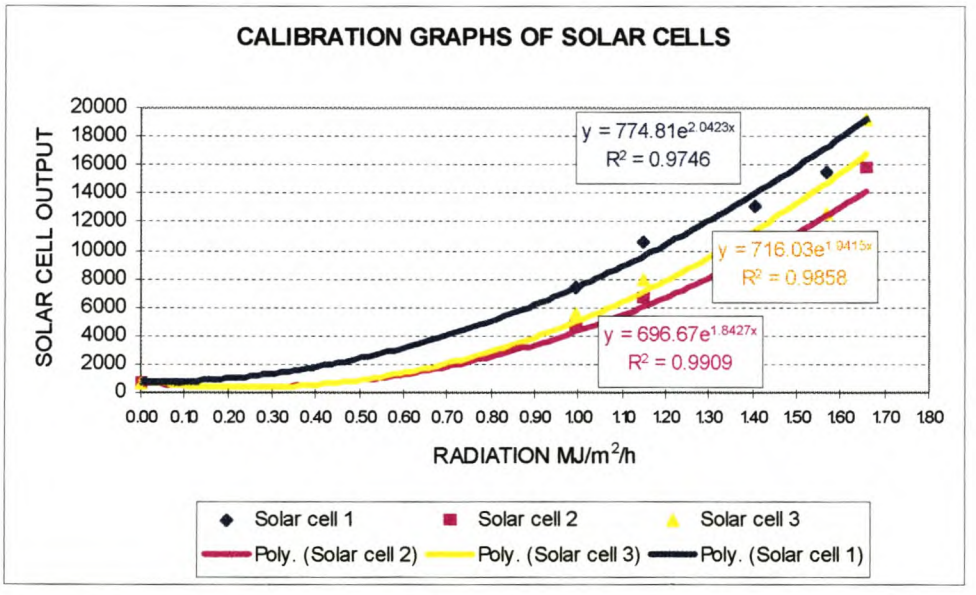

Figure 9.3: Calibration curves for solar cells.

Table 9.1 shows that constant radiation values were obtained with different angles of light incidence.

Table 9.1: Approximate radiation intensities for different light incidence angles

Angle of incidence onto still cover (relative to the horizontal)	Radiation intensity (MJ/m^2)	Underneath cover (MJ/m^2)	Reflectance (MJ/m^2)
97	1,5	1,2	0,1
87	1,5	1,2	0,2
77	1,5	1,2	0,3
67	1,5	1,2	0,3
57	1,5	1,2	0,6
47	1,5	1,2	1,0
37	1,5	1,1	1,4 (*)
27	1,5	1,0	1,5 (*)
17	1,5	0,9	1,8 (*)

(*: includes direct radiation)

Figure 9.4 shows typical radiation results obtained from the solar cells.

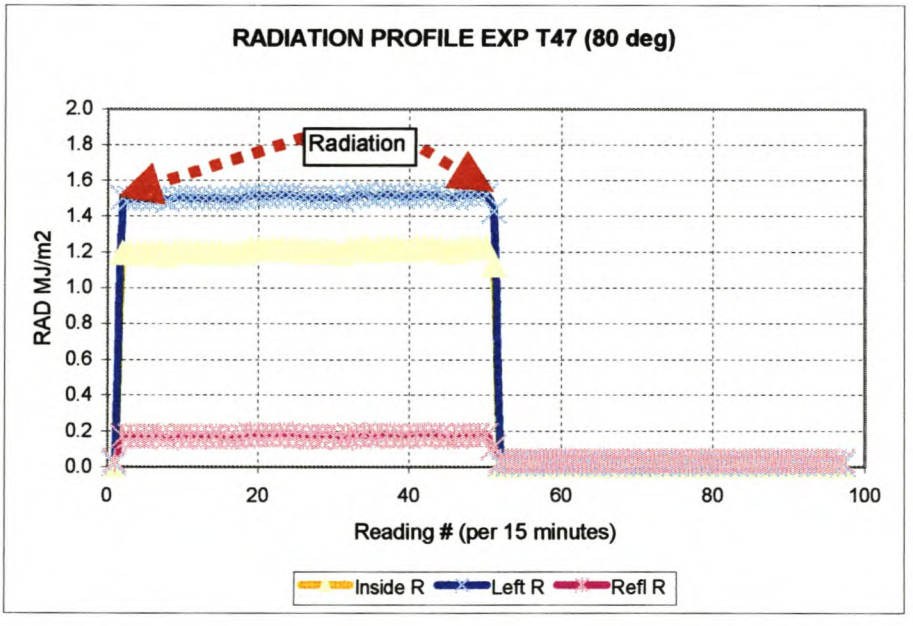

Figure 9.4: Typical radiation profiles as recorded by solar cells (radiation incidence angle 87 degrees).

9.2.3 Productivity

Figure 9.5 shows the average distillate volumes measured over a 24-hour period for different angles of incidence. Production profiles were similar to those in Figure 7.8.

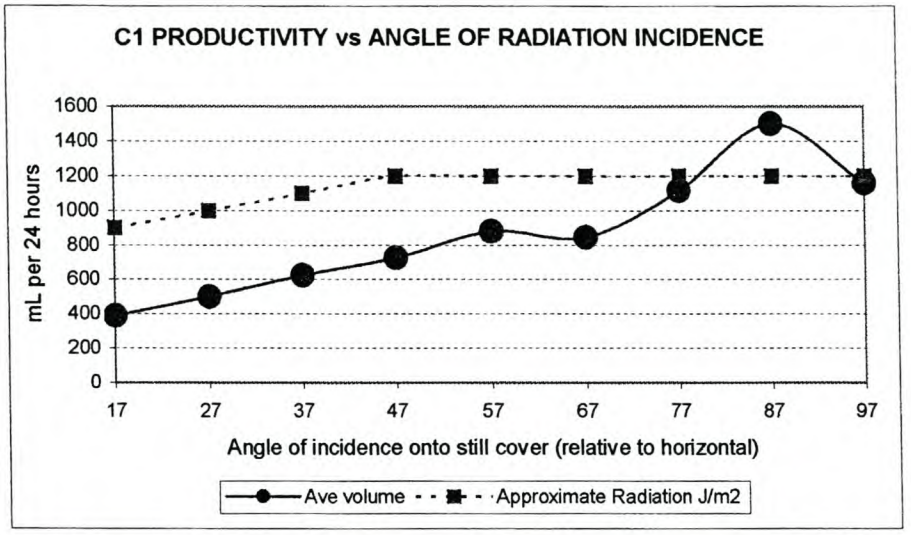

Figure 9.5: Productivity of C1 still radiated from different angles of incidence over a 24-hour period (dots) with radiation values beneath cover (squares).

9.2.4 Heating constants

Heating constants were obtained at the different temperature measurement points using the same approach as described in Section 8.3.2. The different points at which temperatures were recorded were (see Figure 9.2): air inside the still (*inside*), on the lining on the water side (*floor*) and insulation side (*lining*), 10-mm deep water on the lamp side (*N 10 mm*) and opposite side (*S 10 mm*), in the water surface (*surface*), air at different heights above the water surface (*N 60 mm*, *S 70 mm* and *S 120 mm*) and inside the insulation (*foam*). The initial linear heating profiles observed between 150 and 300 minutes of radiation were used to determine the heating behaviour inside the still. Figure 9.6 shows the heating constants for the different measurement points versus radiation incidence angle, while Figure 9.7 compares productivity with different heating constants.

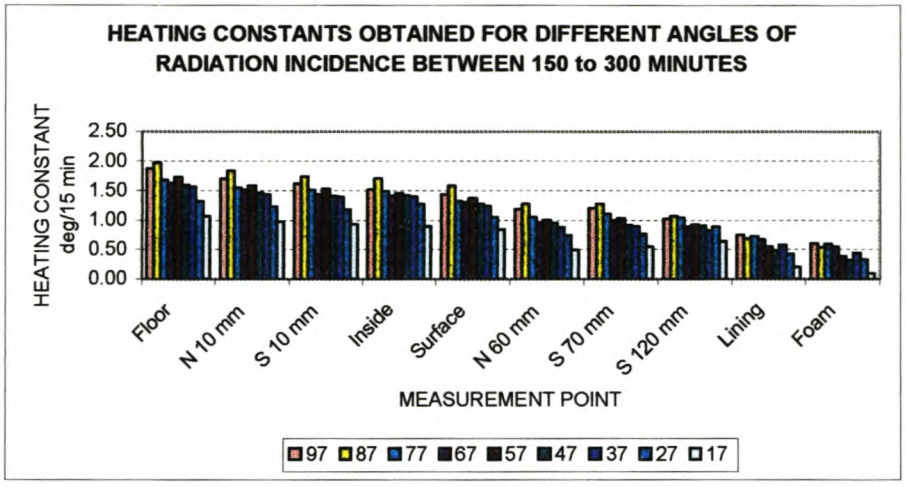

Figure 9.6: Heating constants (as a function of different radiation incidence angles, see legend) at different points inside and around the test still.

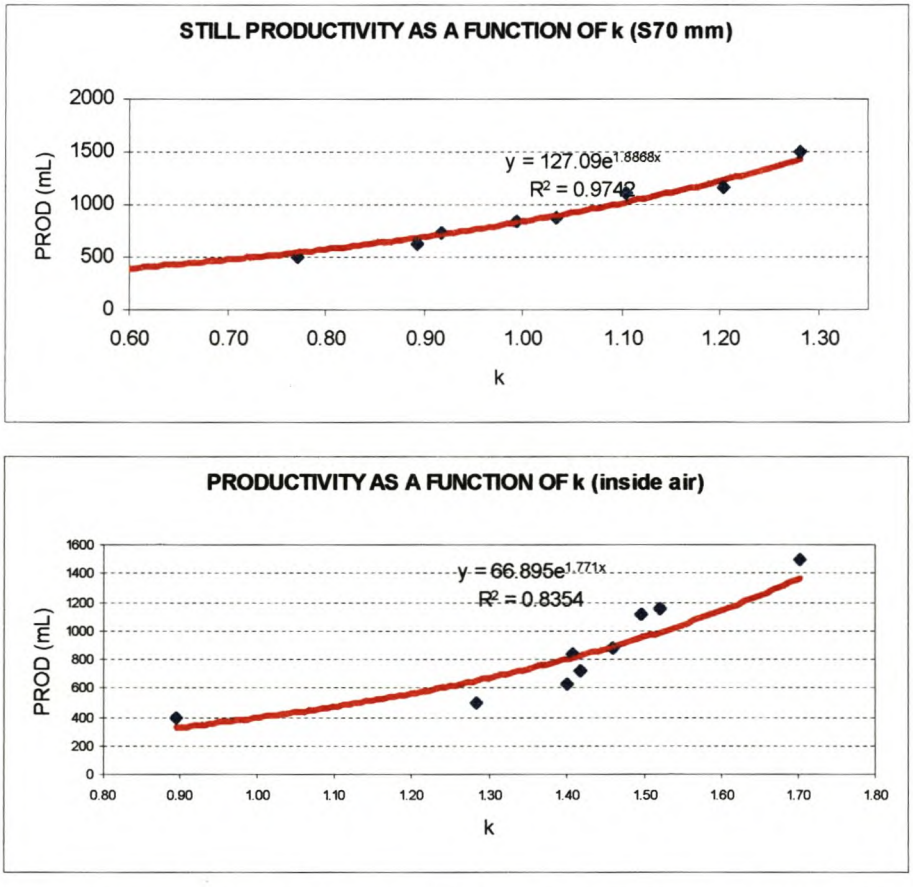

Figure 9.7: Relationship between heating constants and production volumes.

9.3 Discussion

9.3.1 Radiation

Figure 9.1 shows that although the radiation intensity onto the still cover remained constant, the simulated radiation intensity beneath the glass cover decreased when the angle of incidence dropped below 47 °. This is in correlation with the light transmission properties of window glass (see Figure 3.10). In Figure 3.17 it was shown that, under the assumption of two-dimensional radiation trajectory, the maximum amount of radiation hours directly into the basin will decrease by more than 50% from mid-summer to mid-winter, while the winter productivity decreases to about 25% of the summer maximum.

Another relevant factor is the actual water surface area receiving direct light radiation (Figure 9.8). Additional to the decreasing light intensity inside the still, the exposed water surface area also decreases rapidly with decreasing light incidence angle (i.e. the water surface directly radiated, A_i, decreases).

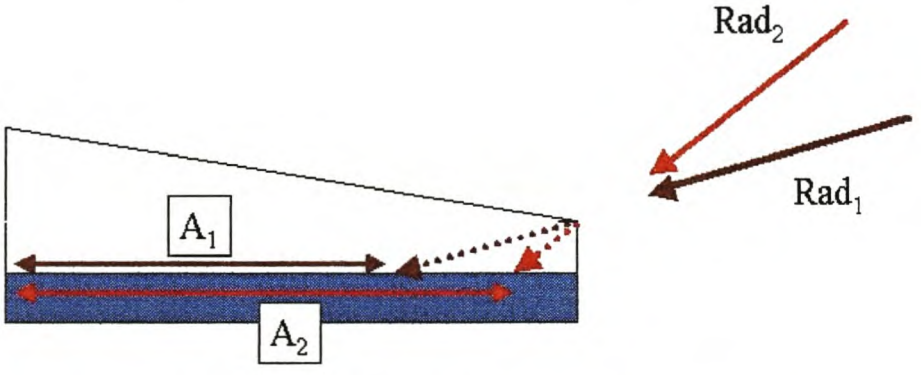

Figure 9.8: Effect of changing angle of light incidence on water surface area directly exposed to radiation.

The directly radiated water surface area as a function of angle of incidence for the test still is presented in Figure 9.9.

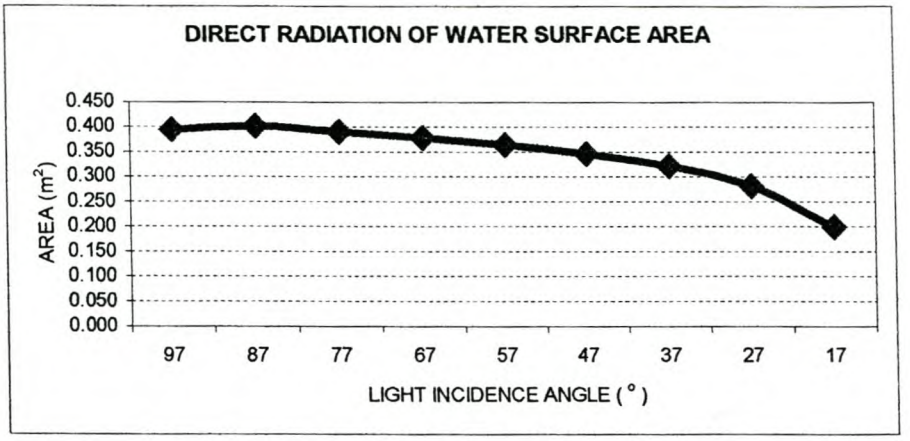

Figure 9.9: Water surface area directly radiated versus angle of light incidence (still water area 0.405 m^2, water depth 30 mm, total height of leading edge frame 100 mm).

9.3.2 Productivity and efficiency

As both the production volume and the radiation intensity onto the still are known, it is possible to calculate the efficiency of the still under the different radiation conditions using the formula explained in Section 3.2.2:

$$\eta = (m_e h_w)/H_s$$

(water surface area = 0.405 m^2). Figure 9.10 plots the efficiency values for the different angles of light incidence, calculated using the actual total water surface area (continuous line) and using the directly radiated water surface area (dotted line). It can be seen that η is higher and more constant when the water surface area exposed to direct radiation is used. This means that η will be influenced by the internal shadows of the North, East and West facing sidewalls of the still, and more so as the angle of light incidence onto the cover decreases (as in the winter months, also see Figure 3.15).

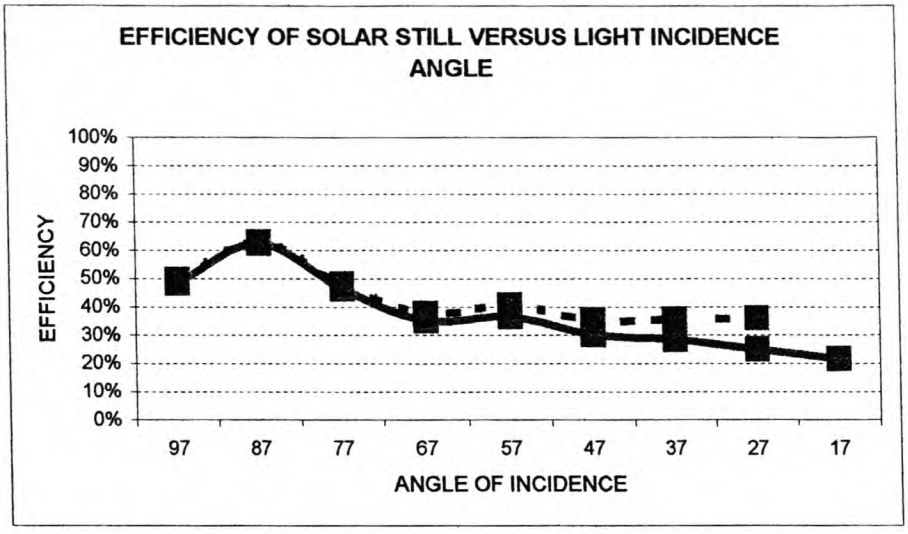

Figure 9.10: Calculated efficiencies for test still radiated from different angles (solid line: using total water surface area; dotted line: using effective directly radiated water surface area).

Under dynamic solar conditions it will be impractical to use the actual radiated water surface area to calculate η. A further reason is that the effect of scattered radiation is ignored. This does however imply that the height of the sidewalls of basin stills should be at a minimum, as the combined effect of decreased amount of internal shadow and increase in cover transmittance will positively affect efficiency. This is best illustrated by the noticeably higher efficiency obtained when the still was radiated directly from above (see Figure 9.10), where the angle of incidence was closest to 90 ° and cover transmittance was at its highest (see Figure 3.10 but note difference in the definition of angle of incidence).

9.3.3 Heating constants

The heating constants (k_{heat}) in Figures 9.6 and 9.7 show that higher k_{heat} values are associated with improved productivity. Further, k_{heat} values at all temperature measurement points decrease with decreasing angles of incidence, with a noticeably faster decrease as the angle of incidence drops below 37 °.

It can also be seen that, for the same angle of incidence, the highest k_{heat} value is obtained in the water on the blackened basin floor. Slightly lower but similar

values are measured along the front and the back sidewalls 10 mm from the basin floor irrespective of shadow. Lower k_{heat} values are measured in the air inside the still, with the lowest value obtained just underneath the glass on the back sidewall of the still where the distance between the water surface and the cover is at a maximum and air convection is at its lowest.

High k_{heat} values indicate fast heating behaviour at the point of measurement, and thus better subsequent still performance and higher productivity. Higher productivity is also associated with higher angles of light incidence onto the still cover (better radiation transmittance through the cover) plus onto smaller shadowed areas inside the still. A reflector placed behind the still during periods when the angles of light incidence are low (e.g. winter in the Southern Hemisphere) can theoretically improve the angle of light incidence onto the cover *and* reduce the shadowed area inside the still. A follow-on study was therefore undertaken to determine the viability of light reflectors placed behind the still, through measurement of still productivity and k_{heat}. These results are presented and discussed in Chapter 10.

CHAPTER 10

IN-HOUSE TESTING:
THE USE OF REFLECTORS TO IMPROVE STILL PRODUCTIVITY

10.1 Introduction

In the previous Chapter it was shown that solar still productivity will drop significantly at lower angles of radiation incidence, as is practically experienced in Southern Africa during the winter months. In this Chapter the use of reflectors to enhance solar still productivity during periods of low solar radiation incidence angles is investigated.

10.2 Experimental and results

10.2.1 Experimental

The experimental set-up presented in Figure 9.2 was used together with a white polystyrene foam sheet placed behind the still (Figure 10.1). The lamps were fixed at 20 degrees below the horizontal i.e. with an angle of direct radiance onto the cover of 27 degrees. The foam sheet was held in position by two clamps on laboratory stands, which also allowed the sheet to be tilted to different angles over the still. The temperature probes described in Section 9.1 were used again. Four solar cells were used to measure incident light intensities (a) directly onto the cover, (b) underneath the cover, (c) reflected from the white foam sheet and (d) reflected from the glass. The same data recording equipment described in Section 9.1 was used.

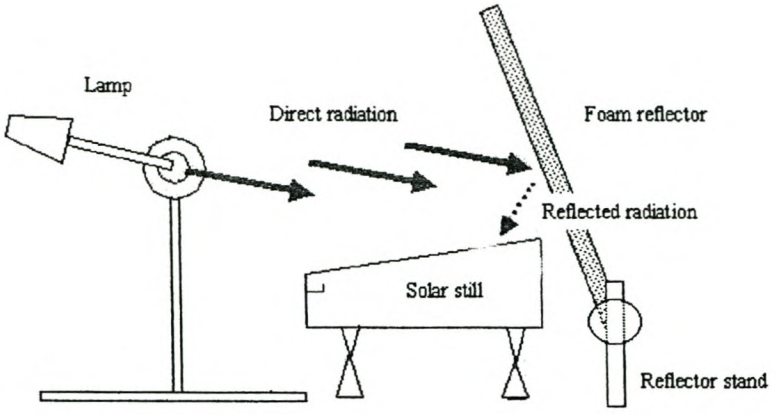

Figure 10.1: Experimental set-up used to measure the influence of reflectors on solar still productivity.

Experiments were carried out in duplicate over a 12-hour heating period where the reflector angle was varied by 10 degree intervals between 0 degrees and 40 degrees (relative to vertical). In order to derive an equation to calculate the angle of incidence of radiation on the still cover, the following geometrical construction was made:

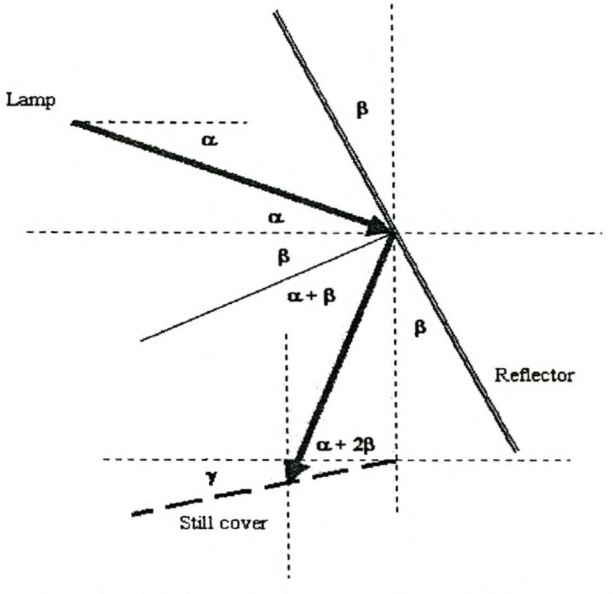

Figure 10.2: Radiation incidence angle on still cover. [α = angle of radiation incidence, β = reflector angle relative to vertical, γ = angle of still cover relative to the horizontal)

From Figure 10.2 it follows that incidence angle on cover = $\alpha + 2\beta + \gamma$.

10.2.2 Light measurement

Due to the low angle of direct radiation incidence, the solar cell measuring radiation for light reflected from the solar still cover (d) was partially also exposed to direct radiation and these radiation values were subsequently ignored (also see Table 9.1). Figure 10.3 shows the radiation values obtained from the other solar cells, including the reference experiment where no reflecting surface was used.

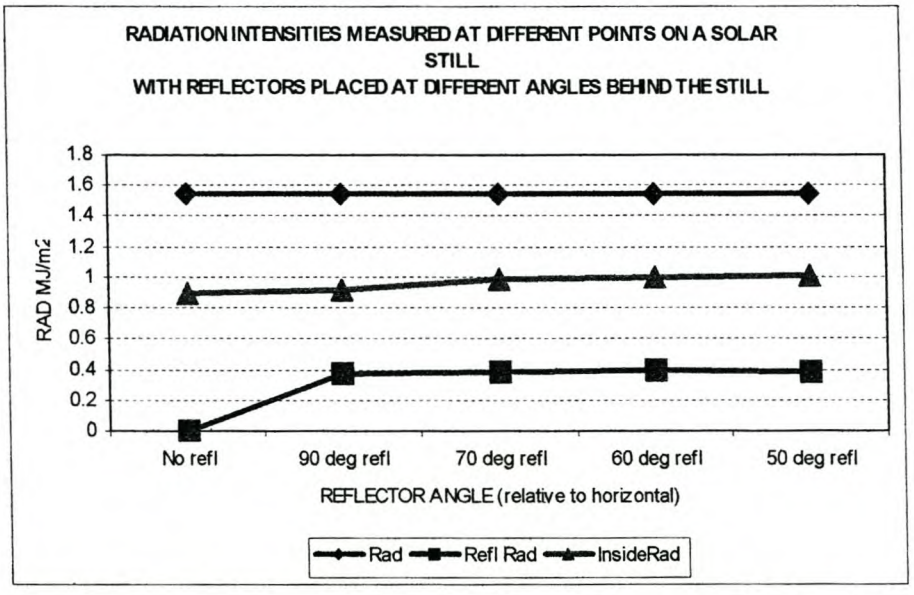

Figure 10.3: Radiation intensity values obtained at different measuring points with reflectors placed at different angles behind a solar still (top: direct radiation on cover with reflector, middle: radiation beneath cover with reflector, bottom: radiation reflected from reflector only).

10.2.3 Productivity

Productivity was measured over a 24-hour period for different reflector angles. Figure 10.4 shows the distillate production volumes for the different test conditions.

10.2.4 Heating constants

The different heating constants obtained at the different measuring points were determined as described in Section 9.2.3 (temperatures measured inside the basin insulation were ignored due to the similarity thereof between experiments). The heating constants are presented in Figure 10.5.

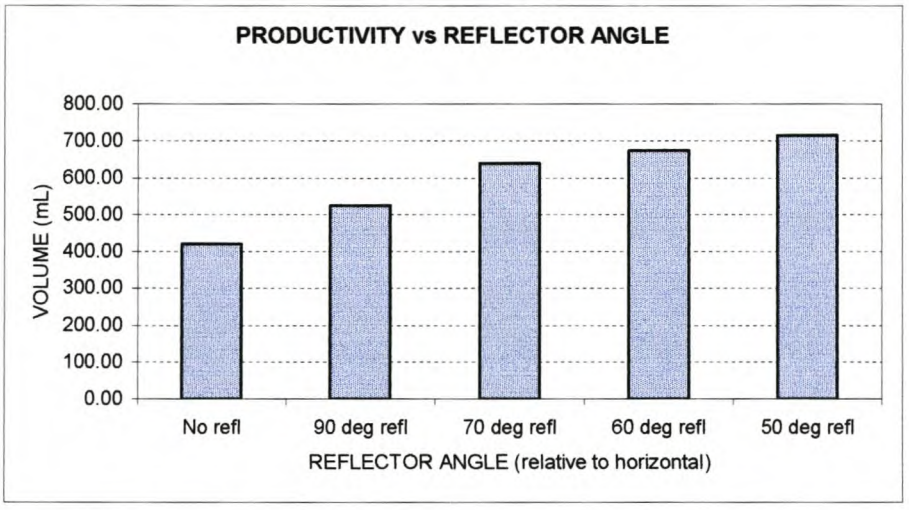

Figure 10.4: Productivity comparison for solar still with reflector placed at different angles behind the still.

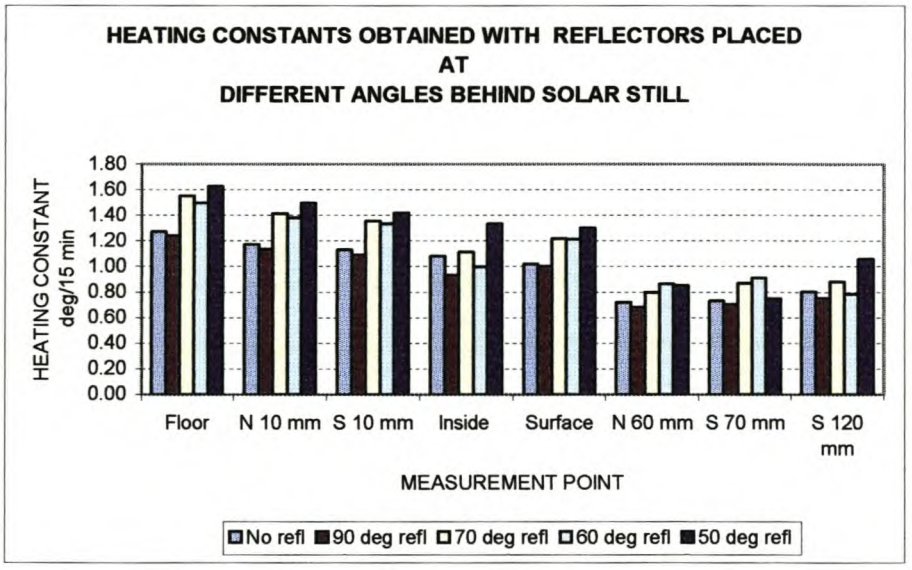

Figure 10.5: Heating constants as a function of reflector angle (reflector angle given relative to horizontal).

10.3 Discussion

From Figure 10.3 it can be seen that the presence of a white reflecting surface placed behind the solar still resulted in light being reflected back over and onto the still cover ('*ReflRad*'), while the direct radiation intensity remained constant ('*Rad*'). The light intensity measured beneath the still cover ('*InsideRad*') increased slightly as the reflector angle relative to the horizontal decreased – an increase of about 12% was measured between having no reflector and a reflector tilted by 40 degrees, an increase which is comparable to the direct light incidence angle being increased by 10 degrees (table 9.1).

As with different angles of light incidence, there was a significant, stronger increase in productivity (Figure 10.4). The amount of distillate produced per 24h cycle increased significantly from when there was no reflector present to where the reflector was tilted by 40 degrees. The presence of a reflector placed vertically behind the still was sufficient to increase the productivity by about 25%, although the angle of incidence of the reflected light onto the cover was 63 ° (where the transmittance of the glass is less than 70% of the maximum). When the reflector was adjusted from 20 ° to 30 ° to 40 °, the productivity increased further with reflected light incidence angles of -23 ° (52%), -3 ° (61%) and +17 ° (70%) respectively. The increase is comparable to the angle of direct light incidence increasing by about 10 to 20 degrees.

The different heating constants (Figure 10.5) indicate that, under the specific test conditions, the initial internal heating behaviour was not influenced by the presence of a vertical reflector, but that significantly higher k-values (Section 9.2.3) were obtained once the reflector was tilted as to allow better reflected light transmittance. As with different angles of direct light incidence, the highest heating rates were measured on and close to the black basin lining ('*Floor*', '*N10 mm*', '*S10 mm*'). The values of k measured close to the sidewalls above the water surface were smaller and more scattered ('*N60 mm*', '*S70 mm*', '*S120 mm*').

From the above results it is clear that the use of reflectors can enhance productivity and therefore efficiency through the improved utilisation of incident

radiation. From Figure 3.10 it can be seen that the transmittance of the 3-mm glass cover of the still will start to decrease when the light incidence angle is less than 50 °, and transmittance will be less than 80% if this angle is less than 30 °. Figure 3.16 compared the monthly total amount of direct sunshine hours in Cape Town with the approximate number of hours where more than 80% of direct radiation reaches the still basin. Figure 10.6 shows the theoretical number of hours where direct and / or reflected light from a reflector positioned directly behind a still passes into the still basin at incidence angles of more than 30 °. Figure 10.7 shows the months with a potential % increase in effective radiation hours i.e. where more than 80% of direct and / or reflected radiation can reach the still basin through the cover, taking into account overhead interference from the reflector on the direct radiation component.

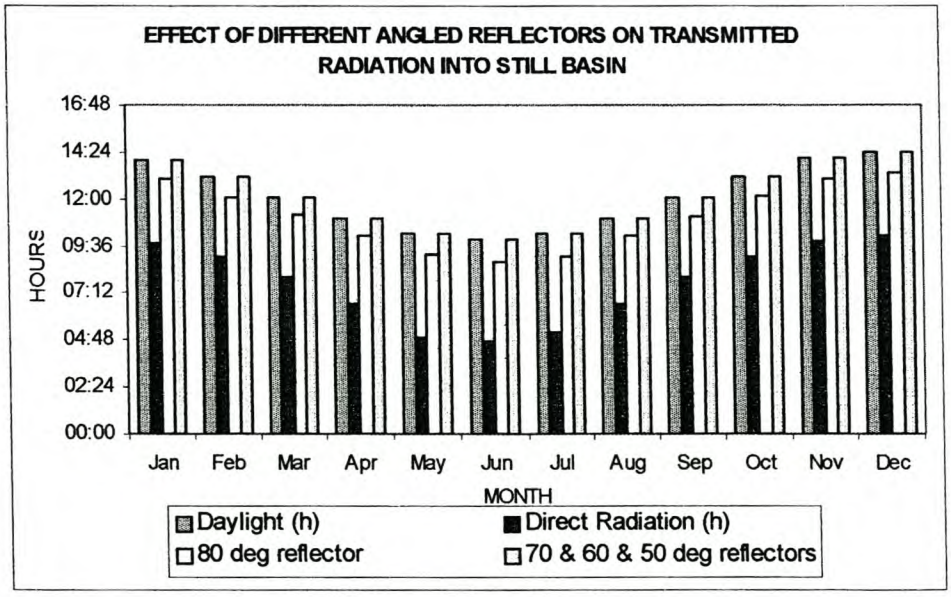

Figure 10.6: Effect of reflectors on availability of light radiated directly into solar still basin (direct radiation plus reflected radiation onto cover at incident angles greater than 30 °, reflector angles relative to horizontal).

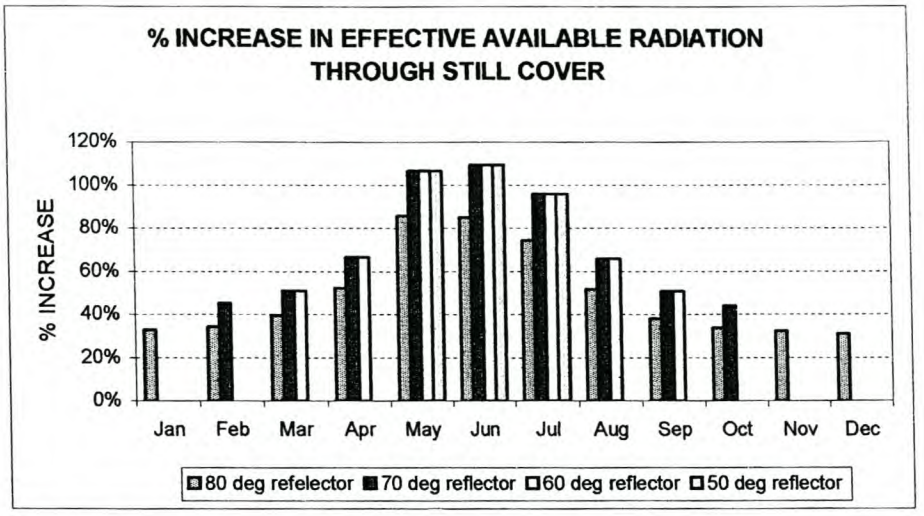

Figure 10.7: Increase in effective number of radiation hours through the use of reflectors at different angles to the horizontal (data points not present indicate either less than 80% of reflected radiation transmitted or physical reflector interference with direct solar radiation, reflector angles relative to horizontal).

Figures 10.6 and 10.7 show that the presence of a reflector will increase the daily amount of radiation reaching the still basin, as simulated for the specific conditions used in the experiments described in this chapter. It can also be seen from Figure 10.7 that the % theoretical gain is better during the months April to August. These are also the months characterised by low productivity (table 3.1). Should a reflector be incorporated temporarily as part of the solar still during the winter months, its tilt angle should be between 60 and 80 ° relative to the horizontal to ensure maximum exposure of the still to the incident radiation. Figure 10.8 presents the potential increase in performance (calculated using Equation 3.1 from Section 3.3.2) through the use of reflectors, confirming that an average productivity increase of about 50% can be obtained over the winter period (Figure 10.4). This is equivalent to a 9% productivity improvement on an annual basis and, therefore, as the amount of radiation received remains the same, an overall efficiency increase of 9%. The additional cost of incorporating a reflector with the solar still must therefore also be less than 9%, else the productivity improvement will be offset by the construction cost increase (see Figure 10.9 for desired economic result).

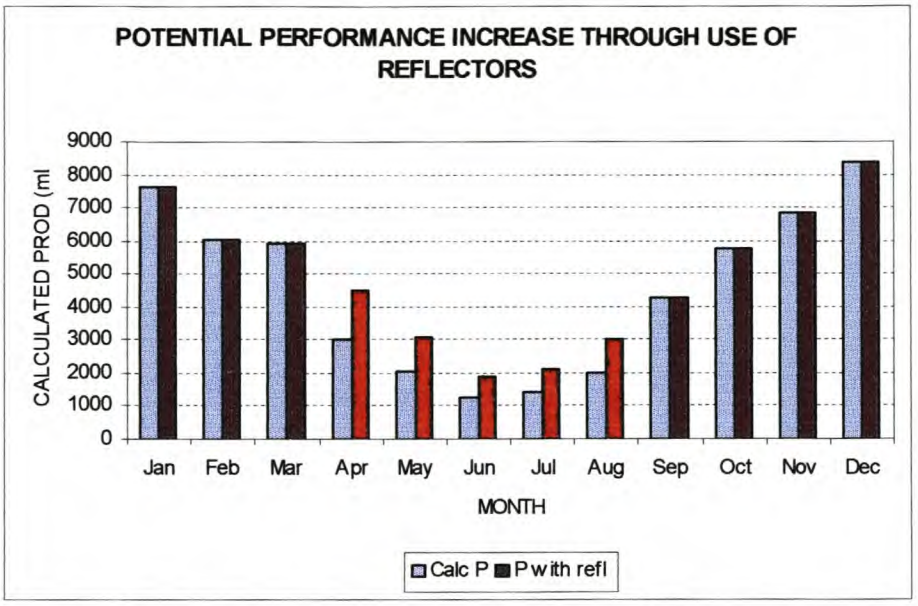

Figure 10.8: Calculated still productivity improvement through use of reflectors during winter months.

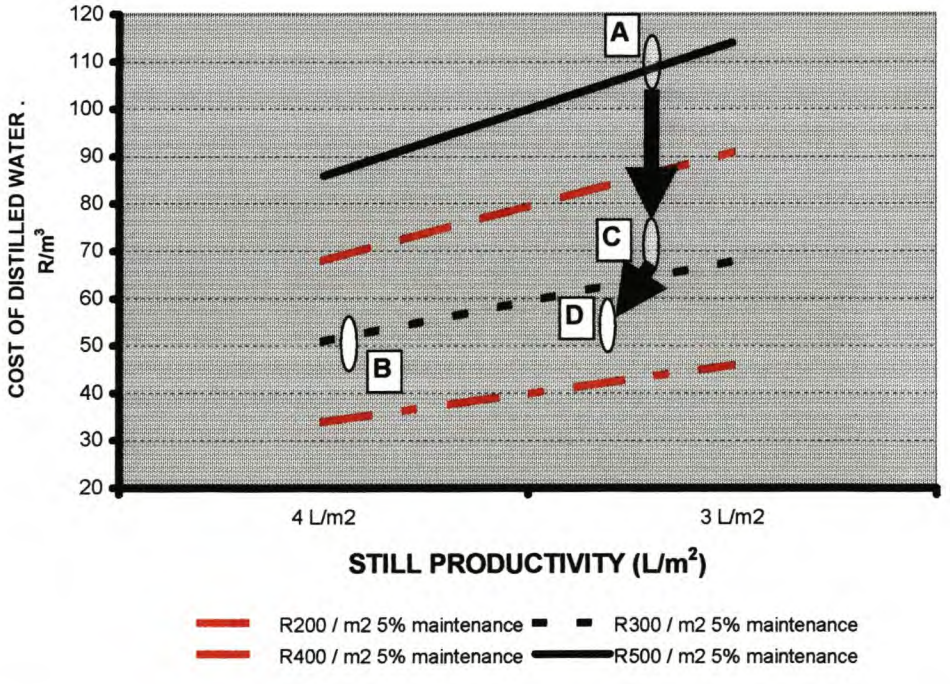

Figure 10.9: Potential distilled water cost improvement through use of economically viable reflectors (reposition from C to D).

10.4 Recommended further investigations

Notwithstanding the improved results obtained, the following aspects of reflectors need to be investigated further before the solar still design is modified to incorporate (temporary) reflectors:

- Different types and colours of reflector materials;
- Number and position of reflectors per still;
- Different light incidence angles to better simulate East-West movement of sun;
- Minimising wind resistance of reflector(s) fixed to basin; and
- Ease of fixing and removal of reflector(s)

CHAPTER 11

IN-HOUSE TESTING: INFLUENCE OF RADATION INTENSITY

11.1 Introduction

From Section 3.3.2 it can be concluded that solar still productivity decreases dramatically as the solar radiation intensity decreases. It was therefore deemed necessary to conduct an investigation into the low-radiance behaviour of these type of solar stills in order to determine the potential for productivity increase under such conditions (e.g. during winter or cloudy periods).

11.2 Experimental and results

11.2.1 Experimental

The experimental set-up presented in Figure 9.1 was used to carry out this part of the study. These experiments were carried by direct vertical radiation onto C1 (black silicone lined still) i.e. angle of light incidence of 97 ^{0} onto the glass cover. Temperature measurement probes were placed as per Figure 9.2, while light intensities were measured on the left side of the still cover directly underneath the lamps, behind the cover directly underneath the lamps, as well as on the right hand front part of the still cover. Productivity was measured volumetrically over a 24-hour period. During this time constant radiation took place over the first 12 hours, after which time the lamps were switched off. The radiation intensity between subsequent experiments was reduced by making use of a calibrated commercial light dimmer.

11.2.2 Radiation intensity

Using the calibration curves for the different solar cells (from Section 9.2.1) it was possible to calibrate the lamps for different dimmer settings. Figure 11.1

shows the measured hourly energy values for the different settings, while Figure 11.2 shows these values as percentages of the maximum measured energy i.e. measured on the still cover directly underneath the lamps. Figure 11.3 gives the total recorded energy per square meter over the 12-hour radiation period.

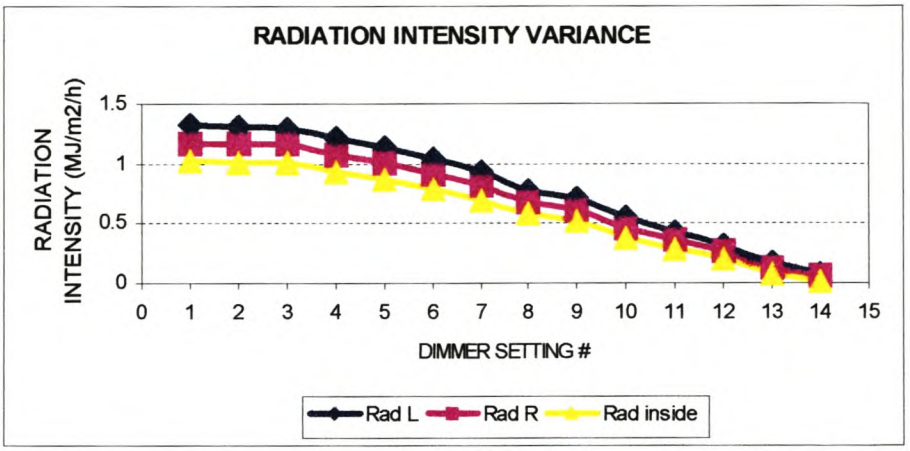

Figure 11.1: Radiation intensity variance per dimmer setting.

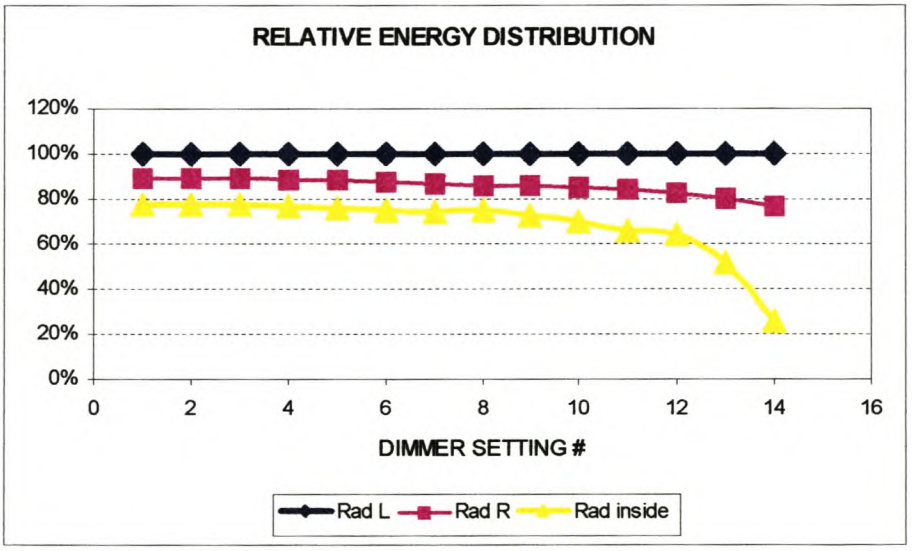

Figure 11.2: Relative energy distribution per radiation measurement point.

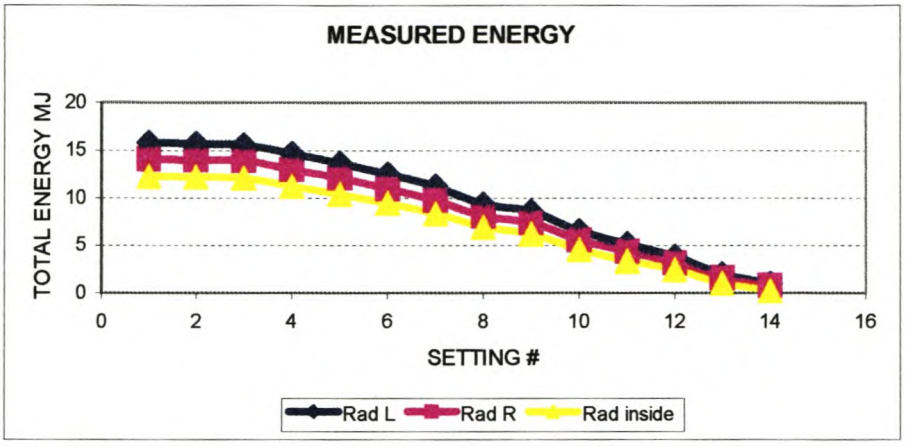

Figure 11.3: 12-hour energy dose per m^2 are for each dimmer setting.

11.2.3 Productivity

The productivity in terms of volume for each experiment is given in Figure 11.4, while the productivity versus total radiation is presented in Figure 11.5. Figure 7.8 shows the correlation between actual and calculated productivity values for different radiation intensities (productivity equation from Figure 3.13).

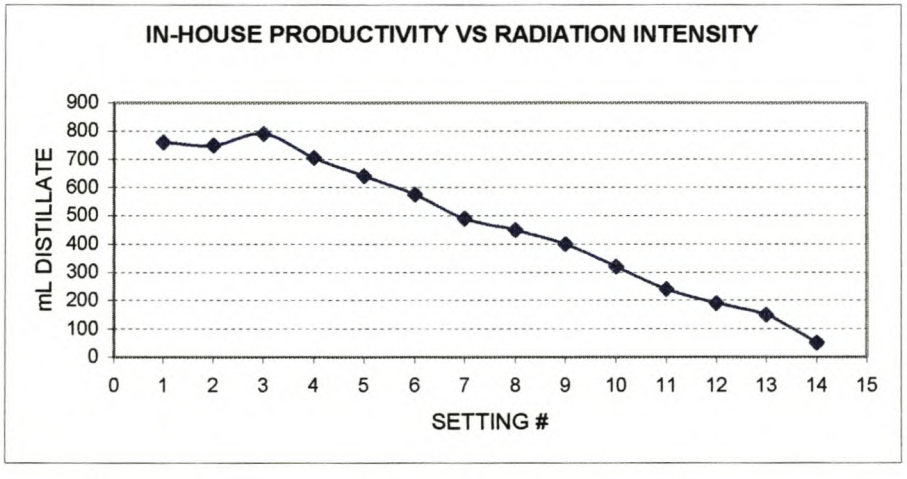

Figure 11.4: In-house productivity per lamp dimmer setting.

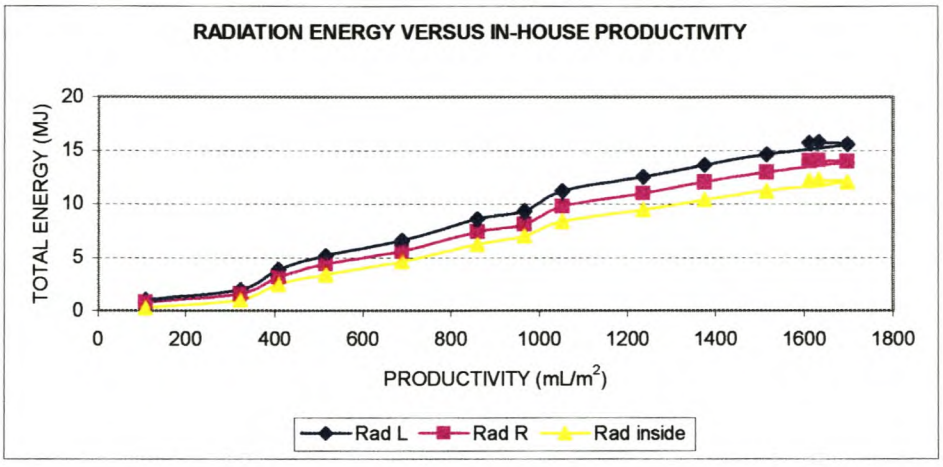

Figure 11.5: Influence of radiation dosage on productivity.

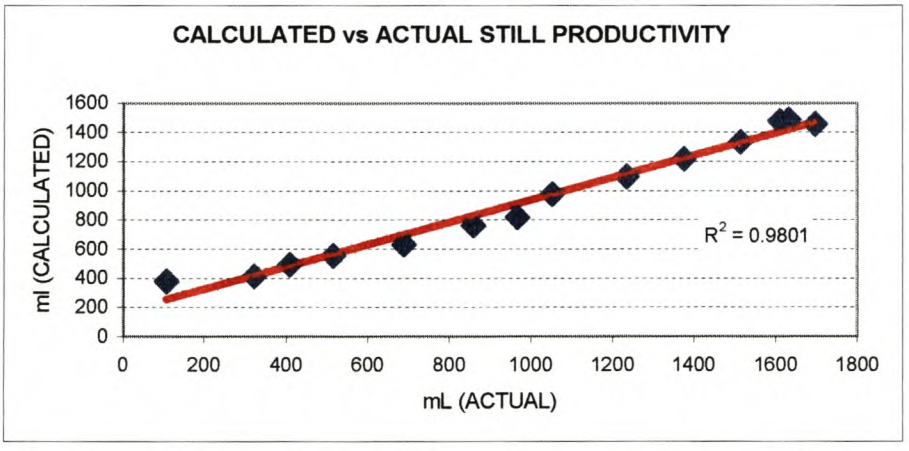

Figure 11.6: Correlation between calculated and measured productivity.

11.2.4 Heating constants

The heating constants over the first 180 minutes at *four* temperature-measuring points (two inside the water and two in the air above the water, see Section 9.2.3) were calculated from the measured temperature profiles. The different heating constants are presented in Figure 11.7.

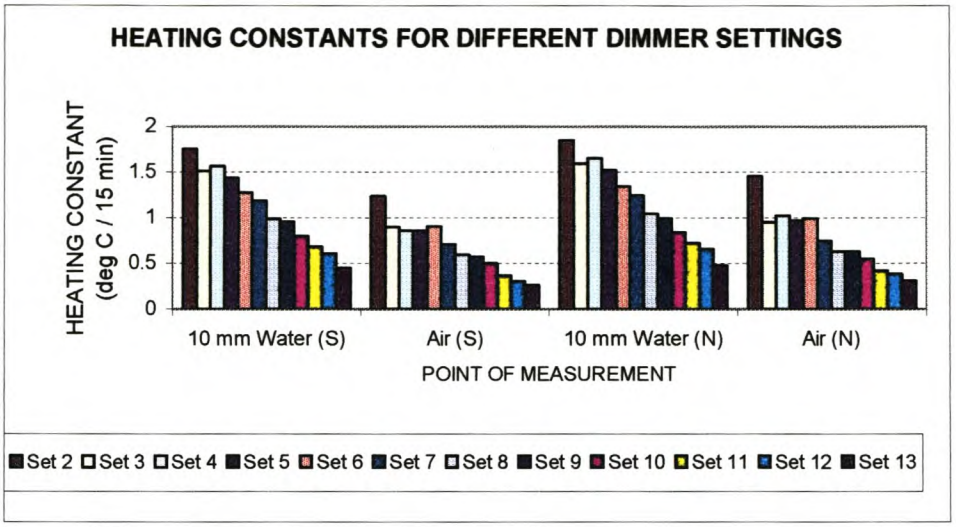

Figure 11.7: Water and air heating constants for different lamp dimmer settings.

11.2.5 Temperatures

The maximum water and air temperatures measured at the probe positions as in Section 11.2.3 were recorded. Results are presented in Figure 11.8.

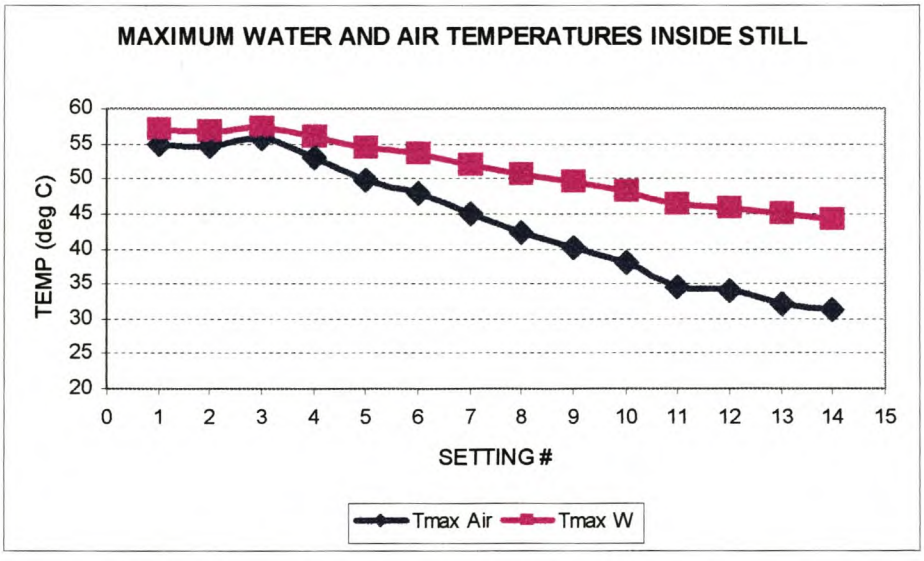

Figure 11.8: Maximum temperatures recorded inside test still at different dimmer settings.

11.3 Discussion

The experiments simulating different solar radiation intensities were carried out over the range of 0 to ca. 1.3 MJ/m^2/h, which simulates conditions of low solar radiation i.e. less than 15 MJ/m^2 (Figures 7.6, 11.1 and 11.3). Such conditions will negatively affect still performance, and can be expected when few daily direct sunshine hours occur e.g. in winter and / or on overcast days.
From Figure 11.5 a near linear relationship between productivity and total radiation energy can be seen under the conditions of direct, nearly perpendicular radiation. It has also been shown in Figure 11.6 that good correlation (within 10%) exists between the formula for productivity:

$$P = 0.3451e^{0.0923R} \quad \text{..... (Equation 3.1, from Figure 3.13)}$$

and the productivity results from these experiments. This means that the above formula is useful for predicting the productivity of a basin solar still for lower daily solar radiation intensities (from Section 3.3.4 the initial lower radiation limit for the equation validity was 8 MJ/m^2/day).

From Figure 11.2 it can be seen that the ratio between the radiation intensities measured on the top of the still cover versus directly underneath the cover remained nearly constant under conditions of very low radiation (3 MJ/m^2), where the radiation intensity beneath the cover decreased faster as less light is transmitted through the cover. Above 3 MJ the transmittance behaviour of the 3 mm glass cover corresponds to measured percentage-transmittance as given in Figure 6.3. Below 3 MJ the greatest deviation from the calculated productivity values is found (> 20%). A lower daily radiation limit of 3 MJ/m^2 is therefore proposed for the application of equation 3.1.

When the maximum operational temperatures are examined (Figures11.2 and 11.8), it can be seen that significant heating of the *basin water* still occurs even under conditions of very low transmittance of incident radiation. The *basin air* temperature, however, is raised only slightly under conditions of very low radiation. The drop in maximum operational temperature is also much faster for

the air than for the water as the radiation intensity decreases below 1.2 MJ/m^2/h, from a difference of 2 ° C to more than 13 ° C. Above 1.2 MJ/m^2/h, the temperature gradient remains less than 2 ° C, with the water temperature higher than the air. This equilibrium difference was also observed in field-testing at much higher radiation energy levels and higher operational temperatures (Section 3.3.4). At decreasing radiation intensities (thus energy dosages less than 1.2 MJ/m^2/h) it seems that not enough longer wave emission energy is generated by the black basin to heat the water *and* the air, resulting in an increasing temperature gradient between the inside water and the air.

Figure 11.9 shows that the calculated efficiencies for the different experimental runs are nearly all between 30% and 34%, except in cases where the total radiation energy drops below 3 MJ/m^2.

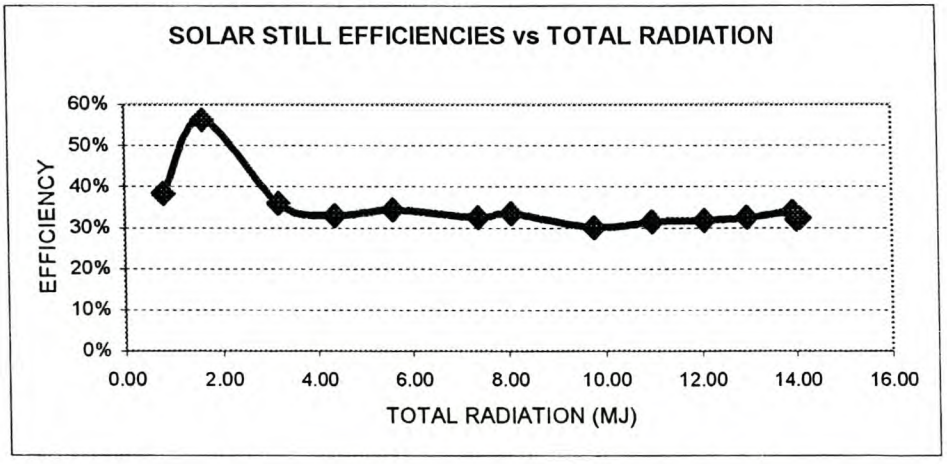

Figure 11.9: Solar still efficiencies under different radiation conditions.

From the above Figure it can be seen that the still's efficiency is independent of the total incident radiation energy (save for the lowest radiation values). This is in contrast with the field results presented in Figure 3.16, which shows a drop in efficiency as the total radiation decreases. These field results were however obtained over a year cycle, i.e. seasonally influenced through the variance in direct radiation incidence angle (as illustrated in Figure 9.10). Figure 11.7 shows the similarity in heating constants obtained for the basin water and air respectively. A decrease in radiation intensity was in all cases

accompanied by a decrease in value of the heating constant, with k_{water} being higher than k_{air} throughout. This, in combination with the heating constants presented in Figure 9.6 (effect of radiation incidence level) illustrates the seasonal impact of the trajectory of the radiation source (sun) on the performance of the solar still and explains the inconsistency of efficiency values calculated from field data (Figure 3.15). In the Southern Hemisphere the low winter radiation intensity combined with the low angle of incidence onto the still cover *both* contribute to lower heating constants, resulting in lower operational temperatures, which in turn results in lower still performance.

From the literature and experimental results of the preceding chapters it has became clear that efficiency values of in the order of 35% can be expected from the basin solar still under investigation. During the Southern Hemisphere's winter months, however, efficiency can drop to as low as 20% due to the factors identified as part of this study. It is this seasonal efficiency drop that should be addressed in future investigations into improving the still's performance, i.e. to attempt to bring the still's overall annual efficiency to about 35%. Higher internal operational temperatures should be sought, which means that more heat energy should be generated inside the basin. For this specific design this can possibly be achieved by externally preheating the saline feed water and / or the use of reflectors to increase the amount of direct radiation into the basin.

11.4 Economic evaluation

The economic viability of the selected solar still design can now be evaluated in the following Chapter by combining the results of the performance improvement studies (Chapters 8 to 11) and improved construction costs (Chapter 5).

CHAPTER 12

ECONOMIC EVALUATION AND ECONOMIC VIABILITY OF SOLAR STILL TECHNOLOGY

12.1 Background

According to the literature the cost of water produced in bulk by solar distillation is high compared with that from fuel-operated distillers, but it is less than the cost of water from other types of plants with similar capacities (Howe 1986). As the production rate of solar distillation plants is proportional to their glass cover area, the cost per unit of water produced is practically consistent regardless of the size of the installation (Bouchekima 1998). Capital and amortization costs vary therefore more or less directly with the size of the projected output (AA Delyannis 1983). A recent study by Kamal (2000) shows that when water production costs for small-scale solar still plants are compared with those for solar-powered membrane distillation, the economics favour solar distillation, and it remains a favourable process for small-capacity water desalination in remote locations. It is therefore of importance to small communities and single-family users in such areas, as it provides the most economical means of supplying potable water (EE Delyannis 1987).

Generally the calculated unit cost of product water is used as the indicator of economic viability. Attempts to decrease the distilled water cost by increasing the efficiency of solar stills through preheating of the feed water or by modifying the basic basin design have been commercially unsuccessful to date because of the additional costs involved in bringing about such modifications. Improvement of performance is not effective where the water cost rate increases at a higher rate than the productivity enhancement. It is more economic to install more units than to try to increase the output of a single still by unconventional methods (EE Delyannis 1985).

12.2 Factors affecting economic feasibility

Several factors can influence the decision to invest in solar stills as a desalination technique for the supply of potable water. The major factors are:

- the constant availability of an adequate capacity of a saline water source;
- the chemical composition of the source water;
- the physical quality of the source water;
- the quantity of product water needed i.e. the supply capacity;
- the quality of the product water;
- the availability of suitable land area for construction of the still plant;
- the site topography;
- geographical location;
- expected local weather conditions;
- the still efficiency;
- the unit cost of a solar still i.e. the materials' purchasing and preparation cost;
- cost of additional infrastructure such as pumps and filters;
- operating and maintenance costs; and
- the expected operational lifetime of the still.

12.2.1 Sustainability of water source

The capacity of the saline water source must be such that it can consistently provide feed water to the still(s). It is preferable that the solar still be positioned as close to the source as possible, otherwise the cost of providing the feed water may become high.

12.2.2 Chemical composition of feed water

Although the performance of a solar still is not directly influenced by the salt content (TDS) of the feed water, it can indirectly impact on its efficiency (e.g. if scaling occurs, Section 8.2.4). The presence of potentially problematic ions must therefore be known beforehand, as water pre-treatment may be necessary, which

has a capital cost impact.

12.2.3 Physical quality of feed water

The presence of suspended physical particles may necessitate the use of inline filters between the water source and the solar still, as such particles will be hard to remove once inside the still. Other preventative measures could include limiting algae growth (Section 4.2). Again, such infrastructure will have a capital cost impact.

12.2.4 Supply capacity

The modular design of the basin solar still (Figure 3.7) lends itself to the construction of a solar still plant consisting of a number of still units. Depending on local and governmental requirements in terms of the expected volume of water per capita, the total volume of water to be supplied per time unit can be calculated. The seasonal productivity of the solar still complicates this calculation, but by making use of equations 3.1 and 3.2, derived from this study, it is possible to predict solar still performance under different conditions (see case studies Section 12.5). Also, if the feed water quality allows it, blending of the distilled water with the feed can increase the supply capacity.

12.2.5 Land area

As the physical space required for a larger capacity solar still plant can be significant, associated costs must be taken into account. Normally, however, such installations are in remote, rural areas where land space is readily available.

Another factor that may have a cost impact is the preparation of the site to ensure horizontal installation of the still unit(s).

12.2.6 Site Topography

In Section 3.3.3 it was shown that a direct relationship exists between direct

radiation and efficiency. Any interference with the amount of direct radiation reaching the still basin will adversely affect the efficiency as calculated from the equation derived from Figure 3.17. This is because it is based on an open horizon with no horizon obstacles (such as mountains or trees). It is therefore important to determine the expected amount of direct sunshine hours per site per month; an applied meteorological computer program such as 'METEONORM' can be used to perform this calculation.

12.2.7 Geographical location

The geographical location of a potential site determines the amount of direct solar radiation hours at any given time, and the fraction of direct radiation reaching the still basin (Figure 9.10). These factors both influence efficiency, thus impacting on the cost of the product water. Again, software programs, in addition to available measured data, can be used to predict still performance at different locations on cloudless days.

12.2.8 Prevailing weather conditions

Cloud cover can negatively influence productivity as it reduces the amount of direct radiation. Wind can improve performance, as it increases the temperature gradient over the condensing surface (glass cover). During conditions of rainfall the productivity is virtually zero. As it is difficult to quantify such dynamic and natural occurring meteorological conditions, forecasts of solar still performance are given based on either historical data (if, statistically, sufficient data exists) or cloudless days (i.e. maximum predicted performance).

12.2.9 Still efficiency

In the preceding Sections a number of factors influencing the solar still efficiency have been highlighted. Other factors that play a role include the characteristics of the still cover and operational procedure. However, for the purposes of this study, the design comprising the materials identified in Section 5.3 are used, and general operational procedures that may negatively

influence the efficiency, are ignored.

12.2.10 Still cost

The capital cost of the still will play a major part in any economic evaluation of a still's economic viability (Figure 5.6). This cost can in turn be related to component costs, the importance of which has been illustrated in Section 5.4.

12.2.11 Additional infrastructure

Additional infrastructure may be necessary for (i) pre-treatment of the feed water (Section 12.2.2 and Section 12.2.3), (ii) blending of the product water (Section 12.2.4) and (iii) supply of the water to the end-user(s). Such infrastructure items will increase the capital cost of the plant.

12.2.12 Operating and maintenance cost

In any cost model, provision has to be made for running costs such as supervision (albeit to a low degree) and maintenance (e.g. replacement of broken glass and repainting).

12.2.13 Operational lifetime

The operational life of a solar still (plant) is related to its construction materials and environmental conditions, and is defined as the total expected period of operational use (including maintenance) until unit disintegration.

The above factors can be summarised as presented in Figure 12.1.

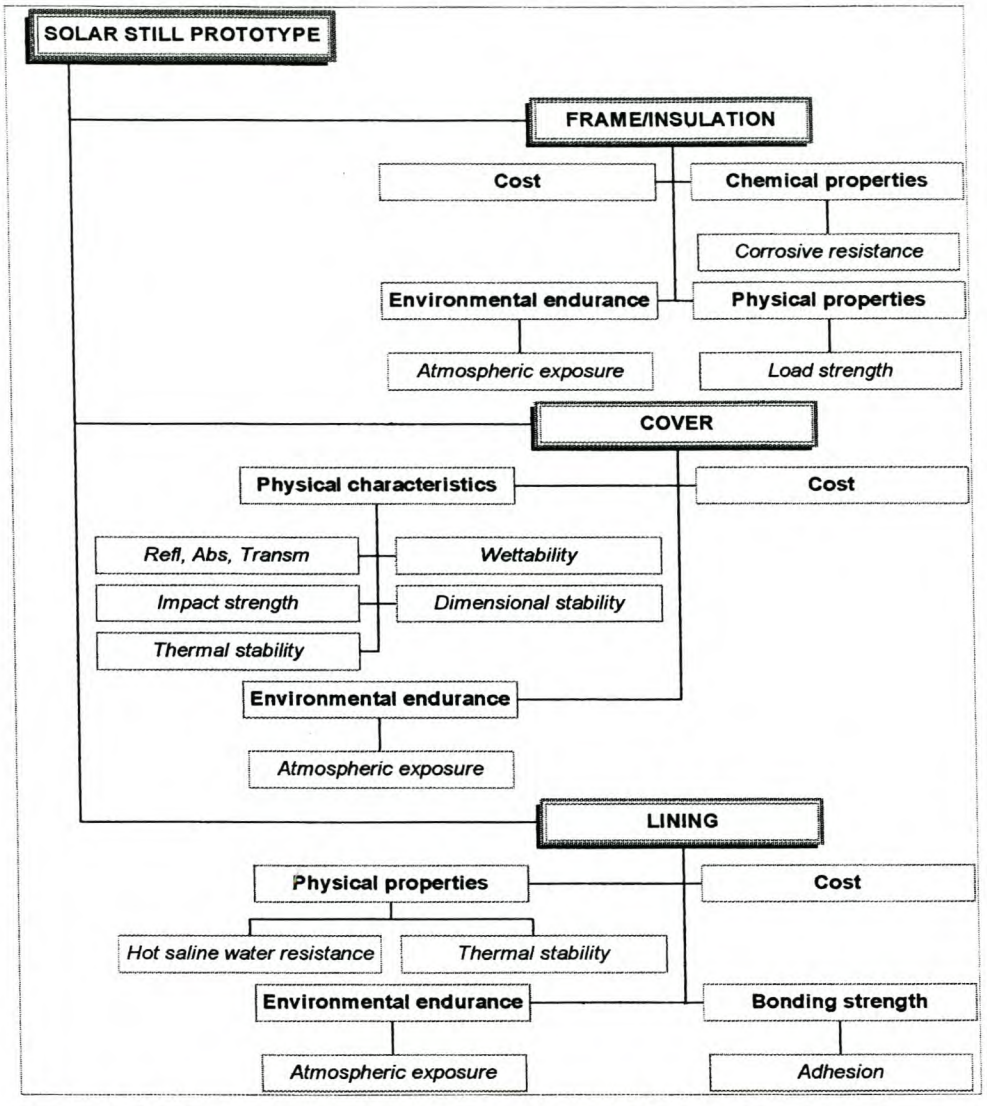

Figure 12.1: Factors influencing the economic viability of solar stills.

12.3 Development of economic evaluation model

The cost contribution factors that need to be incorporated in an economic evaluation model were identified in Section 12.2. Such an evaluation model was considered very important, and could be used to choose between different water supply technologies on a cost-to-user basis, perform sensitivity trade-off analysis e.g. when comparing different construction materials and predict the cost of water produced at a given site under specified operational conditions.

The development of a comprehensive financial cost calculator, which addresses

all the inputs of Section 12.2, is however beyond the scope of this study. It is however possible to make use of simplified models and existing software packages to perform first-order cost calculations.

A simplified cost calculation model in Microsoft Excel ® was developed for this study by Bonthuys (Goldie 2003). This model takes into account capital costs (solar stills plus infrastructure) as well as performance on an annual average basis. Figures 12.2 to 12.4 show the required inputs (shaded cells). For the purposes of this study, the cost of water produced by a solar distillation plant is expressed as South African cents per liter.

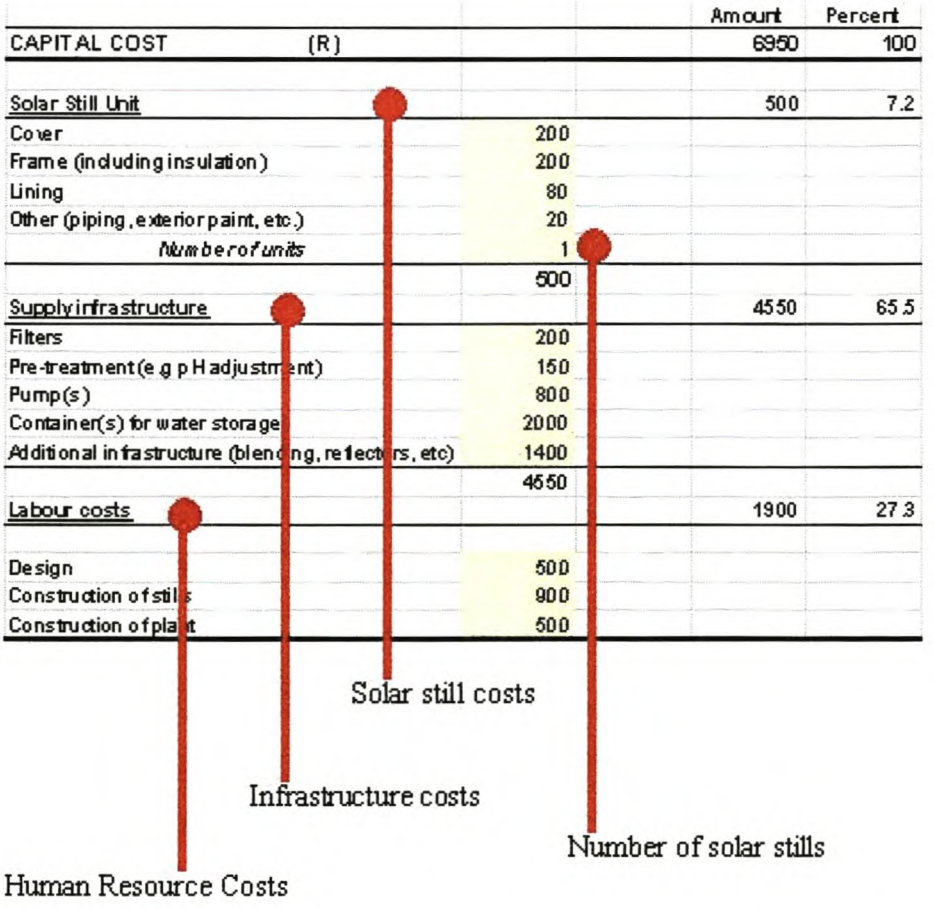

Figure 12.2: Capital cost inputs to solar still water cost model.

			Amount	Percent
RUNNING COST	(/year)		3405	100
Plant supervision:			3000	88.1
Labour	(hours/year)	300		
Rate	(R/Hour)	10		
		3000		
Maintenance			405	11.9
Repair materials (paint, glass, etc.)		30		
Labour	(hours/year)	5		
Rate	(R/Hour)	75		
		405		

Figure 12.3: Inputs to running costs of a solar still plant.

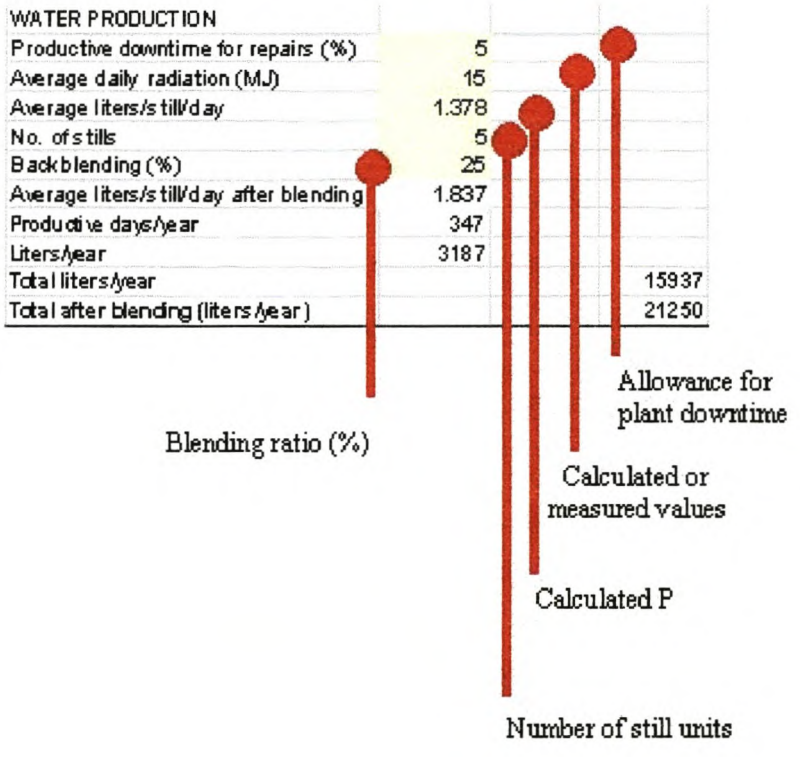

Figure 12.4: Productivity calculation for typical solar still plant (P: productivity).

Other inputs to the above model include useful lifetime and annual cost of capital as well as data generated by other software packages and equations derived from this study.

The following examples will now show how the model can be used to evaluate

the economic viability of solar stills for different applications.

12.4 Capital cost sensitivity analysis

First, Figures 2.10, 3.25 and 5.6 (cost of distilled water as a function of the construction and maintenance cost of a single solar still unit) were revised and refined. The following inputs were used:

- the construction cost of a reference still amounts to R500/m^2 (base area). The cost breakdown of Figure 5.1 was used to calculate the cost of individual components and labour;
- no additional infrastructure cost is taken into account;
- maintenance and operating cost is taken as a percentage of the still unit cost (5% and 10% respectively);
- the still unit is out of operation for 5% annually;
- the average daily global radiation for Cape Town was used, which amounts to 19.26 MJ/m^2 (calculated by using the Swiss METEONORM software package);
- the productivity is calculated by using Equation 3.1 of Section 3.3.2 and 11.3;
- no blending with feed water is taken into the account;
- the useful lifetime of the still is ten years; and
- the annual interest rate is 5%.

When the above values were used in the evaluation, the cost of the distilled water at 5% and 10 % running cost, was R0.127 and R0.162 per liter respectively.

Figure 12.5 shows the influence of decreasing still capital cost on distilled water cost at Cape Town.

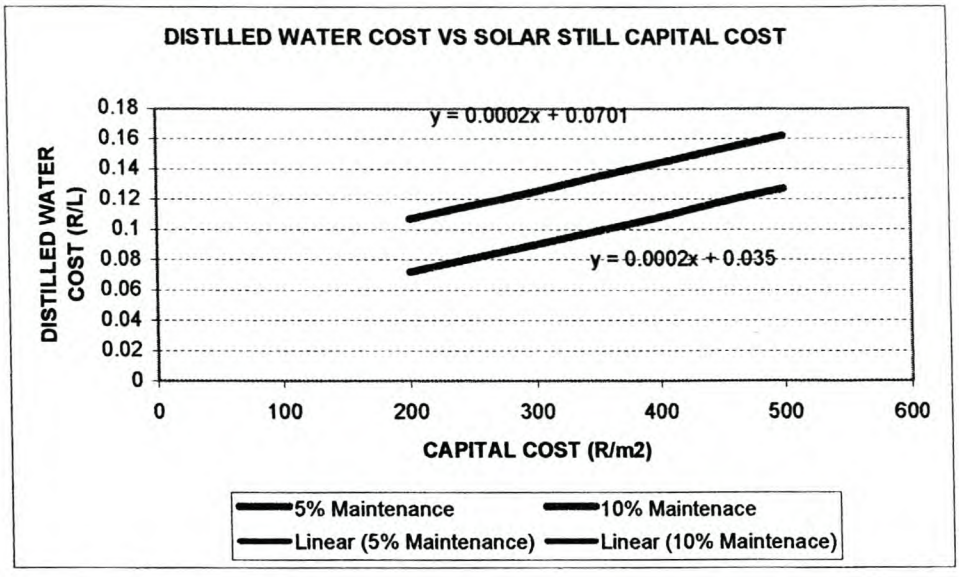

Figure 12.5: Influence of solar still capital cost on distilled water cost.

From Chapter 5 the component cost savings resulting from of this study were frame (40%, Section 5.3.1), cover (33%, Section 5.3.2) and lining (48%). A cost saving on labour of 33% was also found in practise due to the ease of preparation and installation of the new polypropylene lining. Using the economic evaluation model (Section 12.3), the cost of distilled water was now R0.093/L (5% running cost) and R0.128/L (10% running cost) respectively, which amounts to a saving of 27% and 20% relative to the still design used at the beginning of this study.

In Chapter 10 it was found that the use of reflectors could improve the annual productivity of a still by about 9%. Using the cost model, it was possible to calculate the capital cost below which the use of reflectors would be economically viable, namely less than R85/m^2 (5% running cost) or R120/m^2 (10% running cost). If standard white polypropylene sheeting is used (2001: R40/m^2 including frame), the use of reflectors will lower the distilled water cost to R0.086 (-7,5%) and R0.116 (9,3%) respectively.

A lower cost alternative would be to place the solar still array up against the northern wall of a high altitude building structure and affix to the wall silvered or white painted wedges of the correct angle or angles to ensure reflective

enhancement. This could lower reflector costs to < R20/m^2.

The use of blending of the distilled water with the feed water can be considered as long as regulatory standards (see Table 4.1) are not exceeded. Using the cost model, the cost of product water (distilled plus feed) could be calculated for different blending ratios (assuming that blending operation is carried out manually i.e. no associated capital cost). Figure 12.6 illustrates the cost savings potentially associated with blending.

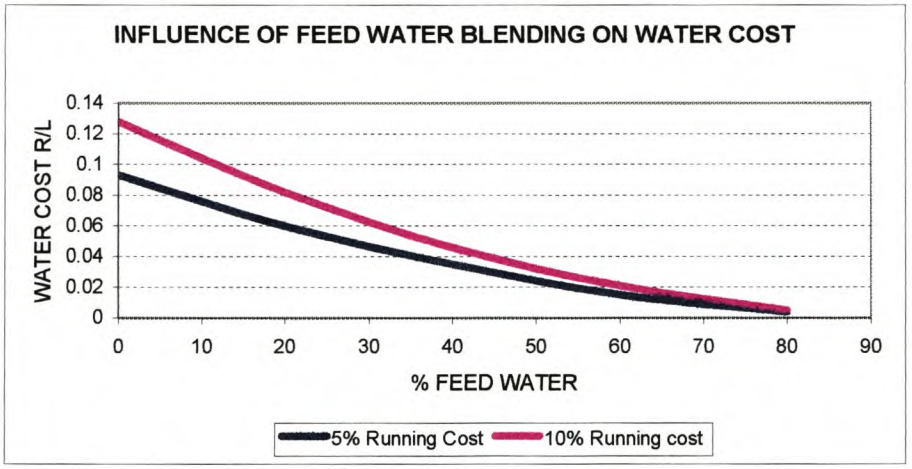

Figure 12.6: Influence of feed water blending on product water cost.

12.5 Performance and economic viability predictions

12.5.1.1 Example 1

Determination of solar still performance, and, subsequently, the cost of distilled water, can be done by using the evaluation model. As an example, Figure 12.7 shows the calculated water cost at different Southern African locations for a basin solar still such as the one developed in this study (with no additional infrastructure and running cost 10% of initial capital cost).

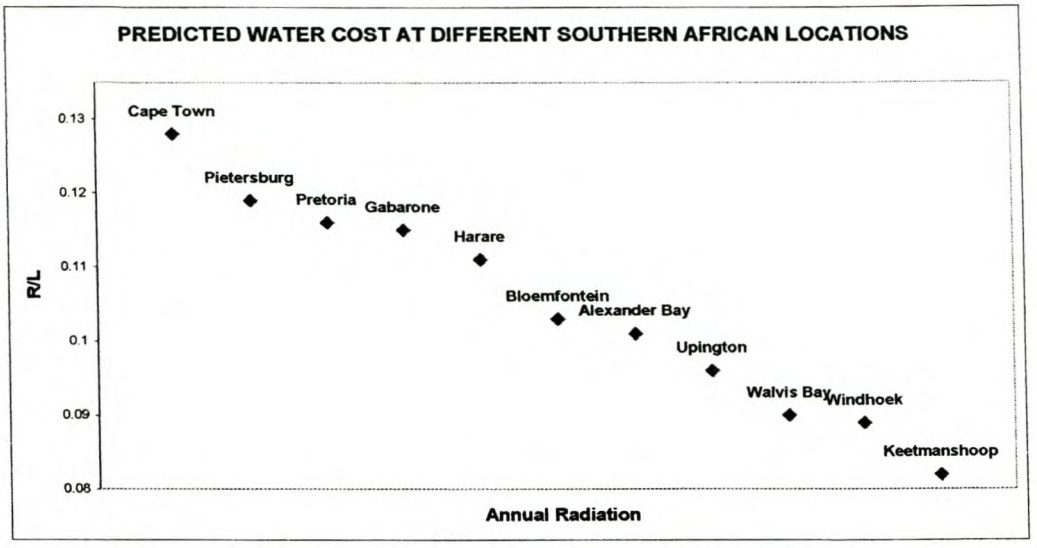

Figure 12.7: Calculated distilled water costs at different Southern African locations (total annual radiation increases from left to right).

12.5.2 Example 2

In Section 3.3.4 it was shown that due to the critical angle of the glass cover, the inherent efficiency η of the basin solar still is not constant for Southern African locations and Equation 3.2:

$$\eta\,(\%) = 2.7256e^{0.0033t}$$

was developed to predict its seasonal efficiency (t being the number of daylight minutes). An average efficiency value could then be calculated, from which the average productivity and thus the distilled water cost can be calculated. The following example was carried out for Gabarone, Botswana, using Eq. 3.2 together with the Cybersky and Meteonorm software packages.

Average annual η (from equation 3.2) = 33,6 %

Average daily water production (from Section 3.2.4) = $(\eta \times Rad\ (MJ)) / 2.43$

= 2,609 Liter

Cost of water = R0.100 / Liter

Similar calculations were performed for different sites. Figure 12.8 shows the different cost values calculated by making use of the productivity and efficiency equations.

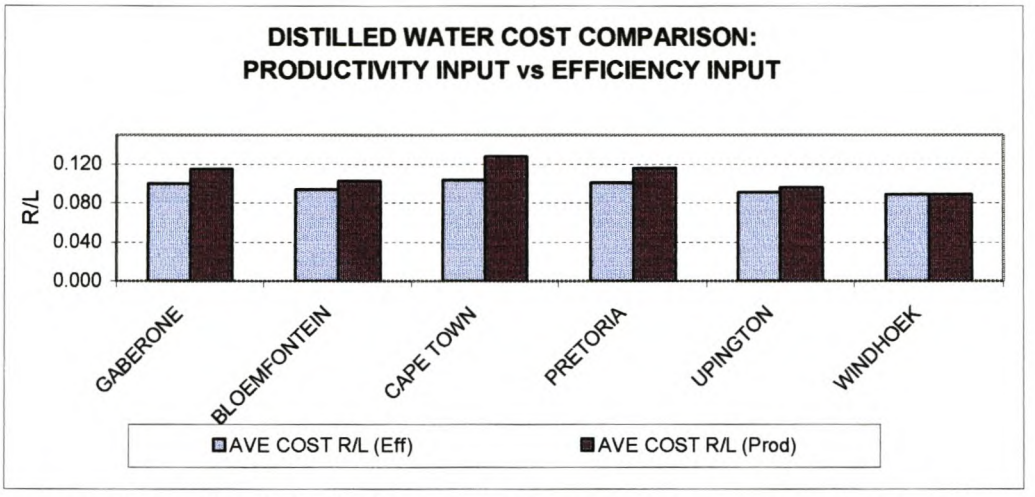

Figure 12.8: Predicted distilled water cost comparison: (a) using efficiency vs. (b) productivity as input.

12.6 Conclusions

A simple cost model to predict the cost of distilled water produced by basin solar stills in the Southern African environment has been developed. It takes into account both capital cost and performance variables, and it provides a useful tool in the first-order evaluation of the economic viability of solar distillation at different locations.

CHAPTER 13

CONCLUSIONS AND RECOMMENDATIONS

13.1 Introduction

The overall aim of this research was to investigate the economic viability of solar stills. Conclusions for this study are drawn within the framework of the aims formulated in Chapter 1:

(A) to understand the factors influencing solar still operation and performance;
(B) to identify the factors contributing to the cost of distilled water produced by solar distillation;
(C) to research and economically optimise the above factors in terms of solar still design and performance to reach a distilled water cost of less than R50/m^3; and

(D) to develop a low cost, low maintenance solar still suitable for use by rural communities and households in arid regions of Southern Africa.

13.2 Conclusions

13.2.1 Factors influencing solar still operation and performance

The most important factor influencing operation and performance of a solar still is its particular design. The study into different solar still designs showed that the basin solar still is the preferred design option despite its seasonal performance. This choice was motivated by its design simplicity (down to component level), ease of operation (no specific operator skills required) and low maintenance, as well as by the degree of worldwide implementation.

The winter productivity of the basin still is very low, about 25% of the summer value. This can be attributed to the lesser amount of solar radiation hours; the lower angles of radiation incidence and the decrease in water area receiving

direct radiation. These factors also result in non-constant efficiency behaviour.

An in-house experimental facility that simulates solar still behaviour under controlled environmental conditions was designed and set up. Of particular importance was the good correlation between conditions of lower radiation intensity and productivity, as this enabled research into performance enhancement under such conditions.

13.2.2 Factors contributing to the cost of distilled water produced by solar distillation

Solar distillation technology can be made more economically attractive through addressing the following cost–contributing factors, i.e. through (1) lowering the construction cost of the solar still and / or (2) increasing the operational life of the still and / or (3) increasing the efficiency of the still. Usually research efforts result in a degree of redesign of existing solar stills, and more than often the search for 'cheaper' water is abandoned in favour of a quest for improved efficiency, despite accompanying cost implications.

In order to identify and incorporate cheaper basin solar still components (parts), it was necessary to form an understanding of what the function of each component is. Given the solar distillation process as formulated in this study, alternative environmentally durable components could be identified and optimised for this design.

13.2.3 Optimisation of solar still design and performance

Under conditions of low radiation intensity, absorption of the radiation by the water plays an important part, although the basin water depth does not seem to be important. It was found, however, that the productivity decrease of the still could be up to 33% as the black interior lining becomes contaminated e.g. through scaling or the use of linings of other colours (care should be taken to keep the still interior as black as possible. It is also important that the height of the basin sidewalls are minimised as to limit the internal shadow areas.

An increase in winter productivity of up to 50% is predicted when a reflector is fixed behind the basin, which relates to about an annual performance increase of about 10%.

A simple cost evaluation model was developed to predict the cost of the product water produced by basin solar stills. Using this model, it was possible to perform an economic optimisation of the solar still and to define the design and possible design improvements. It was found that the eventual basin still should consist of a 3 mm thick window glass cover, black polypropylene lining inside polyurethane insulation, aluminium frame support and PVA exterior coating. This configuration decreased the still cost by about 80% without an apparent drop in performance (= efficiency).

Under conditions of high solar radiation and feed water / product water blending, it will be possible to produce solar distilled water for less than R50/m^3 with the solar still described above. A distilled water cost of about R100/m^3 can be expected when no feed water / product water blending is carried out.

13.2.4 Development of a low cost, low maintenance solar still suitable for use by rural communities

For the purposes of this study, the demographic profile of typical end-users was kept in mind, namely poorer, unskilled people living in small settlements relatively far from the nearest formal town. These are communities in specific geographical areas, for which solar distillation provides the only alternative for drinking water. This means that a solar still has to be simple in design and operation to facilitate easier maintenance necessitated by the logistical and supervisory factors. This also helped to further define the construction materials; in addition to being of relatively low cost, critical components had to be readily available in the case of repairs. In such cases, the application hurdle becomes an economical one, i.e. whether the particular water authority can afford to install solar distillation units or plants at the target communities.

13.2.5 Contributions to the technology emanating from this research

This study played an important role in making solar still technology affordable for use by poor, rural communities, as was demonstrated by the successful use of the research product (basin solar still) in a drinking water plant at a typical target community. This was made possible through the use of evaluation models (also developed as part of the study) for the identification and evaluation of relevant construction and performance factors influencing the economic viability of the still. Further proposed design improvements based on the seasonal use of reflectors which can enhance wintertime performance are also proposed, which can further reduce product water costs.

13.3 **Recommendations**

The following recommendations for further study are made based on the conclusions from Section 13.1.

13.3.1 Recommendation 1

Following from the above conclusions, it is recommended that the basin solar still be considered for general use in the target South African locations as defined in the study framework.

13.3.2 Recommendation 2

The basin solar still components identified in this study should be used as basis for design implementation or serve as reference for future component substitution.

13.3.3 Recommendation 3

Design optimisation to economically enhance solar still performance should be addressed further. This can possibly be achieved by externally preheating the saline feed water and / or the use of reflectors to increase the amount of direct

radiation into the basin.

13.3.4 Recommendation 4

Finally it is recommended that the economic evaluation model developed for this study be used to optimise the solar still design for a particular location. This model can also be developed further to provide more accurate water cost prediction for solar stills in general, as well as to include other desalination techniques (e.g. reverse osmosis).

ADDENDUM

FIELD EVALUATION OF SOLAR STILL AND SOLAR STILL PLANTS

A.I. Inputs from literature study

It was concluded from the literature study (Chapter 2) that solar stills have limited but important application potential in rural, arid regions. The simplicity of the technology combined with its use of renewable energy makes it economically attractive for use by smaller communities and single households in specific target areas, which is best illustrated by maps (see Figures 1.2 to 1.5 for the South African perspective).

Potential for the local use of solar stills thus exists, although similar water provision projects have failed in the past due to (1) the technology being uneconomical to implement or (2) failure to correctly address associated socio-economic issues (Goldie *et al* 2003).

A.II. Field trials

A solar still plant consisting of 20 solar still units was constructed with the materials and components described in Section 5.4. The plant was subsequently tested at sites at the University of Stellenbosch and in Bushmanland in the Northern Cape Province (Figure A.1). Conclusions from these trial runs are presented after the Figures.

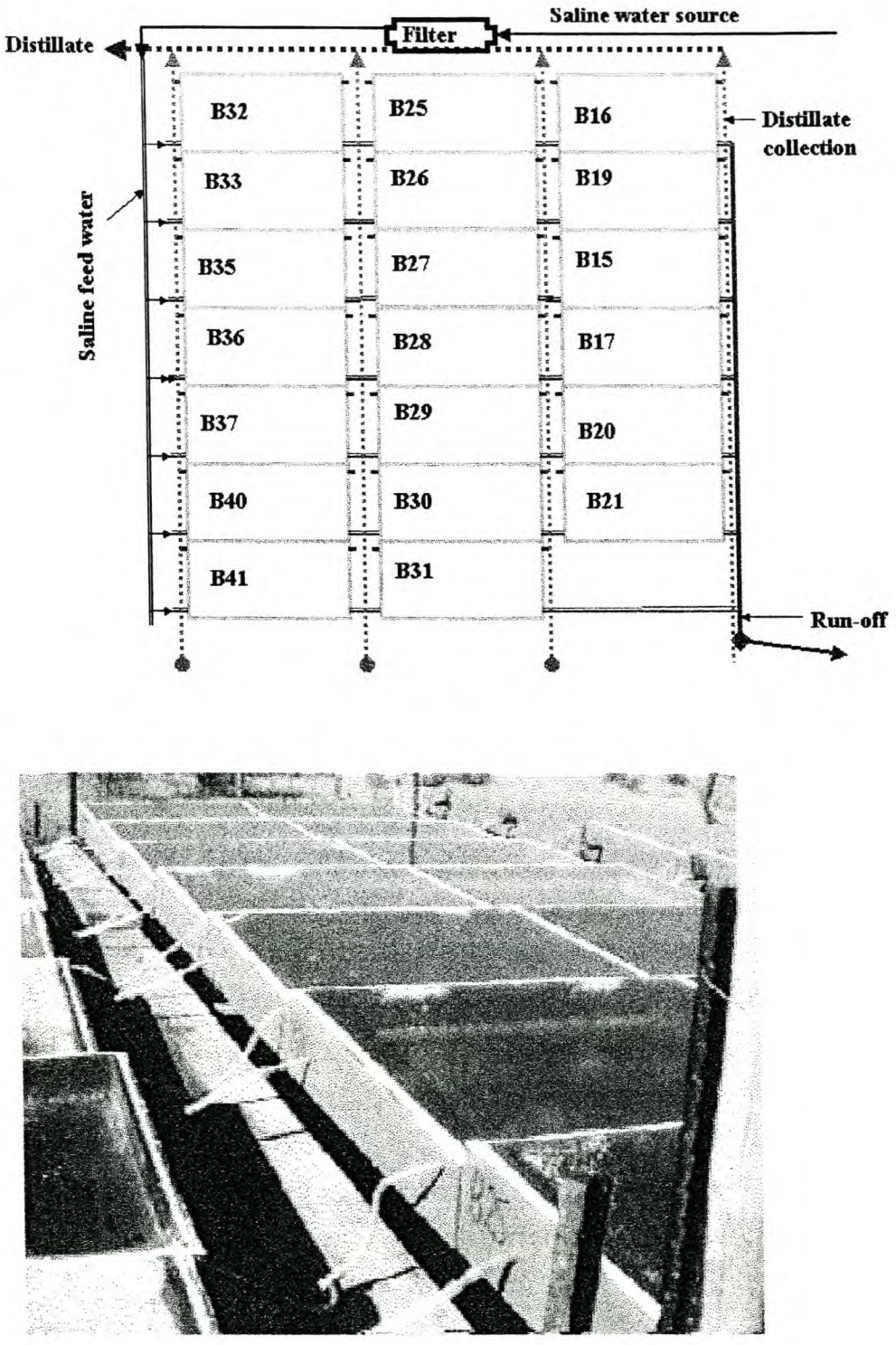

Figure A.1: Solar still plant layout (top) and picture (bottom)

- Solar stills with 'Correx' polypropylene (PP) linings started leaking soon after commissioning. Closer investigation revealed that the welding joints

were not able to withstand the heating / cooling cycles inside the stills. It was therefore decided to rather make use of flexible PP for still linings.

- Stills with plywood frames were able to withstand the frame deformations (due to water filling and prolonged exposure) better than aluminium frames. This was, however, a function of the stand on which the stills were placed, as these frames did not provide sufficient structural support under the still bases. The stand design was subsequently made part of future plant designs.
- Filling and flushing of the rows of stills was very problematic as the overflow piping from one still to the next was too narrow. This extended the nocturnal filling period, which proved to be problematic in winter when freezing in feed pipes could occur. Larger diameter feed piping was incorporated as part of the design review.
- It was shown that with untreated, hard groundwater it may be necessary to routinely clean the inside linings of the stills to maintain a degree of 'blackness' inside the stills. This also confirmed that the cover had to be removable with relative ease. It was also found that removal of scale was easier with a lining of polypropylene than with silicone.
- The actual average performance of the plant was lower than predicted (27% versus 40%). This was attributed to the leaking of the polypropylene-lined stills, incorrect operating procedure which caused some stills to run dry, and a number of stills being tilted too far 'backwards' due to stand deformation.
- The product water from the plant was of a very high quality (constantly less than 30 mg/L TDS versus greater than 8000 mg/L TDS feed water). Feed water spiked with 1% nitrate and fluoride solutions produced distilled water without measurable levels of these contaminants.
- Lastly it was found that it was important to take account of nature: bees trying to get to the 'sweet' water inside the system and porcupines digging up the fresh water pipes were specific problems which had to be addressed during the trial runs.

A.III. Construction and evaluation of a solar still plant for community use

A solar still plant for community use can be defined as a number of solar still units interconnected with pipes and pumps, as well as storage containers from which water for household use can be collected. Distilled water can be blended with feed water to increase the capacity of the plant, and for larger plants the cover areas can also be utilised for rainwater collection.

A.IV. Plant design

The following general procedure was developed for the design of a solar still plant for community use, once there is certainty that a constant feed water source is available:

- First, a site visit is necessary to do basic land surveying, etc. During such a visit the location of the saline water source, relative to the end-user(s), should be determined, and topographical and meteorological information collected (if available). Important design considerations include plant alignment towards true north, available construction area(s) and existing water provision infrastructure.
- A sample from the saline water source should be taken for analysis, as well as a history of any earlier water analysis (if available from the local authority). This enables the plant designer to calculate (a) the economic viability of incorporating distilled water blending, (b) the seasonality of the salinity of the source, (c) the still flushing cycles, and (d) the necessity of additional infrastructure such as in-line filters or anti-scaling equipment.
- The next major design input is determining the number of people who will be dependent on the plant for their potable water. A design base of five liters of drinking and cooking water per capita per day, conforming to the guidelines, is currently being used (van Schalkwyk 1996)
- Lastly the expected productivity of the solar stills should be taken into account. In this case, where modular units are used, the seasonal output

will determine the number of stills to be used.

A.V. Components of solar still plant

Figure A.2 (below) illustrates components of typical solar distillation plants.

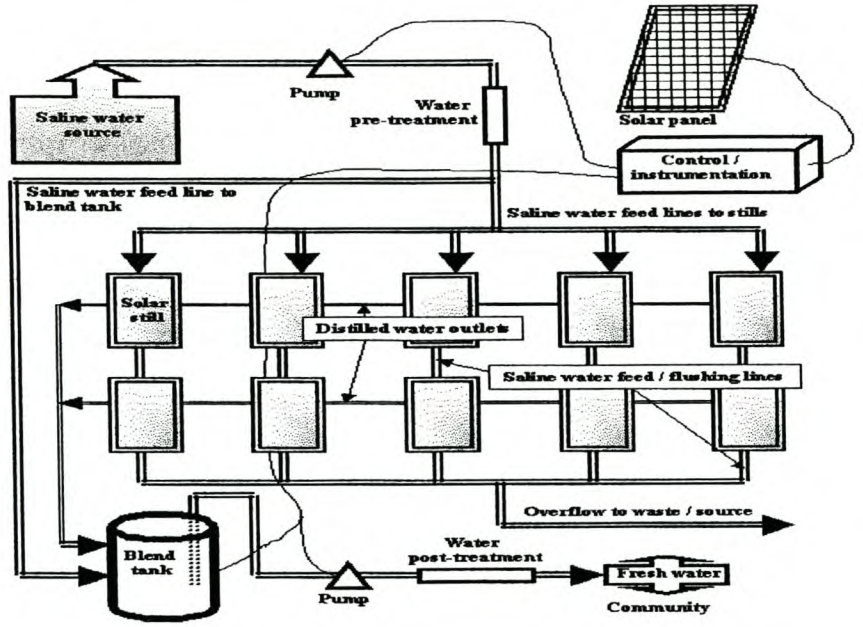

Figure A.2: Typical components of a community solar still plant.

A.VI. Construction of solar still pilot plant

A typical target community was identified at Kerkplaas in the Klein Karoo. Kerkplaas is situated about 30 km from Ladismith, about 300 km from Cape Town. About seven houses, a school and a church are built on the property. The community consists of about 40 people, plus about 20 pupils from neighbouring farms during school terms. Drinking water supply had always been problematic, and during drought spells drinking water had to be trucked to Kerkplaas. Associated costs were high, as the water had been trucked over distances of up to 80 km to the community.

A solar still plant was designed and built according to the general solar still

specification described in Chapter 5. Brackish water (TDS 2200 mg/L) from a nearby dam was used as feed and blend water (see Table A.1 for water analysis before and after blending and in terms of Table 4.1).

The following plant modifications were incorporated to suit local conditions:

- The stills were placed on a sloping steel framework that was high enough (1 meter +) to allow good maintenance accessibility from beneath.
- A two-meter chicken wire fence with lockable gate was erected around the plant. Instrumentation, pumps and valves were placed inside a lockable box beneath the plant.
- A 5 m^3 drinking water tank, connected to the plant outlet, was placed about 20 meters away next to an existing rain water tank.
- In-line water meters were connected into the different feed and outlet lines to record the different water usage Figures.

A picture of the Kerkplaas solar still plant is shown in Figure A.3.

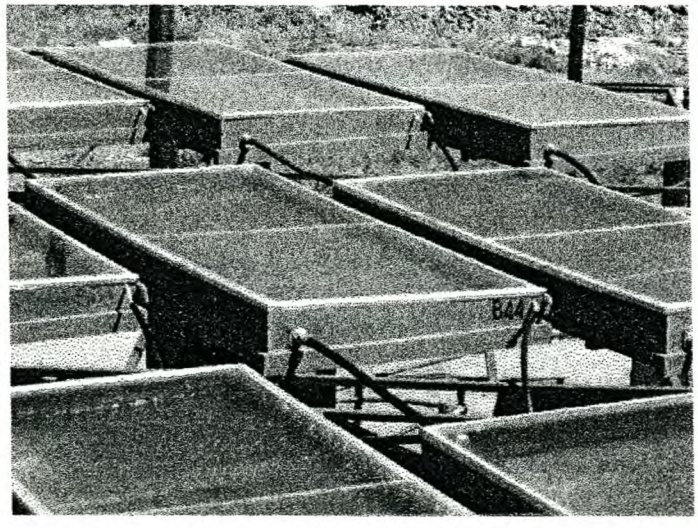

Figure A.3: Kerkplaas solar still plant.

Table A.1: Kerkplaas water analysis versus specifications

Test	Unit	Bore-hole analysis	Percentage dilution with solar-distilled water				
			30	40	50	60	70
Potassium as K	mg/l	6.00	4.20	3.60	3.00	2.40	1.80
Sodium as Na	mg/l	505.00	353.50	303.00	252.50	202.00	151.50
Calcium as Ca	mg/l	132.00	92.40	79.20	66.00	52.80	39.60
Magnesium as Mg	mg/l	78.00	54.60	46.80	39.00	31.20	23.40
Sulphate as SO4	mg/l	333.00	233.10	199.80	166.50	133.20	99.90
Chloride as Cl	mg/l	744.00	520.80	446.40	372.00	297.60	223.20
Alkalinity as CaCO3**	mg/l	389.00	272.30	233.40	194.50	155.60	116.70
Nitrate+nitrite as N	mg/l	1.00	0.70	0.60	0.50	0.40	0.30
Fluoride as F	mg/l	0.83	0.58	0.50	0.42	0.33	0.25
Iron as Fe	mg/l	0.06	0.04	0.04	0.03	0.02	0.02
Manganese as Mn	mg/l	0.26	0.18	0.16	0.13	0.10	0.08
Copper as Cu	mg/l	0.05	0.04	0.03	0.03	0.02	0.02
Cadmium as Cd	mg/l	<0,010	<0,007	<0,006	<0,005	<0,004	<0,003
Zinc as Zn	mg/l	0.23	0.16	0.14	0.12	0.09	0.07
Conductivity	mS/m	342.00	239.40	205.20	171.00	136.80	102.60
pH		7.10	7.10	7.10	7.10	7.10	7.10
Total Dissolved Solids	mg/l	2189.00	1532.30	1313.40	1094.50	875.60	656.70
Hardness as CaCO3	mg/l	651.00	455.70	390.60	325.50	260.40	195.30

** - No specification

Ideal	1	No effects
Good	2	Suitable for lifetime use
Marginal	3	Generally suitable for long term use
Poor	4	Risk of chronic health effects
Unacceptable	5	Severe acute health effects, even with short term use

A.VII. Plant specification and cost

The following Table summarises the most important design and cost aspects of the Kerkplaas plant.

Table A.2: Kerkplaas solar still plant specifications. Plant rinse water approximately equals double the amount of distillate produced per day

Specification / property	Description / remarks
Total plant area (m^2)	45 (level ground)
Saline water capacity at fill (L)	750
Average production capacity (L/day)	90 (unblended, season dependent)
Number of solar still units	15 (5 rows of 3 stills)
Construction materials of solar stills	Glass, PU, PP, aluminium
Additional energy supply equipment	75 W solar panel plus battery
Pumps	2 centrifugal
Filters	In-line cartridge filters
Flushing cycle	Up to 180 minutes every n^{th} day
Maintenance requirements	Routine visual inspection, paint
Water blending ratio	Between 0/100 and 100/0
Distilled water quality	TDS < 10 mg/L
Total component cost (excl framework):	
➢ solar stills	R12000
➢ piping, filters, tanks and pumps	R2500
➢ solar panel and instrumentation	R6000
Construction time (incl stills)	4 weeks
Commissioning period	2 weeks
Imported components	Centrifugal pumps

A.VIII. Plant performance over test period

The technical performance of the test plant was monitored over the period December 2000 to December 2001. Water production, plant durability and water quality were monitored to determine plant performance.

Water production was initially measured by monitoring the water level in the community's fresh water tank. This did not provide sufficient production data as the community continuously used water from the tank. During August 2001 water meters were fitted into the groundwater feed pipes, the plant overflow pipe

and the product water pipe, so that a complete water balance could be calculated for the plant. Figure A.4 shows actual water production averages, as well as calculated (according to formula presented in Section 12.3.1)

.

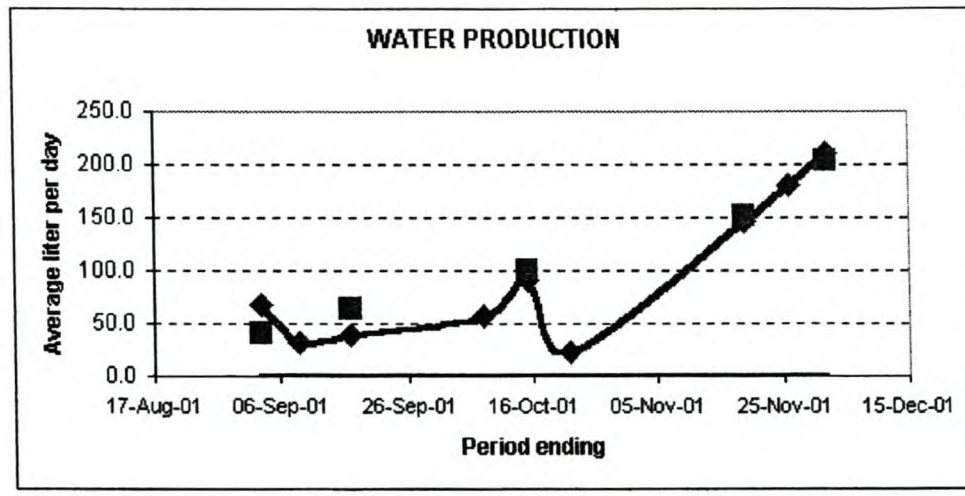

Figure A.4: Average daily water production of Kerkplaas solar still plant (graph) and calculated production volumes (squares).

The seasonal productivity can clearly be seen from the above Figure. The productivity dip in October can be attributed to extended overcast periods plus a weeklong maintenance period when the plant was out of commission. It can be seen that good correlation between expected and actual productivity was found.

Plant durability, in particular water leaks, glass breakages and electronic equipment failure, was visually monitored over the test period. Initially a number of solar still units leaked at their overflows, so a design modification had to be implemented on site to strengthen that interface. No leakages due to rupture of the plastic lining were reported. It was noticed, however, that due to deformation of the still stands, some stills had to be sealed again on the cover/frame interface. Two (uncharacteristic) hailstorms hit the plant during late Spring 2001, and one glass pane broke during the first storm. This was replaced on site without interference to the plant's operation. No electronic equipment failures were reported over the first year of operation. Water quality was managed to a TDS of less than 1000 mg/L (Figure A.5).

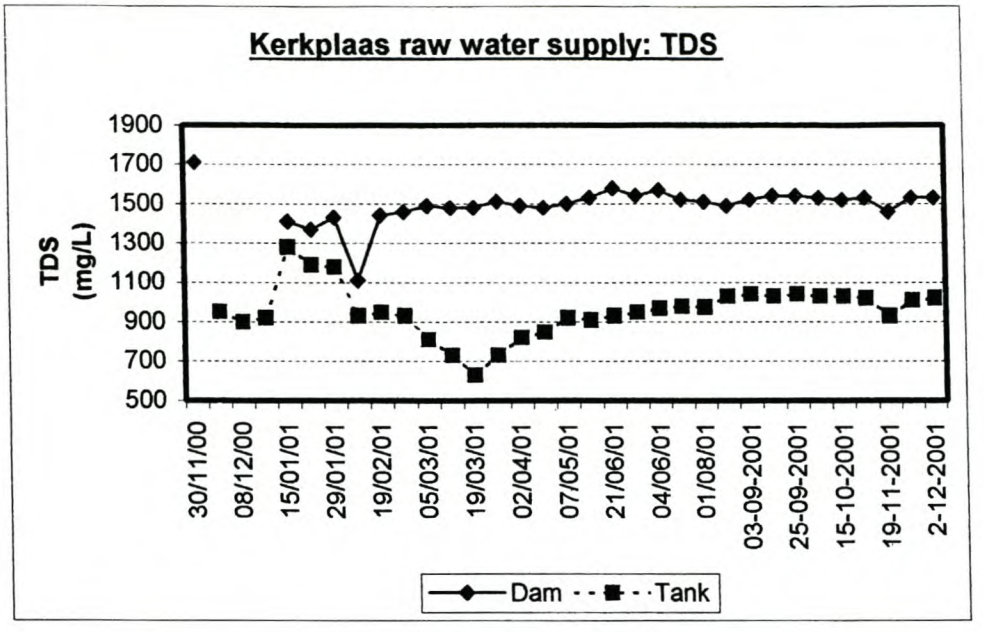

Figure A.5: TDS management of Kerkplaas solar still plant (dam = community drinking water).

Bacterial analyses for total plate count, ecoli and faecal coliforms of the product water were carried out by the District Municipality and the water was found to conform to drinking water standards.

A.IX. Conclusions and recommendations

The following conclusions are drawn at the end of the technology demonstration phase of this study:

- Water supply capacity

  As solar distillation is a season-dependent small-scale water supply technology, it is better suited for summertime fresh water augmentation. It is therefore attractive for use in dry, winter rainfall regions. Blending of feed and product water can be carried out as long as the capital cost implications thereof are beneficial. The use of dual community water supply systems can be considered where the quality of feed water is such

that it can be used for sanitation and / or washing while product water is utilised for drinking and cooking purposes. The number of stills required for a solar still installation will be dependent on the above-mentioned factors.

- Water quality

Solar-distilled water is chemically very pure, with TDS < 10 mg/L. Experimentally it was proven that feed water containing up to 1% dissolved fluorides and nitrates could be purified to contain immeasurable levels thereof (Goldie *et al* 2003). Under normal operational conditions a solar still will not produce water before the feed water temperature exceeds 50 °C, and typically this temperature rises in excess of 60 °, which is sufficient to pasteurise the water. Under conditions of low solar radiation, such as during cloudy winter days, pasteurisation temperatures will not be reached and certain types of microbiological activity in the basin may be enhanced. It is, however, not possible to accurately predict the effect of such contamination on the product water quality as cross-contamination would require a degree of aerial mobility by the microbiological contaminants. Experimentally water produced by the Kerkplaas experimental plant tested negative for microbiological contamination.

- Technical specifications

The basin solar still described in Chapters 3 and 5 was identified as the most appropriate design to fulfil the research requirements of the technology demonstration. These requirements were low construction costs, solar still durability and acceptable production performance. A modular solar still design consisting of readily available, relatively cheap but environmentally durable components was developed and successfully tested, under both controlled and field conditions.

- Economic aspects

The relatively simple financial model that was developed in Chapter 12 can be used to forecast the cost of water delivery to an end user. Using this model, it was shown that although solar still installations are capital intensive, they can produce water at low running costs.

- Socio-economic aspects

As with the provision of other services, community participation largely determines the degree of success of the introduction of solar still technology. It is of great importance that all role-players, from researchers to community leaders and the affected community itself, be involved from the onset of such a project. As the technology is relatively unsophisticated it can be explained quite easily, and operational and maintenance training should not present any major problems. Community ownership is critical in terms of technology sustainability, and also to prevent plant malfunction.

- Additional water usage potential

It has been shown that the quality of product water can be controlled through correct plant management, thus creating the potential for end-users to utilise excess water for purposes other than household. Limited vegetable farming and the establishment of trees and shrubs can potentially be undertaken, given that other factors (such as soil quality and appropriate management) are also addressed. Given the low production volumes and the associated cost, solar stills do not however provide an economically feasible alternative for water supply for general agricultural purposes.

REFERENCES

Abdul-Fattah AF, *Supply of Desalted Water to Remote Arid Zones*, Desalination, 60 (1986) 151 - 164

Abulnour AM, Sorour MH, Hammouda FA, Abdel Dayem AM, *Non-conventional Water Resources for Small Remote Communities in Developing Countries*, Desalination, 47 (1983) 285 - 292

Agua del Sol, *The Water Line*, Monthly Newsletter, July, 1997

Al Kasabi TO, Dix TE, Laporta C, *Design of a Commercial Solar-Powered Greenhouse*, Desalination, 39 (1981) 53 - 62

Al-Abbasi MA, Al-Karaghouli AA, Minasian AN, *Photochemically Assisted Solar Desalination of Saline Water*, Desalination, 86 (1992) 317 - 324

Andreatta D, *A Summary of Water Pasteurisation Techniques*, 29th Intersociety Energy Conversion Engineering Conference, AIAAI, 1994

Arif Ileri AG, *Software to Analyze Solar Stills and an Experimental Study on the Effects of the Cover*, Desalination, 114 (1997) 37 - 44

Ashboren D, Waldman M, *Water for Life: Israel's R&D for Water Renovation and Sweet water Production*, Desalination, 30 (1979) 213 - 221

Belessiotis V, Voropoulos K, Delyannis E, *Experimental and Theoretical Method for the Determination of the Daily Output of a Solar Still: Input-output Method*, Desalination, 100 (1995) 99 - 104

Belessiotis V, Delyannis E, *Solar Energy: Some Proposals for Future Development and Application to Desalination*, Desalination, 105 (1996) 151 - 158

Bouchekima B, Gros B, Ouahes R, Diboun M, *Performance Study of the Capillary Film Solar Distiller*, Desalination, 116 (1998) 185 - 192

Churchill LD, *The water cycle*, http://www.math.montana.edu/~nmp/materials/ess/hydrosphere/ expert/runningwater/runningback.html, K-12 Earth Systems Science Project, University of Montana, United States of America

Delyannis A, Delyannis E, *Recent Solar Distillation Developments*, Desalination, 45 (1983) 361 - 369

Delyannis AA, Delyannis E, *Solar Desalination*, Desalination 50 (1981) 71 - 81

Delyannis EE, Delyannis A, *Economics of Solar Stills*, Desalination, 52 (1985) 167 - 176

Delyannis EE, Belessiotes V, *Solar Application in Desalination: the Greek Islands Experiment*, Desalination, 100 (1995), 27 - 34

Delyannis EE, *Status of Solar Assisted Desalination: A Review*, Desalination, 67 (1987) 3 - 19

Dhiman ND, *Transient Analysis of a Spherical Solar Still*, Desalination, 69 (1988) 47 - 55

Dobrevsky I, Georgieva M, *Some Possibilities for Solar Evaporation Intensification*, Desalination, 45 (1983) 93 - 99

Drinking Water Quality Standards, Environmental Protection Agency of the United States of America, http://www.epa.gov/

El-Haggar SM, Awn AA, *Optimum Conditions for a Solar Still and its Use for a Greenhouse using the Nutrient Film Technique*, Desalination, 94 (1993) 55 - 68

EPSEA Solar water Purification Project, El Paso Solar Energy Association, http://www.epsea.org, 1999

Fath HES, *Solar Distillation: a Promising Alternative for Water Provision with Free Energy, Simple Technology and a Clean Environment*, Desalination, 116 (1998) 45 - 56

Gandhidasan P, Abualhamayel HI, *A Simple Analysis of Solar Desalination of Seawater*, Desalination, 99 (1984) 137 - 147

Geddes KA, Deanin RD *Plastics in Solar Energy Collectors*, Chemtech (1982) 736 - 740

Gerber A, *Guide to the Construction of a Double Tilted Roof Solar Distillation Unit*, Department of Water Affairs (SWA Branch), July 1973

Goldie I, Theunissen A, Bonthuys J, Cloete V, *Cost Effective Solar Still Units for Drinking Water Provision in Remote, Rural Areas of South Africa: A Case Study and Implementation Guidelines,* WRC Report 1032/1/03, February 2003

Gomkale SD, *Operational Experience with Solar Stills in an Indian Village and their Contribution to the Drinking Water Supply*, Desalination, 69 (1988) 171 - 176

Howe ED, *Measurement and Control in Solar Distillation Plants*, Desalination, 59 (1986) 307 - 320

Important characteristics of greenhouse glazing materials, http://www.public.lastate.edu/~greenhouse/unit2.html

Jamieson DT, *Experimental methods for the Determination of the Properties of Salien Water*, Desalination, 59 (1986) 219 - 240

Kamal MR et al, *Cost Comparison of Water Produced from Solar Powered Distillation and Solar Stills*, Desalination & Water Reuse, Vol 9/2 (2000, summary) 74 - 75

Katsifarakis KL, *Solar Distillation of Landfill Leachate. A Case Study in Greece*, Desalination, 94 (1993) 213 - 221

Kirk-Othmer Encyclopedia of Chemical Technology, *Water Analysis*, 4th Edition, Vol 21, 689 – 707

Kulha D, *Clean water from the Sun*, http://sunsite.unc.edu/london/renewable-energy/solar/general-info/msg00383.html, 1994

Kumar S, Tiwari GN, *Optimisation of Collector and Basin Areas for a Higher Yield for Active Solar Stills*, Desalination, 116 (1998) 1-9

Lof GOG, Eibling JA, Bloemer JW, *Energy Balances in Solar Distillers*, AIChE Journal, 7, 4 (1961) 641 – 649

Lowe SK, *Water Purification by Solar Distillation*, http://www.sunseed.org.uk/, 1998

Lynch SD, *Digital Agrohydrological Atlas for Southern Africa*, Department of Agricultural Engineering, University of Natal, South Africa.

Maalej AY, *Solar Still Performance*, Desalination, 82 (1991) 207 - 219

Madani AA, Zaki GM, *Prospective of Two Water Producing Units*, Desalination, 73 (1989) 167 - 180

Maier HB, *Solar energy collecting and trapping apparatus for home heating or cooling*, US patent 4135985, 1979

McCracken H, *Fresh Water from the Sea*, Internet source unknown

McCracken H, *Understanding Solar Stills*, Technical paper # 37, VITA, 1985

Murase K, Kobayashi S, Nakamura M, Toyama S, *Development and Application of a Roof Type Solar Still*, Desalination, 73 (1989) 111 - 118

National Geographic MapMachine, http://plasma.nationalgeographic.com/

Natu GL, Goghari HD, Gomkale SD, Solar *Distillation Plant at Awania*, Gujarat, India, Desalination, 31 (1979) 435 - 441

OSRAM Siccatherm Technical Brochure, www.osram.com

Ouahes E, Ouahes C, Le Goff P, Le Goff J, *A Hardy, High-Yield Solar Distiller of Brackish Water*, Desalination, 67 (1987) 43 - 52

Quality of Domestic Water Supplies, (Second Edition) Volume 1: Assessment Guide, WRC report TT 101/98, Second edition. Second Print. Published by Water Research Commission, The Department of Water Affairs and Forestry, and The Department of Health (South Africa)

Rahim NHA, *Utilization of a Forced Condensing Technique in a Moving Film Inclined Solar Desalination Still*, Desalination, 101 (1995) 255 - 262

Simonic M, *Assessment of Ambient Groundwater Quality on a National Scale in the Republic of South Africa*, Hydromedia Solutions Pty Ltd, 1999

Spiegler KS, El-Sayed Y, *A desalination primer*, Balaban Desalination Publications, 1994

Stark V, *Solar distillation apparatus*, US patent 4270981, 1981

Still AD, *Small Scale Desalination in South Africa with Particular Reference to Solar Distillation*, MSc Theses, University of Cape Town, 1991

Structa Industries Technical Brochure on Structalite, http://www.structa.co.za/structa4.htm

Telkes M, *Solar Stills*, Proc. World Symposium on Applied Solar Energy (1956), 73 – 79

Tiwari GN, Madhuri, *Effect of Water Depth on Daily Yield of the Still*, Desalination, 61 (1987), 67 - 75

Tiwari GN, Kupfermann A, Aggarwal S, *A New Design for a Double-condensing Chamber Solar Still*, Desalination, 114 (1997) 153 - 164

Tiwari GN, Mukherjee K, Ashok KR, Yadav YP, *Comparison of Various Designs of Solar Stills*, Desalination, 60 (1986) 191 - 202

Tiwari GN, Emran Khan Md, Goyal RK, *Experimental Study of Evaporation in Distillation*, Desalination, 115 (1998) 121 - 128

Tiwari GN, Singh AK, *Thermal Efficiency of Double Slope FRP Solar Distiller: Analytical and Experimental Studies*, Desalination, 82 (1991) 223 - 232

Tiwari GN, *Feasibility Study of Solar Distillation Plants in South Pacific Countries*, Desalination, 82 (1991) 233 - 241

Toyama S, Nakamura M, Salah HM, Futamura S, Murase K, *Laboratory Test of a Solar Distillator with a Heat Penetrating Plate*, Desalination, 67 (1987)

67 - 73

van Schalkwyk A, *Guidelines for the Estimation of Domestic Water Demand of Developing Communities in the Northern Transvaal*, The Water Research Commission of South Africa, WRC Report 480/1/96, 1996

Wegelin M, *Solar Water Disinfection*, EAWAG/SANDEC, Duebendorf, Switzerland, 1999

Wilkerson WM, *Solar still assembly*, US patent 5158650, 1992

Workshop Report, *Fluoride and Nitrates in Rural Water Supplies: Health Issues and Removal Techniques*, Water Research Commission, March 1999.

Yadav YP, Tiwari GN, *Monthly Comparative Performance of Solar Stills of Various Designs*, Desalination, 67 (1987) 566 - 578

Yadav YP, *Performance Analysis of a Solar Still Coupled to a Heat Exchanger*, Desalination, 91 (1993) 135 - 144

Yadav YP, *Transient Analysis of a Double-Basin Solar Still Integrated with Collector*, Desalination, 71 (1989) 151 - 164

DIE EINDE VAN KALK, ROES EN ALGE

ISRAELI

P T H

WATER KONDISIONEERDER

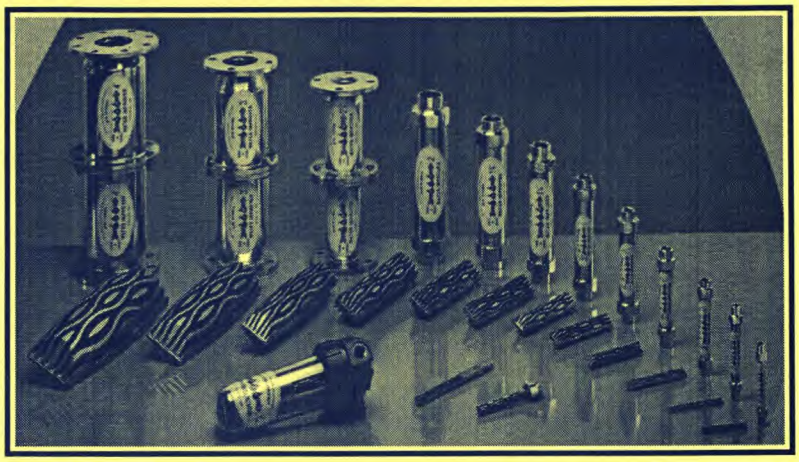

Die Israeli PTH allooi-katalisator waterkondisioneerder, is beskikbaar in groottes van ½ dm tot 12 dm in deursnit om water volumes te hanteer vanaf 1 000 - 1 000 000 lt/uur.

Die toestel het 'n vlekvrye staalomhulsel met skroefdraad sokente vir maklike installasie. Die groter modelle bokant 2 dm, het flense op die ente.

Die PTH kan oopgemaak en skoongemaak word indien dit op die lang termyn nodig sou wees. In so 'n geval kan die katalisator-kern wat bestaan uit allooie van 'n verskeidenheid metale, waaronder ook edel metale, met 'n staalborsel skoongemaak word.

HOE WERK DIE TOESTEL?

Die PTH benodig nie elektrisiteit of enige chemikalieë nie. Wanneer die water deur die toestel vloei, stel die allooi-katalisator-kern selfgeregenereerde elektrone in die water vry. Hierdie elektrone word vanuit die grond aangevul met 'n gronddraad wat saam met die toestel voorsien word. Die elektrone iooniseer die mineralesoute wat in oplossing in die water is, en breek dit op, sodat smaak verbeter en aankalking en roesneerslae voorkom word; terselfdertyd verslap die Waterstofbinding van die H_2O molekules, wat "natter" water tot gevolg het.

WAARVOOR WORD DIE TOESTEL GEBRUIK?

Die PTH waterkondisioneerder is nie 'n waterfilter of 'n watersuiweraar nie. Die word vir die volgende doeleindes gebruik;

- Voorkoming van kalksteenaanpaksels en roes.
- Verwydering van reeds gevormde kalk- en roesneerslae en aanpaksels.
- Bekamping van yster en mangaanneerslae.
- Vermindering van oksidasieprosesse met gepaardgaande neerslae.

- Vermindering van gebreksverwering.
- Verbetering van smaak onder andere brak, chloor en swawel.
- Verbetering van wasvermoë vanweë "natter" water.
- Verhoging van grondinfiltrasievermoë.
- Verbetering van saadontkieming.
- Verbeterde plantegroei en verhoogde produksie.
- Voorkoming van verbrakking.
- Verbeterde benutting van swembadchemikalieë
- Verminderde algegoei in swembaddens en suipkrippe.
- Verbeterde vermenging van vloeibare bemestingstowwe.
- Voorkoming van verstopping van druppers en sproeiers deur aankalking.

WIE GEBRUIK DIE TOESTELLE?

Die PTH word reeds in meer as 30 lande in die wêreld gebruik deur HUISEIENAARS, BOERE, INDUSTRIEË, NYWERHEDE, HOTELLE, KOSHUISE, WOONSTELBLOKKE, KONTOORKOMPLEKSE, MOTORHAWENS, SLAGHUISE, DROOGSKOONMAKERS, WASSERYE, TANDARTSE, KWEKERYE, KELDERS, LABORATORIUMS, MUNISIPALITEITE, MYNE, ens. vir die beskerming van toerusting soos warmwaterinstallasies, verhittingselemente, sonpanele, skoonmaaktoerusting, pasteuriseerders, koeltorings, lugversorgers, steriliseerders, kondensators, kompressors, waterverkoelde enjins, pompe, fonteine, verkoelingstoerusting, ysmasjiene, watervoorsiening vir hoenders, varke, konyne, veesuipings, sprinkel- en drupbesproeiing, swembaddens ens. NIE ALLEENLIK WORD TOERUSTING BESKERM TEEN KALK EN ROESAANPAKSELS NIE, MAAR DIE EFFEKTIWITEIT VAN DIE TOERUSTING IS SOVEEL HOËR, TESAME MET DIE BESPARING OP ENERGIE VERBRUIK.

KALKSTEEN EN ROES KOS GELD!!

MET PTH

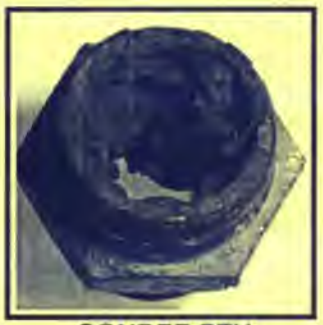

SONDER PTH

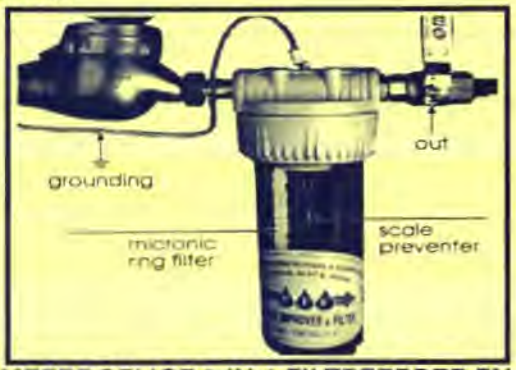

MEERDOELIGE 2-IN-1 FILTREERDER EN KONDISIONEERDER KOMBINASIE.

(1 mm Kalkaanpaksel op 'n verhittingselement verhoog die energieverbruik met gemiddeld 10%. Proewe het die PTH as 94.16% suksesvol bewys teen aankalking, terwyl tot 50% aan chemicalieë vir swembaddens bespaar word.)

WATERVERSAGTING RSA

GAUTENG
POSBUS 17779
PRETORIA NOORD • 0116
TEL : (012) 542-2464
SEL : 082 576 7072
FAKS : (012) 542-5414
E-pos : pth@mweb.co.za

VRYSTAAT
POSBUS 37547
LANGENHOVEN PARK • 9330
TEL : (051) 446-2992
SEL : 083 274 6489
FAKS : (051) 446-2429

KAAP
POSBUS 76
AGULHAS • 7287
TEL : (02846) 56542
SEL : 082 900 9253
FAKS : (02846) 56545
E-pos : pfm@isat.co.za

Falcon Print (012) 542-1711